Treatment of Cryptosporidium and Dye Contaminants Using Photoelectrocatalytic Oxidation

By

Kyana R. L. Young

A dissertation submitted in partial fulfillment of
the requirements for the degree of

Doctor of Philosophy
(Civil and Environmental Engineering)

at the
University of Wisconsin – Madison
2014

Date of final oral examination: 5/30/2014

This dissertation is approved by the following members of the Final Oral Committee:
Gregory W. Harrington, Professor, Civil and Environmental Engineering
Daniel R. Noguera, Professor, Civil and Environmental Engineering
Katherine D. McMahon, Professor, Civil and Environmental Engineering
Christina K. Remucal, Assistant Professor, Civil and Environmental Engineering
Terence Barry, Chief Scientific Officer, AquaMost, Incorporated

ABSTRACT

Water quality is a major concern of the United Nations and the World Health Organization (WHO). Contaminated surface and ground water sources and poorly functioning water distribution systems contribute to transmission of waterborne contaminants (Braghetta, 2006). Worldwide, 1.8 million people die yearly from diarrheal disease (WHO, 2004). Even with regulations and improved treatment methods, waterborne contaminants continue to be present. For the past 30 years, waterborne outbreaks in the United States are a result of emerging infectious diseases caused by microorganisms in the aquatic environment.

Not all water concerns are based on microbial contaminants and their associated outbreaks. With increase in production and the manufacturing of goods that require synthetic dyes comes an increase of the presence of these dyes in environments outside of the manufacturing process. Demand for synthetic dyes accounts for $7x10^5$ metric tons of dyestuffs produced every year (Sahasivam, 2006), and upwards of 15% of that dye accounts as waste for non-production use (Daneshvar, 2005).

Researchers continue to explore methods to provide the highest quality of water. Advanced oxidation processes (AOP) are beneficial for treating contaminants typically not removed, disinfected, or inactivated by conventional water treatment processes such as biological or physical-chemical technologies. This dissertation compares the inactivation of *Cryptosporidium parvum* oocysts by PCO, PECO, electrolysis, and UV reactors; the first order inactivation rate constants for PECO, PCO, electrolysis, and ultraviolet irradiation were $1.0 \times 10^{-2} \pm 1.6 \times 10^{-3}$ sec^{-1}, $3.4 \times 10^{-3} \pm 3.2 \times 10^{-4}$ sec^{-1}, $3.3 \times 10^{-3} \pm 3.0 \times 10^{-3}$ sec^{-1}, and $1.8 \times 10^{-3} \pm 3.2 \times 10^{-3}$ sec^{-1} respectively. Additionally, investigation regarding the degradation of tartrazine (FD&C Acid Yellow No. 23) and erioglaucine (FD&C Acid Blue No. 5), by comparing operational parameters of recirculation rate, tartrazine concentration, chloride ion concentration, and applied bias voltage by treatment with PECO were also explored. For both tartrazine and erioglaucine, the recirculation rate of 4.1 L/min, applied voltage = 9V, chloride ion concentration = 100 mg/L, and dye concentration (tartrazine = 12.0 mg/L, erioglaucine = 10 mg/L) achieved degradation rates of $k = 0.006 \pm 0.0004$ min^{-1} and 0.0173 ± 0.00004 min^{-1} respectively.

TABLE OF CONTENTS

LIST OF TABLES

LIST OF FIGURES

ACKNOWLEDGEMENTS

Thanks to Dr. Gregory W. Harrington for his knowledge, support, encouragement, assistance and advising. I am fortunate to have an advisor who believed in me and allowed for me to explore my academic interests in the lab, within other departments, and projects not entirely engineering focused. I am also grateful to Dr. Christine K. Remucal for her guidance and support with various parts of my writing/editing and experimental approach with this project. I am extremely grateful and honored to have worked with Dr. Terence Barry and the AquaMost, Inc. family; thank you for providing me with an amazing project. Thank you to Katherine D. McMahon for spearheading the phenomenal team who recruited me to this university. I am thankful to Dr. Daniel R. Noguera for his patience and guidance throughout my graduate education.

I am especially grateful to the many colleagues who assisted with my projects, especially Rebecca Hoffman, Martin Collins, Keiva Coppage, Megan McConville, Matthew Russell, YiFan Li, and Nelson Chan.

A special thank you is reserved for my funding groups: National Science Foundation- Integrative Graduate Education and Research Traineeship – Certificate for Humans and the Global Environment, Graduate Engineering Research Scholars, National Science Foundation East Asia Pacific Summer Institute, Global Health Institute.

Thank you to the following people for being instrumental in my life and graduate education career: Nura Dualeh, Dr. Maria Teresa Velez, Dr. Andrew Huerta, Dr. Tong Zhang, Dr. Yang Xin, Raul Amavisca, Dr. Chris Choi, Dr. Sarina Ergas, Dr. Jonathan Patz, Dr. Robert Beattie, Carmela Diosana, Dr. Douglass Henderson, Kelly Burton, Dr. Adrienne Duke, Lorenzo T. Edwards Jr. Esq., Tarah Ausburn, Kelli Wimbley, Priscilla Nunez, Elienisse Rodriguez – Medina, Shannon Roberts, Dr. Edward Cole, Jesus Renteria, Jessica Williams, Dr. Rodolfo Perez, Evan Johnson, Malorie Teich, Fayana Richards, Cesar Martinez, Desiree Alva, Brian Nunez, Dr. Mary Fitzpatrick.

Finally, thank you to my brother, Cameron, and my mother Barbara Bowers. Your continuous love, support, and encouragement was/is extremely appreciated.

1. INTRODUCTION

Water quality in developing countries is a major concern of the United Nations and the World Health Organization (WHO). In 2001, WHO established a goal to both reduce, by half, the numbers for people who do not have access to improved water supply and to those without access to improved water supply and sanitary conditions (WHO, 2004). While this goal has been achieved, there remain 700 million people without access to improved water supply (WHO, 2013). Contaminated surface and ground water sources and poorly functioning water distribution systems contribute to the transmission of waterborne contaminants (Braghetta, 2006). Worldwide, 1.8 million people die every year from diarrheal disease (WHO, 2004).

While the issue of contaminated drinking water occurs on a much larger and rampant scale in developing countries, industrialized nations are not immune to waterborne contaminants or outbreaks. With the overall health concern for populations being exposed to drinking water contaminated with harmful bacteria, pathogens, and viruses, nations with available financial resources have invested in detection and treatment technologies to provide safe drinking water. Laws and regulations supplement treatment technologies by requiring water providers to deliver water based on established standards and regulations. Even with regulations and improved treatment methods, waterborne contaminants continue to be present. For the past 30 years, waterborne outbreaks in the United States are a result of emerging infectious diseases caused by microorganisms in the aquatic environment. In 1984, an outbreak of *Giardia* in treated drinking water in the town of McKeesport, PA forced a national dialogue around intrusive waterborne contaminants. As a result, Congress revised the Surface Drinking Water Act in 1986. In the revision, the USEPA was granted authority to write and revise water regulations such as the Safe Water Treatment Rule (NAP, 2005); the rule required that filtration be used and set minimum levels of disinfection for all surface water being treated. After a 1984 outbreak of *Cryptosporidium* in Carrolton, GA, and a 1993 outbreak in Milwaukee, WI, where 403,000 people were infected (MacKenzie, 1994), the Enhanced Surface Water Treatment Rules were established in 1994, 1998, 2000, and 2002 (revision). These rules were established after finding that pathogens entered drinking water systems through failure of conventional water treatment facilities that were designed to prevent breakthrough of the pathogen (Harrington, 2003).

After monitoring 82 surface water treatment plants in the United States, Aboytes (2004) showed that 1.4% of treated water samples were positive for infectious *Cryptosporidium*. From

the study, a risk of 52 infections per 10,000 people per year was calculated for surface water systems. This raised general concern, as the target set by the United States Environmental Protection Agency allows for a risk of 1 infection per 10,000 people per year (Aboytes, 2004). The majority (70%) of the positive filtered water samples occurred in waters with low turbidity, less than 0.1 nephelometric turbidity units (ntu). Twenty percent (20%) of the samples were from water with less than 0.05 ntu. This finding is in disagreement with the conclusion that turbidity removal is correlated with pathogen removal in conventional filtration plants (Nieminksi, 1992). However, the results are consistent with those of Xagoraraki (2004), who reported no correlation between pathogen removal and turbidity removal.

Not all water concerns are based on microbial contaminants and their associated outbreaks. With the increase in production and the manufacturing of goods that require synthetic dyes comes an increase of the presence of these dyes in environments outside of the manufacturing process. The demand for synthetic dyes accounts for $7x10^5$ metric tons of dyestuffs produced every year (Sahasivam, 2006), and upwards of 15% of that dye accounts as waste for non-production use (Daneshvar, 2005). Additionally, the widely accepted use of synthetic dyes to be used as coloring for drinks, food, candies, and sweets also contributes to demand. Large volumes are also wasted and disposed, untreated, to the environment where regulations are often times not enforced. Such locations primarily include China and India (Gleick, 2009). Often times, the waste and excess of beauty, health, electronic, and textile goods are disposed of improperly, where they eventually find their way to the natural environment (Flury, 1994).

One particular mode of contamination occurs through various waterways, where the dye is detected in trace amounts in water streams, groundwater, and lakes. In various geographic locations such as the United States, Germany, Switzerland, and France, there is a direct correlation between the presence of an industrial manufacturer using dye and the presence of dye in the water near the manufacturer (Travis, 2002). While the ingestion of these contaminants is deemed permissible, the effects of prolonged exposure, along with ingestion of a heterogeneous mixture of contaminants, have not been explored. Thus, it is important to investigate a drinking water treatment option that not only is able to treat one type of contaminant, but also can successfully treat a host of contaminants.

Nationally, as improvement over the past 30 years has occurred as a direct result of implementing several drinking water regulations, researchers continue to explore methods to provide the highest quality of water. One method for treatment is the use of advanced oxidation processes (AOPs), a group of technologies used to generate hydroxyl radicals for treating contaminated drinking water. One set of AOP methods involves the use of ultraviolet (UV) radiation to irradiate a titanium dioxide (TiO_2) semiconductor, producing hydroxyl radicals on the surface of the semiconductor. The hydroxyl radical, a powerful oxidant, is instrumental in inactivating waterborne pathogens and degrading synthetic dyes (Curtis, 2000; Saien, 2006). One alternative approach to combining UV and TiO_2 is with photoelectrocatalytic oxidation (PECO) systems. Studies using PECO reactors have been successful in degrading orange 16 dye (Roselin, 2011), brilliant orange (Wang, 2010), and methylene blue (Wen-Yu Wang, 2010).

Based on several research papers (Jain, 2008; Molot, 2003; Wawrzkiewicz, 2009; Sanchez-Martin, 2011; Yu, 2010; Aber, 2011; Saien, 2007, Yu, 2011, Gupta, 2011) it is clear that operational parameters have a significant effect on the removal and degradation of target contaminants by AOPs. Parameters include light intensity, recirculatioin rate, pH, contaminant concentration, catalyst concentration, applied voltage, and reactor design. These operational parameters affect the decolorization of dyes and inactivation of microbial contaminants due to hydroxyl radical production, ultraviolet irradiation, and chlorine production.

1.1. RESEARCH OBJECTIVES

The goal of this study was to demonstrate the use of PECO to degrade or inactivate the target contaminants of erioglaucine dye, tartrazine dye, and the waterborne pathogen *Cryptosporidium*.

The first objective of this research was to evaluate the ability of PECO to inactivate *Cryptosporidium parvum*, to evaluate the influence of recirculation rate on the rate of *Cryptosporidium* inactivation, and to compare PECO performance with that of UV, photocatalytic oxidation (PCO), and electrolysis. The second objective of this research was to evaluate the influence of operational parameters such as recirculation rate, chloride ion concentration, dye concentration, and applied voltage for the degradation of tartrazine, erioglaucine.

1.2. REFERENCES

Aber, S., H. Mehrizade, and A. R. Khataee (2011), Preparation of ZnS nanocrystal and investigation of its photocatalytic activity in removal of CI acid blue 9 from contaminated water, Desalination and Water Treatment, 28(1-3), 92-96.

Aboytes, R., G. D. Di Giovanni, F. A. Abrams, C. Rheinecker, W. McElroy, N. Shaw, and M. W. LeChevallier (2004), Detection of infectious Cryptosporidium in filtered drinking water, American Water Works Association Journal, 96(9), 88-98.

Braghetta A (2006) Drawing the connection between malnutrition and lack of safe drinking water in Guatemala. American Water Works 98: 97–106.

Curtis, T. P., G. Walker, G. M. Dowling, and P. A. Christensen (2002), Fate of Cryptosporidium oocysts in an immobilised titanium dioxide reactor with electric field enhancement, Water Research, 36(9), 2410-2413.

Daneshvar, N., D. Salari, A. Niaei, and A. R. Khataee (2006), Photocatalytic degradation of the herbicide erioglaucine in the presence of nanosized titanium dioxide: Comparison and modeling of reaction kinetics, Journal of Environmental Science and Health Part B-Pesticides Food Contaminants and Agricultural Wastes, 41(8), 1273-1290.

Flury, M., and H. Fluhler (1994), Brilliant Blue FCF as a dye tracer for solute transport studies – a toxicological overview, Journal of Environmental Quality, 23(5), 1108-1112.

Gleick, P.H. (2008). China and Water. *The World's Water*. Chapter 5.

Gupta, V. K., R. Jain, A. Nayak, S. Agarwal, and M. Shrivastava (2011), Removal of the hazardous dye-Tartrazine by photodegradation on titanium dioxide surface, Materials Science & Engineering C-Materials for Biological Applications, 31(5), 1062-1067.

Harrington, G. W., I. Xagoraraki, P. Assavasilavasukul, and J. H. Standridge (2003), Effect of filtration conditions on removal of emerging waterborne pathogens, Journal American Water Works Association, 95(12), 95-104.

Jain, R., and S. Sikarwar (2008), Photodestruction and COD removal of toxic dye erioglaucine by TiO(2)-UV process: influence of operational parameters, International Journal of Physical Sciences, 3(12), 299-305.

Mackenzie, W. R., et al. (1994), A massive outbreak in Milwaukee of *Cryptosporidium* infection transmitted through the public water supply, New England Journal of Medicine, 331(3), 161-167.

Molot, L. A., S. A. Miller, P. J. Dillon, and C. G. Trick (2003), A simple method for assaying extracellular hydroxyl radical activity and its application to natural and synthetic waters, Canadian Journal of Fisheries and Aquatic Sciences, 60(2), 203-213.

Nieminski, E. C., and J. E. Ongerth (1995), Removing Giardia and *Cryptosporidium* by conventional treatment and direct filtration, Journal American Water Works Association, 87(9), 96-106.

Roselin, L. S., and R. Selvin (2011), Photocatalytic Degradation of Reactive Orange 16 dye in a ZnO coated thin film flow photoreactor, Science of Advanced Materials, 3(2), 251-258.

Sadhasivam, S., S. Savitha, and K. Swaminathan (2007), Feasibility of using Trichoderma harzianum biomass for the removal of erioglaucine from aqueous solution, World Journal of Microbiology & Biotechnology, 23(8), 1075-1081.

Saien, J., and A. R. Soleymani (2007), Degradation and mineralization of Direct Blue 71 in a circulating upflow reactor by UV/TiO2 process and employing a new method in kinetic study, Journal of Hazardous Materials, 144(1-2), 506-512.

Sanchez-Martin, J., J. Beltran-Heredia, and M. T. Rodriguez-Sanchez (2012), Removal of Erioglaucine (Acid Blue 9) with a new coagulant agent from Acacia mearnsii tannin extract, Coloration Technology, 128(1), 15-20.

Travis, A. S. (2002), Contaminated earth and water: a legacy of the synthetic dyestuffs industry, Ambix, 49(1), 21-50.

Unites States Environmental Protection Agency. (2013). Surface Water Treatment Rules. *What do they mean to you?* water.epa.gov

Wang, W.-Y., M.-L. Yang, and Y. Ku (2010), Photoelectrocatalytic decomposition of dye in aqueous solution using Nafion as an electrolyte, Chemical Engineering Journal, 165(1), 273-280.

Wawrzkiewicz, M., and Z. Hubicki (2009), Removal of tartrazine from aqueous solutions by strongly basic polystyrene anion exchange resins, Journal of Hazardous Materials, 164(2-3), 502-509.

World Health Organization. (2013). Data and Statistics: Causes of Death 2002. http://www.who.int/

World Health Organization. (2013). Millennium Development Goals. http://www.who.int/

Xagoraraki, I., G. W. Harrington, P. Assavasilavasukul, and J. H. Standridge (2004), Removal of emerging waterborne pathogens and pathogen indicators by pilot-scale conventional treatment, Journal American Water Works Association, 96(5), 102-113.

Yu, C.-H., C.-H. Wu, T.-H. Ho, and P. K. A. Hong (2010), Decolorization of CI Reactive Black 5 in UV/TiO2, UV/oxidant and UV/TiO2/oxidant systems: A comparative study, Chemical Engineering Journal, 158(3), 578-583.

2. LITERATURE REVIEW

2.1. *CRYPTOSPORIDIUM PARVUM*

2.1.a *C. parvum* properties

Cryptosporidium parvum is a waterborne pathogenic organism that is known to infect humans through ingestion of water, causing cryptosporidiosis; this is a severe diarrheal and potentially fatal disease for the immunocompromised, elderly, and children (Messner, 2001). Dupont (1995) evaluated the ID_{50}, the dose that will infect 50% of the experimental group of healthy volunteers after ingestion of *Cryptosporidium* ranging from 30 to 1,000,000 oocysts. The study found that the ID_{50} for healthy adults was 132 oocysts, while the ID_{50} for immunocompromised adults was 9 to 30.

From 2009 to 2010, *C. parvum* accounted for 2 waterborne outbreaks in the United States (Pennsylvania and Vermont). During the same year, community water systems were accountable for 75.8% of the total number of waterborne outbreaks in the U.S. (CDC, 2013). The deadliest known U.S. waterborne outbreak of *C. parvum* occurred in Milwaukee in 1993. This outbreak infected 400,000 people, accounting for over 100 deaths (MacKenzie, 1994). While the conventional surface water treatment system was functional at the time of the outbreak, breakthrough of the oocysts through the filtration system was one of the main faults/causes of the outbreak (Fox, 1996). With the implementation of regulations, including three Enhanced Surface Water Treatment Rules, occurrences of outbreaks have decreased significantly (Brunkard, 2011).

The pathogen is an intercellular coccidian protozoan parasite found in animal stool, drinking water, and soils. The typical oocyst, the encysted stage of *C. parvum*, is spheroid in shape with a diameter of 4-7 μm, and is very resistant to conventional chemical treatment (rapid mix, flocculation, sedimentation, filtration, chemical disinfection). From a negative staining technique, the oocyst has been shown to have filamentous array (mesh) of the outer layer (Reduker, 1985). This layer, when exposed to trypsin, a digestive enzyme, can be degraded over time. Ultrasonication, the agitation of a liquid sample that is activated by sound waves and pressure creating sonic waves, shows that the rigorous movement has no effect on the structural integrity of the oocyst wall. Most forms of treatment focus on the treatment of the zoite stages, rather than the destruction of the oocyst wall (Reduker, 1985).

The oocyst wall consists of three protein rich layers, which provide protection and structural support for the sporozoites inside the oocyst. The inner layer is the layer with the most

durability, since the outer layer can be compromised with proteinase K without compromising the overall structure of the wall (Nina, 1992).

The life cycle is similar to other coccidians, with the infection beginning with the ingestion of oocysts. As shown in Figure 2-1, the oocyst enters the host, and attaches to the epithelial lining of the intestines (1). The oocyst wall opens, whether by wall compromise or intentional asexual reproduction (2). The sporozoites emerge from the oocyst (3), and attach to epithelial lining of the host's intestines (4) to begin asexual reproduction (5,6). Asexual reproduction occurs, producing a male (microgamonts) and female (macrogamonts) for sexual reproduction (7). The microgamonts and microgametes then reproduce (8) and eventually form a zygote (9). The zygote may propagate the infection or produce an oocyst that may be released to the environment (10).

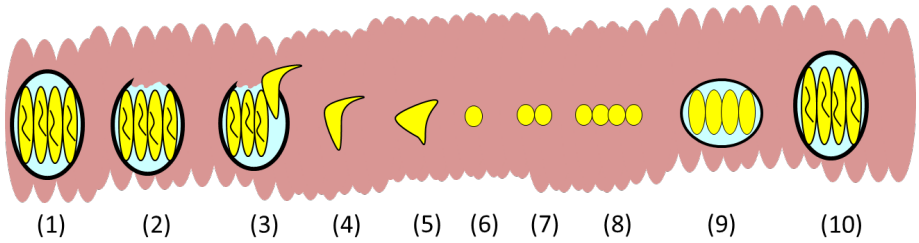

Figure 2-1: Life cycle of the *Cryptosporidium* oocyst in the epithelial lining of the host.

Reproducibility of the oocyst is compromised once the DNA and RNA structure of the sporozoite is destroyed, which is noted with the application of UV irradiation of the oocyst (Morita, 2002). Due to the recalcitrant nature of oocysts, Robertson (1998) conducted a study to determine the survival of oocysts in varying extreme environmental situations, and concluded that some oocysts were even able to survive in environments for 775 hours at -22°C. This recalcitrant nature of the oocysts was beneficial when determining the source of cryptosporidiosis from the Milwaukee outbreak; *Cryptosporidium* was detected in ice made during the time period of the water treatment plant failure (MacKenzie, 1994). Oocysts are also able to survive 4-6 days in water with chlorine levels of 1-3 mg/L (Robertson, 1992).

2.1.b *C. parvum* occurrence and treatment

In 1995, LeChevallier explored the potential for breakthrough of *Cryptosporidium* in water utilities that were compliant with the Surface Water Treatment Rule (SWTR), Long Term 1 Enhanced Surface Water Treatment Rule (LT1ESWTR) and Long Term 2 Enhanced Surface Water Treatment Rule (LT2ESWTR).

Out of the 66 water utilities evaluated, 22 were found to have breakthrough of *Cryptosporidium* with a mean concentration of 1.52 oocysts/100 liters. All 66 water utilities were in compliance with the aforementioned regulations. The systems where the most breakthroughs occurred included granular activated carbon and rapid sand filtration as their filtration method. Typical treatment measures for *Cryptosporidium* have included ozone, chlorination, UV, and coagulation.

Due to the sturdy nature of the oocyst wall, treatment via conventional disinfection processes has been rendered ineffective. Concentrations of chlorine required to penetrate the oocyst wall, or damage the structure, would be too toxic for human ingestion after treatment. Alternate treatment methods, such as UV irradiation, have been very effective at inactivating the oocyst when applied. The UV rays are able to penetrate through the oocyst wall, damage the DNA and RNA cellular structure of the oocyst, and prevent the reproduction of the oocyst in a host (Morita, 2002). However, the lack of residual disinfectant not provided by UV is a legitimate concern for water utilities. Despite the research and operational adjustments at water utilities, *Cryptosporidium* continues to break through and is present in drinking water.

In the Harrington (2003) study, to determine the effects of filter run time, loading rates, filter media, and pH on microorganism (*Cryptosporidium parvum* oocysts, *Encephalitozoon intestinalis* spores, enteropathogenic *E. coli*, *Aeromonas hydrophila*, and bacteriophage MS2) removal, turbidity was found to have a reduction of risk relating to pathogen breakthrough when there was a decrease of turbidity in the filter effluent. The conventional water treatment design included a rapid mix tank with alum coagulation, flocculation, sedimentation and filtration consisting of anthracite and sand. Coagulation at a lower pH value affects the overall removal of some pathogens and helps prevent the breakthrough of some pathogens (Harrington, 2003). Filtration rate and filter media type had no effect on pathogen removal. Influent concentrations were significantly high for each pathogen; for example, *Cryptosporidium* had an influent concentration of $1x10^5$ oocysts/L (Harrington 2003).

2.1.c Detection of *C. parvum* with Immunofluorescence Assay

The three most common assays for detection of *C. parvum* infectivity are cell culture with reverse transcriptase PCR (Rochelle, 1997), polymerase chain reaction, and immunofluorescence assay (IFA). Johnson (2012) conducted a study to determine which of these three assays produced the lowest frequency of false positives, highest reproducibility, and greatest sensitivity to accurate values; the IFA method was the highest performer of the three. IFA was a procedure developed for the detection of *C. parvum* oocysts in humans, animals, and bovine fecal smears (Stibbs, 1986). Subsequently, the method was modified to detect *C. parvum* in bodies of water (Ongerth, 1987). The modified method uses antiserum from rabbits, dyes to stain oocysts, and epifluorescence microscopy at x250 and x400 magnification to detect oocysts (Ongerth, 1987). The modification provided an effective alternative method to locate and identify low concentrations of oocysts, compared to the conventional staining methods of glass slide mounted materials (Ongerth, 1987).

Recent studies have investigated the use of a primary antibody specific for reproductive stages and a secondary fluorescein isothiocyanate-conjugated (FITC) anti-body, to detect infected foci (Slifko, 1997). Other studies (Schets, 2005, Bukhari 2006) investigated IFA's ability to detect infectious *C. parvum* oocysts grown in cell culture. When compared to neonatal mouse infectivity assays, the original gold standard of infectivity analysis, the viability of the oocysts were often comparable (Rochelle, 2002). Knowing the infectivity of oocysts is the key component of calculating risk for individuals (Aboytes, 2004).

The current assay requires use of HCT-8 monolayers to support the treated oocysts (Upton, 1995). Sterilized oocysts were applied on the monolayers of HCT-8 cells, with the intention of determining the best medium supplements to support *C. parvum* development on the HCT-8 cells. The growth of the parasite, on the HCT-8 cell with the specified supplement, is determined by counting the stages under a microscope. The ideal medium contains RPMI 1640, 10% fetal bovine serum, HEPES, glucose, ascorbic acid, folic acid, aminobenzoic acid, calcium pantothenate, insulin, penicillin, streptomycin, and amphotericin. This method was developed as a simple and reproducible method for viable and surface sterilized oocysts *in vitro*.

2.1.d Chemical Disinfectants

2.1.d.1 Chlorine

While chlorine is a common disinfectant used for drinking water treatment (WHO, 2010), its use does not result in a complete alleviation of drinking water concerns. "*Cryptosporidium* are extremely resistant to common disinfectants (Campbell, 1982);" it is highly resistant to typical concentrations of chlorine, even when chlorine is applied at concentrations toxic to humans (Peeters, 1989). Ruffell (1998) analyzed chlorine dioxide (0.4 to 2.0 mg/L) as a disinfectant for Iowa strain *Cryptosporidium parvum* oocysts (4 to 5 x 10^6 oocysts/mL), and reported that a CT of 20 to 1000 mg min/L achieved 6-log inactivation. Campbell (1982) discovered that two hours of chlorine disinfectant incubation, at concentrations typical in drinking water (0.2 to 1.0 mg/L), had no effect on oocyst inactivation. Quinn (1993) reported that viability of oocysts was not reduced when exposing oocysts to 2.5 and 5 mg/L of chlorine, with a CT of 75 and 150 mg min/L respectively. A study in 2010 (Zhi, 2013) demonstrated that treatment conditions of pH 7, 6.3 mg/L of chlorine, and treatment time of 360 minutes, achieved 99% reduction of *Cryptosporidium* with an initial concentration of 1 x 10^6 oocysts/mL. There is a significant increase in required CT with a modest decrease in temperature for inactivation of *Cryptosporidium* (King, 2007; Zhi, 2013). However, oocysts are extremely resistant to a host of environmental factors, including, but not limited to, freezing, dessication, disinfectants, and man-made chemicals. Due to their resistant nature, the oocysts are able to survive in a plethora of natural and engineered environments.

2.1.d.2 Ozone

Various disinfection processes have been studied for the purpose of replacing the current wide use of chlorine as the primary disinfectant agent. Free chlorine and chloramines, the most widely used disinfectants in the world (WHO, 2012), are not effective at inactivating *Cryptosporidium*. Korich (1990) compared the treatment methods of ozone (1 mg/L at 5 minutes), chlorine dioxide (1.3 mg/L at 60 minutes), chlorine (80 mg/L at 90 minutes), and chloramines (80 mg/L at 90 minutes), finding that inactivation of *Cryptosporidium* occurred most in ozone and chlorine dioxide; 1 log removal at initial concentration of 2.8 x 10^5 oocysts/mL.

Ozone, as a primary disinfectant is effective; however, the lack of residual concentration in the bulk water to continue treatment as water travels through the distribution system prevents ozone from being used more universally. Ozone and UV are the primary alternative disinfection agents, but cost and maintenance have prevented both options from becoming wide spread applications.

2.1.d.3 Synergistic Treatment

A Corona-Vasquez study (2002) analyzed inactivation through synergistic treatment methods with ozone as the primary disinfectant, followed by free chlorine as the secondary disinfectant. Based on previous studies that showed a significant dependence on temperature and inactivation kinetics, the temperature (1 to 20°C) was also tested for its contribution to inactivation. The variability of inactivation kinetics, amongst different lots and *in-vitro* excystation were also tested. The concentration of dissolved ozone was 0.45 to 4.83 mg/L for primary disinfection. For secondary disinfection, 0.45 to 3.78 mg/L of free chlorine was used. A pH of 6.0 was monitored to ensure that the free chlorine was mostly in the form of hypochlorous acid. Experiments were performed in a batch reactor, where *in vitro* mouse assays were used to detect infectivity. Varying oocyst lots did indeed have an effect on the inactivation efficiency, regardless of concentration, synergy, pH, and temperature; age of oocysts was also a factor. Ozone pretreatment also increased the efficacy of chlorine treatment up to 6x the original level.

The Surface Water Treatment Rule was established to regulate enteric viruses and *Giardia lamblia*. However, the CT values for treating viruses and *Giardia* are much lower than what is required for the inactivation of *Cryptosporidium*. Because of this, new treatment technologies/configurations must be analyzed, in order to effectively remove, degrade, or inactivate *Cryptosporidium* from drinking water. Rennecker (1999) also analyzed the use of ozone, free chlorine, monochloramine and their synergistic effects on the inactivation of *Cryptosporidium* in a semi-batch reactor, with operational conditions of dissolved oxygen (0.35 to 1.0 mg/L), temperature (4 to 20°C), pH 6 to 8, and oocyst doses of 7×10^5. Synergistic approach to inactivation of *Cryptosporidium* was much more effective than using one treatment method as the primary method. To achieve 2-log inactivation, the required CT for monochloramine was 11,000 mg·min/L, and free chlorine 2500 mg·min/L. When used in

conjunction with ozone as the primary disinfectant (at 1.4 mg·min/L), CT for monochloramine and free chlorine decreased to 1000 and 900 mg·min/L respectively.

2.1.d.4 Ultraviolet (UV) Irradiation

Based on previous studies (Amoah, 2005; Zimmer, 2003; Linden 2001; Shin, 2001), medium pressure (MP), 1 kW, UV lamps provided 0.4 to 2 log inactivation of *Cryptosporidium* at low doses of 2 mJ/cm^2. Low pressure (LP) (30W) lamps are practical, and widely used, due to "availability, cost, ease of use, and measurement of UV output." Craik, (2001) demonstrated that the use of UV has been effective at other wavelengths aside from the standard 254 nm provided by LP UV lamps. Wavelengths of 245 to 275 nm achieved the highest log inactivation (1.8 to 2.3) for the range studied. The absorption of UV by *Cryptosporidium* DNA results in the compromise of the nuclei, rendering the microorganism incapable of reproducing itself (Morita, 2002) Using the range of wavelengths (245 to 275 nm), there is no significant difference between LP and MP in the inactivation of *Cryptosporidium*.

Two-log inactivation of *Cryptosporidium* was observed when using a LP UV light, applying a dosage of 9,000 mWs/cm^2; the inactivation was observed through DAPI/PI staining (Campbell, 1995). Nucleic acids stains may be used for quantifying damaged oocysts that were treated by ozone, chlorine, and chlorine dioxide (Belosevic, 1997). However, nucleic staining is not applicable for oocysts treated by UV irradiation; the UV damages the DNA structure of the oocysts, rather than the physical morphology of the oocysts (Morita, 2002). Additionally, other studies (Clancy 1998, Bukhari 1999) found that the correlation of infected oocysts using *in vivo* and *in vitro* assays was not strong, and therefore considered nullified. Mouse infectivity studies and immunofluorescnce assays are reliable methods to analyze infectivity in oocyst samples (You, 1996; Shin, 2001). When using UV as part of an enclosed configuration of a reactor, as opposed to med/low pressure mercury lamp with an open plastic Petri dish exposure, a significant difference in inactivation occurs; 4 log vs. 0.6 log inactivation for identical UV output and dose. Low doses of UV (1 mJ/cm^2) achieved 3.4 to 4.0 log inactivation of *Cryptosporidium*.

The advantages of using UV to inactivate *Cryptosporidium* are:

- Highly effective with inactivation
- No additional chemical required

- Short contact times
- No regulated byproducts

The disadvantages of using UV to inactivate *Cryptosporidium* are:

- Difference in output for each UV lamp
- Cannot measure lamp dose
- Interference by turbidity
- No lasting residual disinfectant

2.2. DYE CONTAMINANTS

2.2.a. Introduction

Many of the dyes used in the textile industry are azo (-N=N-) dyes, which are water soluble, toxic, and nonbiodegradable. These include the tartrazine and erioglaucine dyes used in this study. Dyes can be among the most difficult contaminants to remove using conventional wastewater treatment plants (Delee, 1998) or using oxidation, coagulation, membrane technology, and biological treatment (Jain, 2008). Because of the recalcitrant characteristic of these dyes during conventional treatment, AOP have been explored as a treatment option (Daneshvar, 2004). Unfortunately, the treatment of contaminated water using AOP requires lengthy treatment times (> 3 hours) to remove the target dye (Mittal, 2006; Jain, 2008, Sanchez-Martin; 2011).

Methylene blue (Franke, 1999; Houas, 2001), malachite green (Chen, 2007), indigo/indigo carmine (Vautier, 2001), Reactive Orange 84 (Rao, 1998), erioglaucine (Jain, 2008), and Direct Blue 71 (Saien, 2007) have all been degraded using the AOP of TiO_2/UV, with TiO_2 in the anatase form. However, the kinetics vary with the configuration of the operational system in place. The most extensive study of azo dye degradation compared the degradation of eight dyes using the UV/TiO_2 treatment technique (Gonçalves, 1999). The operational parameters had the most effect on the degradation, rather than the dye type/characteristic itself.

2.2.b. TARTRAZINE (FD&C Yellow 5)

Tartrazine is a water soluble, yellow synthetic dye, with a maximum absorbance wavelength of 426 nm, and is used in a variety of products such as clothing, food, and paint; It is

also used as a component of Aquashade®. Tartrazine can safely be consumed at 7.5 mg kg^{-1} day^{-1}, based on studies showing that subcutaneous injection in mice yielded an acute LD_{50} of 2000 mg/kg and that oral ingestion by rats yielded an acute LD_{50} of 12,750 mg/kg (JECFA, 1964). Acute fish toxicity was determined at an LC_{50} of 1.14 x 10^{14} mg/L (USEPA, 2000). In 2013, Shawish published a study to determine the concentration of tartrazine in food products. The research was motivated by information that tartrazine is known to cause asthma attacks and urticaria, a skin rash caused by allergic reaction, in children at 50 mg/day. Ingestion of tartrazine may result in the development of lupus, thyroid cancer, migraines, and eczema in humans in dosages of 20 mg/day (Mittal, 2006).

Regarding treatment, Ghezzar (2013) focused on the use of Dielectric Barrier Discharge, coupled with TiO_2 as a semiconductor, to mineralize and discolor tartrazine solutions. Wawrzkkiewicz (2009) investigated the use of polystyrene anion exchange resins to adsorb tartrazine from water streams polluted by textile, food processing, and paper factories. Another resin, melamine – formaldehyde – tartaric acid resin, has been shown to remove tartrazine through adsorptive mechanisms as well (Baraka, 2012). Adsorptive media, such as rice, peanut hull, orange peel, and fly ash (Wawrzkiewicz, 2009) have been explored for their use in removal of tartrazine from water.

While studies have been successful in the removal of tartrazine using anion exchange resins (Wawrzkiewicz, 2009), methods involving post treatment remediation also becomes a concern. Typically when an adsorbent or coagulant is used, there is concern about the secondary removal of the contaminant to the adsorbent. Thus, exploration of alternative technologies, where the secondary removal is not a concern, was greatly needed.

Oancea (2014) was able to achieve a 30% degradation rate of tartrazine at an initial concentration of 1.035 x 10^{-5} M, with an irradiation time of 60 minutes, using UV alone. With the addition of the photocatalyst TiO_2, Gupta (2011) showed that use of the anatase form of TiO_2 at 0.02 g/L, pH 11, and 30°C achieved 96% degradation in 40 minutes of treatment. Gupta (2011) and Oancea (2013) also reported 60-minute UV/H_2O_2 treatment times to achieve tartrazine degradation of 94% and 83% for initial concentrations of 6 x 10^{-5} M and 1.03 x 10^{-5} M, respectively.

2.2.c. ERIOGLAUCINE (FD&C Blue 1)

Erioglaucine is an anionic synthetic dye that has a blue color, a maximum absorbance wavelength of 630 nm, a low octanol-water coefficient, and a half-life of two months. It is stable in the dark, but susceptible to degradation when treated with hydroxyl radicals (Molot, 2003). Erioglaucine can be seen, without visual detection equipment, at concentrations as low as 1 mg/L (Sadhasivam, 2007). Erioglaucine is also component of Aquashade®. The dye is also used in a host of industrial processes, such as textile, paper, printing, and photography production. Other uses include chemical coloring in toilet bowl cleaners, agriculture, indicator stains for biological research, cakes, dry mix beverages, and pharmaceuticals. These additional applications provide more opportunity for erioglaucine to be introduced to the natural environment via production waste or improper disposal.

With respect to the use in food, erioglaucine is used strictly for the appearance of processed foods and is commonly used to restore food colors that are lost to food processing, achieving uniformity of products for consumer appeal (Sabnis, 2010). The dye adds no nutritional value or taste to the food to which it is added. Fortunately, there are no reports of carcinogenicity or mutagenicity when administered to rats and other rodents (Sabnis, 2010). Subcutaneous injection in mice has yielded an acute LD_{50} of 4600 mg/kg while oral ingestion by rats has yielded an acute LD_{50} of 2000 mg/kg (USEPA, 2005). All erioglaucine consumed by rats was completely excreted in the feces. An acute LC_{50} of 3000 mg/L has been reported for fish and amphibians. Because of the low toxicity, the Federal Drug Administration has approved its use in foods, drugs, and cosmetics (Sabnis, 2010).

There is literature to suggest effective methods to treat water contaminated with erioglaucine. For example, one study used the fungus *Trichoderma harzianum* for 88% removal of erioglaucine in a batch reactor (Sadhasivam, 2006). The dyes adsorb to the surface of the biomass, thus removing the dye from the water. However, secondary treatment must now be applied to the biomass; the contaminant has been removed from the system, but not completely treated to mineralization. Tannins, a water soluble polyphenolic compound derived from trees, have been shown to be an effective coagulant to treat erioglaucine (Sanchez-Martin, 2011). Sanchez Martin explored the use of tannins from *Schinopsis balansae, Casanea sativa, and Acacia meansii* as sources of tannin coagulant. The tannins were effective at the removal of erioglaucine with optimal doses of 50 mg/L. While not practical for everyday use, the batch

reactor, with 200 mg/L of the coagulant, achieved 80% dye removal when the pH was less than 5.

2.2.d. AQUASHADE®

Aquashade® is a blend of tartrazine (2.39% of Aquashade® mass) and erioglaucine (23.64% of Aquashade® mass) dyes, and it is used as an aquatic growth inhibitor. As a photosystem II pigment, Aquashade® blocks spectrum wavelengths which are required by aquatic plant life (Spencer 1984). Because of the lack of natural degradation after application, users are instructed to only use Aquashade® for recreational or fully contained bodies of water. There are several first aid response instructions for accidental ingestion, skin contact, or exposure to the eye of Aquashade® in the concentrated bottled form (MSDS, 2013).

Because of the application of the dye to bodies of water, studies have investigated the abundance of food supply available to aquatic animal life once Aquashade® has been applied. According to Ludwig (2010), use of the dye is not detrimental to the aquatic animal life relying on the Aquashade®-treated water, at concentrations more than 2X the recommended dose of 2 mg/L. To date, much of the research regarding Aquashade® has focused on the effect of its application on various aquatic ecosystems (Spencer, 1984; Ludwig, 2010; Bristow 1996; Manker, 1984).

2.3 ADVANCED OXIDATION PROCESSES

Advanced oxidation processes (AOP) are beneficial for treating contaminants that are typically not removed, disinfected, or inactivated by conventional water treatment processes such as biological or physical-chemical technologies. Typically, AOP involves the use of ozone/OH^-, ozone/UV, ozone/H_2O_2, H_2O_2/UV, UV/TiO_2 (photocatalysis), H_2O_2/Fe(II), or H_2O_2/Fe(III) (Fenton Reaction) for hydroxyl radical production. The effective component of AOP is the generation of hydroxyl radicals ($^{\bullet}OH$; Equations 2-1 through 2-8).

This study focuses on the use of UV/TiO_2 (photocatalysis) for hydroxyl radical generation. When a TiO_2 catalyst is exposed to ultraviolet irradiation, holes (h^+_{vb}) are generated in the valence band of the TiO_2 catalyst and electrons (e^-_{cb}) exist in the conduction band (Equation 2-1) (Hoffmann, 1995). The oxygen in the bulk water accepts an electron to form the moderately reactive superoxide ($O_2^{\bullet-}$, Equation 2-2). The superoxide accepts another electron

along with two protons (H^+) to form hydrogen peroxide (H_2O_2, Equation 2-3). Reactions of hydrogen peroxide with superoxide produce hydroxyl radicals ($^{\bullet}OH$), hydroxide ions (^{-}OH), and oxygen (O_2) (Equation 2-4). The further reactions of irradiation of hydrogen peroxide by UV create more hydroxyl radicals in the bulk water (Equation 2-9) (Jakob, 1993). Some hydroxyl radicals combine to create more hydrogen peroxide.

$$TiO_2 \xrightarrow{hv} TiO_2\left(h_{vb}^{+} + e_{cb}^{-}\right) \quad \text{(Equation 2-1)}$$

$$O_2 + e_{cb}^{-} \longrightarrow O_2^{\bullet -} \quad \text{(Equation 2-2)}$$

$$O_2^{\bullet -} + e_{cb}^{-} + 2H^{+} \longrightarrow H_2O_2 \quad \text{(Equation 2-3)}$$

$$O_2^{\bullet -} + H_2O_2 \longrightarrow {}^{\bullet}OH + OH^{-} + O_2 \quad \text{(Equation 2-4)}$$

$$e_{cb}^{-} + H_2O_2 \longrightarrow {}^{\bullet}OH + OH^{-} \quad \text{(Equation 2-5)}$$

$$h_{vb}^{+} + OH^{-} \longrightarrow {}^{\bullet}OH \quad \text{(Equation 2-6)}$$

$$h_{vb}^{+} + H_2O \longrightarrow H^{+} + {}^{\bullet}OH \quad \text{(Equation 2-7)}$$

$$2\,{}^{\bullet}OH \longrightarrow H_2O_2 \quad \text{(Equation 2-8)}$$

$$H_2O_2 \xrightarrow{hv} {}^{\bullet}OH + {}^{\bullet}OH \quad \text{(Equation 2-9)}$$

These $^{\bullet}OH$ have a high oxidizing potential (2.8 V), with the potential to transform many organic pollutants such as pesticides, dichloroacetic acid, phenol, and organo-halogenated compounds into CO_2, H_2O, and inorganic residues. For laboratory settings, hydroxyl radicals have been a key component in degrading dyes (Molot, 2003) and inactivating microorganisms (Cho, 2010).

Bicarbonate, carbonate, and dissolved organic matter (DOM) are known to act as hydroxyl radical scavengers, which means that they consume hydroxyl radicals that are intended to oxidize a target contaminant. Hydroxyl radicals oxidize DOM, decreasing both the concentration of hydroxyl radicals and DOM when reaction between the constituents, while producing organic byproducts in the process (Page, 2013). The reaction between hydroxyl radicals and bicarbonate occurs with a rate constant of 8.5 x 10^6 $M^{-1}s^{-1}$, and the reaction between hydroxyl radicals and carbonate occurs at a rate constant of 4.2 x 10^8 $M^{-1}s^{-1}$. The pH of the

solution determines the concentrations of carbonate and bicarbonate. At pH below 6.3, carbonic acid is the dominant form of dissolved inorganic carbon whereas at pH above 10.3, carbonate is the dominant form. Bicarbonate is the dominant form between these two pH values.

2.3.c.1 Ultraviolet Irradiation and Titanium Dioxide

Titanium dioxide is a widely used catalyst, due to its low cost, stable nature, and high photoreactivity when exposed to UV. The use of titanium dioxide has shown potential, in conjunction with UV, for the inactivation of coliform bacteria and viruses in water supply and wastewater effluents (Shang, 2009, Rizzo 2009, Rahmani 2011). The most common pairing of semi-conductor and light source is TiO_2 and UV at 356 nm (Maness, 1999). When the UV light is applied to the TiO_2 surface, electrons are promoted from the valence band to the conduction band. As the electrons move from lower energy states to higher energy states, their absence in the valence band leaves a hole in the valence band. If the mobile electron does not get moved away from the valence band by an electrical current or does not bind with an electron acceptor within nanoseconds, the electron then recombines with a hole in the valence band (Hoffmann 1995, Maness 1999, Chen 2004, Li 2010, Ryu 2008).

If the system is successful at preventing electron-hole recombination, one route for hydroxyl radical generation is the reaction of hydroxide with holes at the surface of the TiO_2 (Equation 2-6). However, as demonstrated in Equations 2-1 through 2-8, other routes of hydroxyl radical generation are also possible. Hydroxyl radicals are the primary oxidant in the aqueous phase of the photocatalytic system. This generation of hydroxyl radicals allows for redox reactions to occur within the bulk water phase or within the mass transfer layer between the surface and the bulk water.

2.3.c.2. Photocatalytic Oxidation (PCO)

With the powder or anatase form of TiO_2, a slurry can be created as the catalyst for reactions within the system. Research has shown effective use of a TiO_2 slurry for bactericidal treatment and dye treatment, but the slurry must be filtered/removed from the bulk water once the experiment is complete (Matsunaga 1988, Maness 1999).

With TiO_2, the semiconductor is used in several physical forms. Regardless of the form of TiO_2 (e.g., rutile, anatase), if it is attached to other media such as glass beads, coated tubes,

and silica-based material, the hydroxyl radicals are generated on the surface of the irradiated TiO_2 (Mills 2007). The distance of the bulk water contaminant from the surface of the TiO_2, where the hydroxyl radicals are generated, affects the degradation kinetics of the target contaminant. Degradation kinetics decrease as the distance of the contaminant increases from the surface catalyst (Egerton, 2006). This is what makes suspended particles more attractive to implement for treatment, compared to a TiO_2 coated surface. With this case, the suspended TiO_2 catalyst is evenly dispersed throughout the bulk water, therefore increasing the likelihood that the target contaminant would come into contact with hydroxyl radicals. However, the photon flux is more attenuated with suspended particles and, thus, the suspended particles of TiO_2 furthest from the UV lamp might be poorly illuminated. In addition, the added step of filtering the suspended catalyst particles makes it a less desirable option for the degradation of target contaminants. The surface reaction rate between hydroxyl radicals and contaminants is higher than the diffusion rate of hydroxyl radicals in the bulk water solution; the hydroxyl radical does not diffuse far in to the solution. The reaction between hydroxyl radicals and contaminants must occur within nanoseconds of contact, else recombination of electrons to their hole pair occurs while releasing heat in the process (Hoffman, 1995).

The presence of electron acceptors such as O_2 and H_2O_2 in the bulk water is important, or the holes on the surface of the catalyst would recombine with electrons from the conduction band and prohibit degradation from taking place. In order to achieve optimal degradation, the prevention of the recombination of electron-hole pairs is desirable.

Immobilization of the semi-conductor can be achieved by using a TiO_2 coated material, to reduce the need for filtration or sedimentation after treatment. Unlike many other experiments using TiO_2 as the semiconductor, Mills (2007) used a TiO_2 coated glass mesh, instead of a TiO_2 slurry to serve as the catalyst for photocatalysis. As previously stated, the use of this technology in water treatment has been applied for inactivation of *E. coli*, MS2, and *Cryptosporidium* and the degradation of dyes.

2.3.c.3 Photoelectrocatalytic Oxidation (PECO)

Some of the challenges posed by the use of photocatalytic oxidation are: (1) slurries need filtration after use, (2) electron-hole recombination rates are high, and (3) costs for operation are high. While the activation of the TiO_2 is effective only so far as much as there is UV presence,

the addition of an applied electrical bias to an immobilized TiO_2 surface reduces the rate of electron-hole recombination; this is photoelectrocataytic oxidation (PECO). Because the device is connected to the applied voltage, electrons are transferred through the electrical current to the cathode surface. This abundance of electrons on the cathode surface allows for reduction reactions to occur with aqueous-phase substances at the surface. A reactor system with an anode, a cathode, a titanium dioxide film, a UV lamp, and a potentiostatic electrical current, can now be used as the reactor. Reactions no longer need to occur within the first nanoseconds, because electrons are continually shuttled away from the valence band by the electric current, allowing oxidation reactions to occur between aqueous-phase substances and electron holes at the anode surface.

Because of its potential for superior treatment, variations of PECO have been studied for inactivation, removal, and degradation of a host of contaminants: MTBE (Wu, 2011), Gram-negative bacteria (Li, 2013), and bio-particulates (Markowska-Szczupak, 2011). The use of PECO is effective for the degradation of dyes, but the intermediates can take longer to degrade within the same reactor (Egerton, 2010). Studies using photoelectrocatalytic reactors as a dye removal device have been successful in reporting the degradation of the following reactive dyes: Orange 16 dye (Roselin, 2011), Brilliant Orange (Wang, 2010), and Methylene Blue (Wang, 2010).

PECO has proven to be more efficient of an advanced oxidation process application. For example, PCO only achieved 1-log inactivation of *C. parvum* compared to that of 6-log with PECO in a treatment time of 10 minutes, with a direct relationship between the increase of applied voltage and the increase of the reaction rate (Baram, 2009). With the lower applied bias, the quick recombination of the electron hole, similar to that of photocatalysis, prevents the mechanism from being applied.

Results from the experiment also indicated that the configuration of the reactor has a great effect on the efficiency of removal/degradation. PECO can be more effective at treatment, but can be prevented from maximum efficiency based on the design of the distance between the bulk phase, electrodes, and the UV light in the reactor. The effectiveness of the device relies heavily on the design of the reactor, also by the thickness of the bulk water phase, and the type of contaminant being analyzed (Egerton, 2010).

2.4 PHOTOLYSIS OF WATER

While most research involving the use of UV focuses on the direct impact the germicidal technology has on treating microorganisms, another method of treatment is available with a shorter irradiation wavelength. At wavelengths of 136 nm to 185 nm, UV is absorbed by water molecules causing the homolysis of water molecule to produce hydrogen atoms and hydroxyl radicals (Jakob 1993, Crovisier 1989, Weeks 1963) (Equation 2-10).

$$H_2O \xrightarrow{h\nu} \frac{1}{2} H_2 + {}^{\bullet}OH$$

Equation 2-10

The use of photolysis, and subsequent use of hydroxyl radicals, to treat contaminants requires the use of a medium-pressure lamp that can produce wavelengths short enough to split the water molecule; low pressure lamps only emit wavelengths of 254 nm, while medium pressure lamps emit wavelengths of 180 nm to 410 nm (Craik, 2001). Manufacturing of the germicidal low-pressure UV lamp has widespread implementation, as it is an effective treatment option for water disinfection (Shang, 2009, Rizzo 2009, Rahmani 2011).

2.5 ELECTROLYSIS OF WATER

Researchers have also explored the use of electrochemistry to inactivate target contaminants in water. Electrochemistry, as a treatment option, involves the charge transfer between a semiconductor, such as TiO_2, and the reaction between electrolytes in the bulk water. Electrolysis may either occur by an oxidant being produced on the surface of the anode within the reactor, or by electron transfer between electrode surface and the targeted contaminant (Grimm 1998, Li 2010). The decomposition of water to H_2 and O_2 may occur when a potential of more than 1.23 V is applied between electrodes (Fujishima, 1972). It is in the bulk water system that the presence of hydroxyl radicals assists in electrochemical oxidation of target contaminants into water and CO_2 (Grimm, 1988).

The bulk of electrochemistry research details the use an additive (i.e. Fenton Reagent) to facilitate generation of hydroxyl radicals within the system (Oturan 2000). Cong (2007) used Na_2SO_4 as an electrolyte additive to assist in conductivity, where hydroxyl radicals were generated in the bulk water system after applying a voltage of 7.5 V for 2 minutes (Cong, 2007).

Limited research has focused on only using electrolysis without an additive to produce hydroxyl radicals. Kesselman (1997) generated hydroxyl radicals on the surface of TiO_2, with the sole use of current at 1.0 mA. The [OH] on the surface of the TiO_2 was calculated to be 1.6×10^{-13} mol cm^{-2}. The use of only applied voltage reduces the need for a light source (i.e. UV) to generate hydroxyl radicals with a system.

2.6 REFERENCES

Aboytes, R., G. D. Di Giovanni, F. A. Abrams, C. Rheinecker, W. McElroy, N. Shaw, and M. W. LeChevallier (2004), Detection of infectious Cryptosporidium in filtered drinking water, American Water Works Association Journal, 96(9), 88-98.

Amoah, K., S. Craik, D. W. Smith, and M. Belosevic (2005), Inactivation of Cryptosporidium oocysts and Giardia cysts by ultraviolet light in the presence of natural particulate matter, Journal of Water Supply Research and Technology-Aqua, 54(3), 165-178.

Baraka, A. (2012), Adsorptive removal of tartrazine and methylene blue from wastewater using melamine-formaldehyde-tartaric acid resin (and a discussion about pseudo second order model), Desalination and Water Treatment, 44(1-3), 128-141.

Baram, N., D. Starosvetsky, J. Starosvetsky, M. Epshtein, R. Armon, and Y. Ein-Eli (2011), Photocatalytic inactivation of microorganisms using nanotubular TiO2, Applied Catalysis B-Environmental, 101(3-4), 212-219.

Belosevic, M., R. A. Guy, R. TaghiKilani, N. F. Neumann, L. L. Gyurek, L. R. J. Liyanage, P. J. Millard, and G. R. Finch (1997), Nucleic acid stains as indicators of Cryptosporidium parvum oocyst viability, International Journal for Parasitology, 27(7), 787-798.

Bristow, B. T., R. C. Summerfelt, and R. D. Clayton (1996), Comparative performance of intensively cultured larval walleye in clear, turbid, and colored water, Progressive Fish-Culturist, 58(1), 1-10.

Brunkard, J. M., Ailes, E., Roberts, V.A., Hill, V., Hilborn, Elizabeth. (2011), Surveillance for Waterborne Disease Outbreaks Associated with Drinking Water-United States, 2007-2008, Morbidity and Mortality Weekly Report, 60(SS12, Suppl. S), 38-75.

Bukhari, Z., D. M. Holt, M. W. Ware, and F. W. Schaefer, III (2007), Blind trials evaluating in vitro infectivity of Cryptosporidium oocysts using cell culture immunofluorescence, Canadian Journal of Microbiology, 53(5), 656-663.

Bukhari, Z., T. M. Hargy, J. R. Bolton, B. Dussert, and J. L. Clancy (1999), Medium-pressure UV for oocyst inactivation, Journal American Water Works Association, 91(3), 86-94.

Campbell, A. T., L. J. Robertson, and H. V. Smith (1992), Viability of *Cryptosporidium parvum* oocysts – coorelation of invitro excystation with inclusion or exclusion of fluorogenic vital dyes, Applied and Environmental Microbiology, 58(11), 3488-3493.

Campbell, A. T., L. J. Robertson, M. R. Snowball, and H. V. Smith (1995), Inactivation of oocysts of *Cryptosporidium parvum* by ultraviolet irradiation, Water Research, 29(11), 2583-2586.

Campbell, I., S. Tzipori, G. Hutchison, and K. W. Angus (1982), Effect of disinfectants on survival of *Cryptosporidium* oocysts, Veterinary Record, 111(18), 414-415.

Centers for Disease Control and, P. (2013), Surveillance for waterborne disease outbreaks associated with drinking water and other nonrecreational water - United States, 2009-2010, MMWR. Morbidity and mortality weekly report, 62(35), 714-720.

Chen, C. C., P. X. Lei, H. W. Ji, W. H. Ma, J. C. Zhao, H. Hidaka, and N. Serpone (2004), Photocatalysis by titanium dioxide and polyoxometalate/TiO2 cocatalysts. Intermediates and mechanistic study, Environmental Science & Technology, 38(1), 329-337.

Cho, M., E. L. Cates, and J.-H. Kim (2011), Inactivation and surface interactions of MS-2 bacteriophage in a TiO2 photoelectrocatalytic reactor, Water Research, 45(5), 2104-2110.

Clancy, J. L., T. M. Hargy, M. M. Marshall, and J. E. Dyksen (1998), UV light inactivation of Cryptosporidium oocysts, Journal American Water Works Association, 90(9), 92-102.

Cong, Y., Z. Wu, and Y. Li (2007), Hydroxyl radical electrochemically generated with water as the complete atom source and its environmental application, Chinese Science Bulletin, 52(10), 1432-1435.

Corona-Vasquez, B., J. L. Rennecker, A. M. Driedger, and B. J. Marinas (2002), Sequential inactivation of Cryptosporidium parvum oocysts with chlorine dioxide followed by free chlorine or monochloramine, Water Research, 36(1), 178-188.

Craik, S. A., D. Weldon, G. R. Finch, J. R. Bolton, and M. Belosevic (2001), Inactivation of Cryptosporidium parvum oocysts using medium- and low-pressure ultraviolet radiation, Water Research, 35(6), 1387-1398.

Crovisier, J. (1994), Photodestruction rates for cometary parent molecules, Journal of Geophysical Research-Planets, 99(E2), 3777-3781.

Daneshvar, N., D. Salari, A. Niaei, and A. R. Khataee (2006), Photocatalytic degradation of the herbicide erioglaucine in the presence of nanosized titanium dioxide: Comparison and modeling of reaction kinetics, Journal of Environmental Science and Health Part B-Pesticides Food Contaminants and Agricultural Wastes, 41(8), 1273-1290.

Delee, W., C. O'Neill, F. R. Hawkes, and H. M. Pinheiro (1998), Anaerobic treatment of textile effluents: A review, Journal of Chemical Technology and Biotechnology, 73(4), 323-335.

Dupont, H. L., C. L. Chappell, C. R. Sterling, P. C. Okhuysen, J. B. Rose, and W. Jakubowski (1995), The infectivity f *Cryptosporidium parvum* in healthy volunteers, New England Journal of Medicine, 332(13), 855-859.

Egerton, T. A., P. A. Christensen, S. A. M. Kosa, B. Onoka, J. C. Harper, and J. R. Tinlin (2006), Photoelectrocatalysis by titanium dioxide for water treatment, International Journal of Environment and Pollution, 27(1-3), 2-19.

Fox, K. R., and D. A. Lytle (1996), Milwaukee's crypto outbreak: Investigation and recommendations, American Water Works Association Journal, 88(9), 87-94.

Franke, R., and C. Franke (1999), Model reactor for photocatalytic degradation of persistent chemicals in ponds and waste water, Chemosphere, 39(15), 2651-2659.

Fujishima, A., and K. Honda (1972), Electrochemical photolysis of water at a semiconductor electrode, Nature, 238(5358), 37-+.

Ghezzar, M. R., S. Ognier, S. Cavadias, F. Abdelmalek, and A. Addou (2013), DBDplate-TiO2 treatment of Yellow Tartrazine azo dye solution in falling film, Separation and Purification Technology, 104, 250-255.

Goncalves, M. S. T., A. M. F. Oliveira-Campos, E. Pinto, P. M. S. Plasencia, and M. Queiroz (1999), Photochemical treatment of solutions of azo dyes containing TiO(2), Chemosphere, 39(5), 781-786.

Grimm, J., D. Bessarabov, and R. Sanderson (1998), Review of electro-assisted methods for water purification, Desalination, 115(3), 285-294.

Gupta, V. K., R. Jain, A. Nayak, S. Agarwal, and M. Shrivastava (2011), Removal of the hazardous dye-Tartrazine by photodegradation on titanium dioxide surface, Materials Science & Engineering C-Materials for Biological Applications, 31(5), 1062-1067.

Harrington, G. W., I. Xagoraraki, P. Assavasilavasukul, and J. H. Standridge (2003), Effect of filtration conditions on removal of emerging waterborne pathogens, Journal American Water Works Association, 95(12), 95-104.

Hoffmann, M. R., S. T. Martin, W. Y. Choi, and D. W. Bahnemann (1995), Environmental applications of semiconductor photocatalysis, Chemical Reviews, 95(1), 69-96.

Houas, A., H. Lachheb, M. Ksibi, E. Elaloui, C. Guillard, and J. M. Herrmann (2001), Photocatalytic degradation pathway of methylene blue in water, Applied Catalysis B-Environmental, 31(2), 145-157.

Jain, R., and S. Sikarwar (2008), Photodestruction and COD removal of toxic dye erioglaucine by TiO(2)-UV process: influence of operational parameters, International Journal of Physical Sciences, 3(12), 299-305.

Jain, R., and S. Sikarwar (2010), Adsorptive and Desorption Studies on Toxic Dye Erioglaucine Over Deoiled Mustard, Journal of Dispersion Science and Technology, 31(7), 883-893.

Jakob, L., T. M. Hashem, S. Burki, N. M. Guindy, and A. M. Braun (1993), Vacuum ultraviolet (VUV) photolysis of water – oxidative degradation of 4-chlorophenol, Journal of Photochemistry and Photobiology a-Chemistry, 75(2), 97-103.

Johnson, A. M., G. D. Di Giovanni, and P. A. Rochelle (2012), Comparison of Assays for Sensitive and Reproducible Detection of Cell Culture-Infectious Cryptosporidium parvum and Cryptosporidium hominis in Drinking Water, Applied and Environmental Microbiology, 78(1), 156-162.

Kesselman, J. M., O. Weres, N. S. Lewis, and M. R. Hoffmann (1997), Electrochemical production of hydroxyl radical at polycrystalline Nb-doped TiO2 electrodes and estimation of the partitioning between hydroxyl radical and direct Hole oxidation pathways, Journal of Physical Chemistry B, 101(14), 2637-2643.

King, B. J., and P. T. Monis (2007), Critical processes affecting Cryptosporidium oocyst survival in the environment, Parasitology, 134, 309-323.

Korich, D. G., J. R. Mead, M. S. Madore, N. A. Sinclair, and C. R. Sterling (1990), Effects of ozone, chlorine dioxide, chlorine, and monochloramine on *Cryptosporidium parvum* oocyst viability, Applied and Environmental Microbiology, 56(5), 1423-1428.

Lechevallier, M. W., W. D. Norton, and R. G. Lee (1991), Giardia and *Cryptosporidium spp* in filtered drinking water supplies, Applied and Environmental Microbiology, 57(9), 2617-2621.

Li, L., and R. K. Goel (2010), Role of hydroxyl radical during electrolytic degradation of contaminants, Journal of Hazardous Materials, 181(1-3), 521-525.
Linden, K. G., G. Shin, and M. D. Sobsey (2001), Comparative effectiveness of UV wavelengths for the inactivation of Cryptosporidium parvum oocysts in water, Water Science and Technology, 43(12), 171-174.

Ludwig, G. M., P. Perschbacher, and R. Edziyie (2010), The Effect of the Dye Aquashade (R) on Water Quality, Phytoplankton, Zooplankton, and Sunshine Bass, Morone chrysops x M-saxatilis, Fingerling Production in Fertilized Culture Ponds, Journal of the World Aquaculture Society, 41, 40-48.

Mackenzie, W. R., Hoxie, N.J., Proctor, M.E., Gradus, M.S. (1994), A massive outbreak in Milwaukee of *Cryptosporidium* infection transmitted through the public water supply, New England Journal of Medicine, 331(3), 161-167.

Maness, P. C., S. Smolinski, D. M. Blake, Z. Huang, E. J. Wolfrum, and W. A. Jacoby (1999), Bactericidal activity of photocatalytic TiO2 reaction: Toward an understanding of its killing mechanism, Applied and Environmental Microbiology, 65(9), 4094-4098.

Manker, D. C., and D. F. Martin (1984), Investigation of 2 possible modes of action of the inert dye Aquashade on Hydrilla, Journal of Environmental Science and Health Part a-Environmental Science and Engineering & Toxic and Hazardous Substance Control, 19(6), 725-733.

Markowska-Szczupak, A., K. Ulfig, and A. W. Morawski (2011), The application of titanium dioxide for deactivation of bioparticulates: An overview, Catalysis Today, 169(1), 249-257.

Matsunaga, T., R. Tomoda, T. Nakajima, N. Nakamura, and T. Komine (1988), Continuous sterilization system that uses photosemiconductor powders, Applied and Environmental Microbiology, 54(6), 1330-1333.

Messner, M. J., C. L. Chappell, and P. C. Okhuysen (2001), Risk assessment for Cryptosporidium: A hierarchical Bayesian analysis of human dose response data, Water Research, 35(16), 3934-3940.

Mills, A., M. Crow, J. Wang, I. P. Parkin, and N. Boscher (2007), Photocatalytic oxidation of deposited sulfur and gaseous sulfur dioxide by TiO2 films, Journal of Physical Chemistry C, 111(14), 5520-5525.

Mittal, A., J. Mittal, and L. Kurup (2006), Adsorption isotherms, kinetics and column operations for the removal of hazardous dye, Tartrazine from aqueous solutions using waste materials - Bottom Ash and De-Oiled Soya, as adsorbents, Journal of Hazardous Materials, 136(3), 567-578.

Molot, L. A., S. A. Miller, P. J. Dillon, and C. G. Trick (2003), A simple method for assaying extracellular hydroxyl radical activity and its application to natural and synthetic waters, Canadian Journal of Fisheries and Aquatic Sciences, 60(2), 203-213.

Morita, S., A. Namikoshi, T. Hirata, K. Oguma, H. Katayama, S. Ohgaki, N. Motoyama, and M. Fujiwara (2002), Efficacy of UV irradiation in inactivating Cryptosporidium parvum oocysts, Applied and Environmental Microbiology, 68(11), 5387-5393.

Nina, J. M. S., V. McDonald, D. A. Dyson, J. Catchpole, S. Uni, M. Iseki, P. L. Chiodini, and K. McAdam (1992), Analysis of oocyst wall and sporozoite antigens from 3 *cryptosporidium* species, Infection and Immunity, 60(4), 1509-1513.

Oancea, P., and V. Meltzer (2014), Kinetics of tartrazine photodegradation by UV/H2O2 in aqueous solution, Chemical Papers, 68(1), 105-111.

Ongerth, J. E., and H. H. Stibbs (1987), Identification of *Cryptosporidium* oocysts in river water, Applied and Environmental Microbiology, 53(4), 672-676.

Oturan, M. A. (2000), An ecologically effective water treatment technique using electrochemically generated hydroxyl radicals for in situ destruction of organic pollutants: Application to herbicide 2,4-D, Journal of Applied Electrochemistry, 30(4), 475-482.

Page, S. E., J. R. Logan, R. M. Cory, and K. McNeill (2014), Evidence for dissolved organic matter as the primary source and sink of photochemically produced hydroxyl radical in arctic surface waters, Environmental Science-Processes & Impacts, 16(4), 807-822.

Peeters, J. E., E. A. Mazas, W. J. Masschelein, I. V. M. Dematurana, and E. Debacker (1989), Effect of disinfection of drinking water with ozone or chlorine dioxide on survival of *Cryptosporidium parvum* oocysts, Applied and Environmental Microbiology, 55(6), 1519-1522.

Quinn, C. M., and W. B. Betts (1993), Longer term viability status of chlorine-treated Cryptosporidium oocysts in tap water, Biomedical Letters, 48(192), 315-318.

Rahmani, A., M. Samarghandi, M. Samadi, and F. Nazemi (2009), Photocatalytic Disinfection of Coliform Bacteria Using UV/TiO2, Journal of research in health sciences, 9(1), 1-6.

Rao, N. N., and S. Dube (1998), Photocatalytic degradation of Reactive Orange 84 (RO 84) in dye-house effluent using single pass reactor, Recent Advances in Basic and Applied Aspects of Industrial Catalysis, 113, 1045-1050.

Reduker, D. W., C. A. Speer, and J. A. Blixt (1985), Ultrastructural changes in the oocyst wall during excystation of *Cryptosporidium parvum* (Apicomplexa, Euccidiordia), Canadian Journal of Zoology-Revue Canadienne De Zoologie, 63(8), 1892-1896.

Rennecker, J. L., B. Corona-Vasquez, A. M. Driedger, S. A. Rubin, and B. J. Marinas (2001), Inactivation of Cryptosporidium parvum oocysts with sequential application of ozone and combined chlorine, Water Science and Technology, 43(12), 167-170.

Rizzo, L., S. Meric, M. Guida, D. Kassinos, and V. Belgiorno (2009), Heterogenous photocatalytic degradation kinetics and detoxification of an urban wastewater treatment plant effluent contaminated with pharmaceuticals, Water Research, 43(16), 4070-4078.

Robertson, L. J., A. T. Campbell, and H. V. Smith (1992), Survval of *Cryptosporidium parvum* under various environmental pressures, Applied and Environmental Microbiology, 58(11), 3494-3500.

Rochelle, P. A., R. DeLeon, M. H. Stewart, and R. L. Wolfe (1997), Comparison of primers and optimization of PCR conditions for detection of Cryptosporidium parvum and Giardia lamblia in water, Applied and Environmental Microbiology, 63(1), 106-114.

Rochelle, P. A., M. M. Marshall, J. R. Mead, A. M. Johnson, D. G. Korich, J. S. Rosen, and R. De Leon (2002), Comparison of in vitro cell culture and a mouse assay for measuring infectivity of Cryptosporidium parvum, Applied and Environmental Microbiology, 68(8), 3809-3817.

Roselin, L. S., and R. Selvin (2011), Photocatalytic Degradation of Reactive Orange 16 Dye in a ZnO Coated Thin Film Flow Photoreactor, Science of Advanced Materials, 3(2), 251-258.

Ruffell, K.M., Rennecker, J.L., and Marinas, B.J. (1998). Inactivation kinetics of *Cryptosporidium parvum* with chlorine dioxide. Proceedings of the American Water Works Association Water Quality Technology Conference , San Diego, CA.

Ryu, H., D. Gerrity, J. C. Crittenden, and M. Abbaszadegan (2008), Photocatalytic inactivation of Cryptosporidium parvum with TiO2 and low-pressure ultraviolet irradiation, Water Research, 42(6-7), 1523-1530.

Sabnis, R. W. (2010). *Handbook of biological dyes and stains: synthesis and industrial applications*. John Wiley & Sons.

Sadhasivam, S., S. Savitha, and K. Swaminathan (2007), Feasibility of using Trichoderma harzianum biomass for the removal of erioglaucine from aqueous solution, World Journal of Microbiology & Biotechnology, 23(8), 1075-1081.

Saien, J., and A. R. Soleymani (2007), Degradation and mineralization of Direct Blue 71 in a circulating upflow reactor by UV/TiO2 process and employing a new method in kinetic study, Journal of Hazardous Materials, 144(1-2), 506-512.

Sanchez-Martin, J., J. Beltran-Heredia, and M. T. Rodriguez-Sanchez (2012), Removal of Erioglaucine (Acid Blue 9) with a new coagulant agent from Acacia mearnsii tannin extract, Coloration Technology, 128(1), 15-20.

Schets, F. M., G. B. Engels, A. During, and A. A. D. Husman (2005), Detection of infectious Cryptosporidium oocysts by cell culture immunofluorescence assay: Applicability to environmental samples, Applied and Environmental Microbiology, 71(11), 6793-6798.

Shang, C., L. M. Cheung, C.-M. Ho, and M. Zeng (2009), Repression of photoreactivation and dark repair of coliform bacteria by TiO2-modified UV-C disinfection, Applied Catalysis B-Environmental, 89(3-4), 536-542.

Shin, G. A., K. G. Linden, M. J. Arrowood, and M. D. Sobsey (2001), Low-pressure UV inactivation and DNA repair potential of Cryptosporidium parvum oocysts, Applied and Environmental Microbiology, 67(7), 3029-3032.

Slifko, T. R., D. Freidman, J. B. Rose, and W. Jakubowski (1997), An in vitro method for detecting infectious Cryptosporidium oocysts with cell culture, Applied and Environmental Microbiology, 63(9), 3669-3675.

Spencer, D. F. (1984), Influence of Aquashade on growth, photosynthesis, and phosphorous uptake of microalgae, Journal of Aquatic Plant Management, 22(JUL), 80-84.

Stibbs, H. H., and J. E. Ongerth (1986), Immunofluorescence detection of *Cryptosporidium* oocysts in fecal smears, Journal of Clinical Microbiology, 24(4), 517-521.

Upton, S. J., M. Tilley, and D. B. Brillhart (1995), Effects of select medium supplements on in-vitro development of *Cryptosporidium parvum* in HCT-8 cells, Journal of Clinical Microbiology, 33(2), 371-375.

Vautier, M., C. Guillard, and J. M. Herrmann (2001), Photocatalytic degradation of dyes in water: Case study of indigo and of indigo carmine, Journal of Catalysis, 201(1), 46-59.

Wang, W.-Y., M.-L. Yang, and Y. Ku (2010), Photoelectrocatalytic decomposition of dye in aqueous solution using Nafion as an electrolyte, Chemical Engineering Journal, 165(1), 273-280.

Wawrzkiewicz, M., and Z. Hubicki (2009), Removal of tartrazine from aqueous solutions by strongly basic polystyrene anion exchange resins, Journal of Hazardous Materials, 164(2-3), 502-509.

Weeks, J. L., G. M. Meaburn, and S. Gordon (1963), Absorption coefficients of liquid water and aqueous solutions in the far ultraviolet, Radiation research, 19, 559-567.

Wu, T.-N. (2011), Electrochemical removal of MTBE from water using the iridium dioxide coated electrode, Separation and Purification Technology, 79(2), 216-220.

Wu, T.-N., T.-C. Pan, and L.-C. Chen (2012), Electrophotocatalysis of aqueous methyl tert-butyl ether on a titanium dioxide coated electrode, Electrochimica Acta, 86, 170-176.

You, X. D., M. J. Arrowood, M. Lejkowski, L. T. Xie, R. F. Schinazi, and J. R. Mead (1996), In vitro evaluation of anticryptosporidial agents using MDCK cell culture and chemiluminescence immunoassay, Journal of Eukaryotic Microbiology, 43(5), S87-S87.

Zimmer, J. L., R. M. Slawson, and P. M. Huck (2003), Inactivation and potential repair of Cryptosporidium parvum following low- and medium-pressure ultraviolet irradiation, Water Research, 37(14), 3517-3523.

Zhi L.R., Shaofeng, L. (2013), Applied Mechanics and Materials, 361-363, 623

3. INACTIVATION OF CRYPTOSPORIDIUM PARVUM BY PHOTOELECTROCATALYTIC OXIDATION

Kyana R.L. Young[a], Rebecca Hoffman[c], Christina K. Remucal[a,b], Gregory W. Harrington[a]
[a]University of Wisconsin – Madison, Civil and Environmental Engineering, Madison, WI
[b] University of Wisconsin – Madison, Environmental Chemistry and Technology, Madison, WI
[c] University of Wisconsin – Madison, Wisconsin State Laboratory of Hygiene, Madison, WI

3.1 ABSTRACT

Advanced oxidation processes (AOP) are beneficial for treating pathogens typically not removed or inactivated using conventional biological or physical-chemical technologies. AOP technologies that can produce hydroxyl radicals, a powerful oxidant, include photocatalytic oxidation (PCO) and photoelectrocatalytic oxidation (PECO). These systems are effective when electrons move into a higher energy state leaving a hole capable of oxidation work, and when the rate of radical generation is faster than the rate at which the electron recombines with the hole.

This chapter compares the inactivation of *Cryptosporidium parvum* oocysts by PCO, PECO, electrolysis, and UV. Experiments were conducted in a recirculating batch reactor with *C. parvum* spiked at 2.0 x 10^7 oocysts/L. Inactivation was measured with cell culture combined with immunofluorescence assay. The first order inactivation rate constants for PECO, PCO, electrolysis, and ultraviolet irradiation were 1.0 x 10^{-2} ± 1.6 x 10^{-3} sec^{-1}, 3.4 x 10^{-3} ± 3.2 x 10^{-4} sec^{-1}, 3.3 x 10^{-3} ± 3.0 x 10^{-3} sec^{-1}, and 1.8 x 10^{-3} ± 3.2 x 10^{-3} sec^{-1} respectively. The hydroxyl radical production rates for the same four systems were 0.15 ± 0.02 μM/min, 0.11 ± 0.02 μM/min, 0.006 ± 0.001 μM/min, and 0.28 ± 0.01 μM/min, respectively. With the reactor configurations used in this study, it appears that electrolysis may be a significant contributing factor to the inactivation of *Cryptosporidium* in PECO systems.

3.2 INTRODUCTION

Cryptosporidium parvum is a waterborne pathogenic organism known to infect humans through ingestion of water, causing a severe diarrheal disease known as cryptosporidiosis. The disease is potentially fatal for the immunocompromised, elderly, and children (Messner, 2001). The pathogen is an intercellular coccidian protozoan parasite found in animal stool, drinking water, and soils. Between 1995 and 2010, *C. parvum* accounted for 16 waterborne disease outbreaks in the United States. Over the same time period, conventional water treatment facilities were accountable for 75.8% of the total waterborne outbreaks in the US (CDC, 2013). The deadliest known U.S. waterborne cryptosporidiosis outbreak occurred in Milwaukee in 1993,

infecting 400,000 people and accounting for over 100 deaths (MacKenzie, 1994). While the conventional surface water treatment system was functional at the time of the outbreak, breakthrough of the oocysts through the filtration system was a contributing factor in the outbreak (Fox, 1996).

The level of *C. parvum* breakthrough is a concern for immunocompromised individuals. In one study, the dose that infected 50% of healthy volunteers after ingestion of *C. parvum* was 132 oocysts, while the dose that infected 50% of immunocompromised adults was between 9 and 30 (Dupont, 1995). A dose of $6x10^{-6}$ oocysts per exposure leads to 10^{-4} infections per capita per year (Englehardt, 2006). With the implementation of United States Environmental Protection Agency regulations, including three Enhanced Surface Water Treatment Rules, occurrences of cryptosporidiosis outbreaks have decreased significantly (CDC, 2013). Nevertheless, studies have shown the ability of live oocysts to evade removal by conventional surface water treatment (Assavasilavasukul, 2008; Xagoraraki, 2004; Harrington, 2003). Despite the increased monitoring and operational adjustments that water utilities have made in response to regulations, breakthrough of *C. parvum* continues to occur in relatively sophisticated water treatment systems. For example, from May 2012 to June 2012, Seoul, Korea experienced a *C. parvum* outbreak in their water distribution system (Cho, 2013). In central China, the effluent of wastewater treatment plants along the Three Gorges Reservoir serves as the influent source water for the drinking water plants. At the drinking water treatment plant, 61 influent water samples were taken and were discovered to have *C. parvum* present in 86.4% of the samples, with presence of *C. parvum* in concentrations as high as 2.88 oocysts/L (Xiao, 2012).

As a general rule, disinfection processes are employed to augment the physical separation processes present in a treatment plant. However, due to the sturdy nature of the oocyst wall and its ability to protect the sporozoites and their nucleic acid structure, treatment via conventional disinfection processes is generally ineffective. *C. parvum* is highly resistant to typical treatment concentrations of chlorine (0.2 to 1.0 mg/L), even when chlorine is applied at high concentrations of 20 mg/L for 765 minutes of treatment (Peeters, 1989). Campbell (1992) discovered that two hours of chlorination, at concentrations typical in drinking water, had no effect on oocyst inactivation. Ozone oxidation is an alternative to chlorine, but cost and maintenance have prevented ozone from becoming widely applied for *Cryptosporidium* inactivation in the U.S. The CT for 2.5-log ozone inactivation of *C. parvum* is 4 mg·min/L

(Rennecker, 2001). The sequential treatment application of ozone followed by monochloramine, requires a monochloramine CT of 2000 mg·min/L to achieve 2.5 log inactivation (Rennecker, 2001).

Ultraviolet (UV) irradiation is a promising method to treat water for *C. parvum* inactivation. The absorption of UV by the *C. parvum* DNA results in the compromise of the nuclei, rendering the microorganism incapable of reproduction (Morita, 2002). Craik (2001) demonstrated that the use of UV has been effective at 1.8 to 2.3 log inactivation of *C. parvum* at UV wavelengths of 245 to 275 nm and doses of 10 to 25 mJ/cm^2. Medium pressure, 1 kW, UV lamps provided 0.8 log inactivation of *C. parvum* at low doses of 5 to 40 mJ/cm^2 (Amoah, 2005, Zimmer, 2003, Linden 2001). Low pressure, 30 W, UV lamps are also practical and widely used, due to availability, cost, ease of use, and measurement of UV output. A 1.7 log inactivation of *C. parvum* was observed when a low pressure UV light was applied at a dosage of 2 mJ/cm^2; the inactivation was observed through cell culture infectivity (Shin, 2001).

Alternatively, advanced oxidation processes (AOP) are processes that produce hydroxyl radicals and several AOP have been studied for their ability to inactivate waterborne pathogens. For example, photocatalytic oxidation (PCO) with the simultaneous use of titanium dioxide and ultraviolet irradiation, UV+TiO_2, has shown promising results for the inactivation of *C. parvum* in water (Cho, 2008, Ryu, 2008). A hydroxyl radical CT value of 9.3 x 10^{-5} mg·min/L has been reported for 2-log inactivation (Cho, 2008). TiO_2, as a semi-conductor, is electrochemically stable, resistant to corrosion, and conductive, making it a useful catalyst for advanced oxidation processes (Zanoni, 2004).

When the TiO_2 absorbs UV light having energy greater than 3.2 eV, electrons (e^-) move from its valence band to its conduction band, leaving holes in the valence band (h^+). The subsequent transfer of electrons from the surrounding water towards the hole is likely to occur within nanoseconds, creating a highly oxidizing surface that promotes the production of hydroxyl radical (Hoffmann, 1995). However, recombination of electrons and holes may also occur within the catalyst, rendering the process inefficient. AOP have shown inefficiencies when chloride ions, bicarbonate, and dissolved organic matter (DOM) are present. Hydroxyl radicals generated by AOP are scavenged by the chloride, bicarbonate and DOM, rather than attacking/reacting with the target contaminants. This renders the powerful hydroxyl radical oxidant null or ineffective (Liao, 2001).

If the TiO_2 is used as an anode in a photocatalytic system with sufficient UV radiation (>3.2 eV) applied, the electrons (e^-) on the surface of the TiO_2 move from the valence band to the conduction band (Fujishima 1972, Hoffmann 1995). If an applied bias is applied between the TiO_2 anode and the Ti cathode, the electrons in the conduction band will move to the liquid cathode interface, where they participate in reduction reactions. The resulting separation of the electron-hole pair reduces the amount of electron-hole recombination and allows the e^- to directly participate in reduction reactions at the cathode-water interface (Linsebigler, 1995). The holes can then more efficiently produce hydroxyl radicals at the anode-water interface and these radicals can oxidize contaminants in the bulk water of the system. Using this electrochemical system in conjunction with applied UV energy is known as photoelectrocatalytic oxidation (PECO). Another advantage of this process is that it can be used at the small scales needed for point-of-use (POU) treatment.

The goal of this study was to compare the inactivation of *C. parvum* by use of four different POU technologies: PECO, PCO, UV irradiation, and electrolysis. Each experiment was designed to compare each POU device along with the effect of water recirculation rate through each system.

3.3 METHODS

3.3.a. Inactivation experiments

Experiments were run to compare the effect of recirculation rate and treatment technology on the inactivation of *C. parvum*. The treatment technologies were (1) control, (2) UV irradiation, (3) electrolysis with TiO_2, (4) PCO with UV + TiO_2, and (5) PECO with UV + TiO_2 + electrolysis. Experiments were conducted in a recirculating reactor system, shown in Figure 3-1 and the components of the reactor are shown in Figure 3-2. For PCO operation, all components of the reactor were intact, the UV lamp was turned on, and no voltage was applied across the anode and cathode. When PECO was tested, all components of the reactor were intact, the UV lamp was turned on, and voltage was applied across the anode and cathode. The reactor properties for all five treatment technologies are shown in Table 3-1.

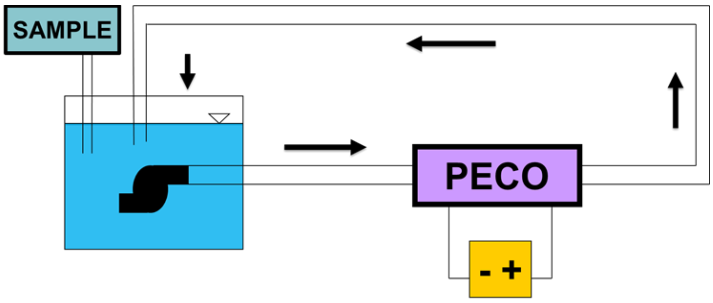

Figure 3-1: Schematic of one POU reactor unit; a 7 L tank, 12 V Power Supply, ½" ID x ¾" OD Vinyl Connector Tubes, POU Reactor device, Pump (Max Q = 5.4 L/min).

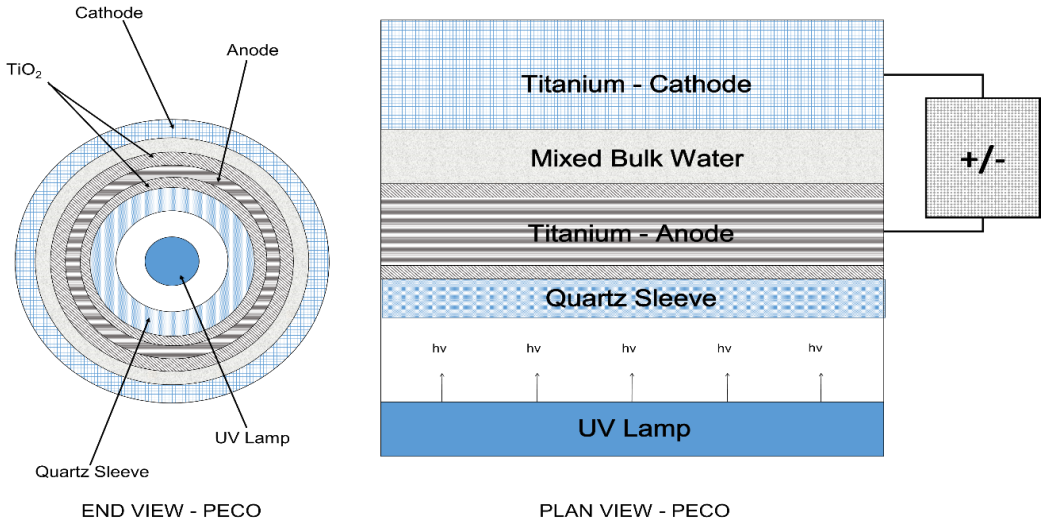

Figure 3-2: End view and plan view of the reactor with all components installed for PECO operation.

Device	Ultraviolet Irradiation	TiO_2	Voltage
Control	Off	Absent	Not applied
Ultraviolet Irradiation	On	Absent	Not applied
Electrolysis with TiO_2	Off	Present	Applied
Photocatalysis	On	Present	Not applied
Photoelectrocatalysis	On	Present	Applied

Table 3-1: Active components within the reactor for each treatment technology.

Each experiment required three 7.0 L capacity aquarium tanks, filled with 4.0 L of tap water. Two of the tanks were run with identical experimental conditions to assess variability, while the third tank was run as a control. For the device serving as the control, the TiO_2 semiconductor and the unlit UV light source remained housed within the POU treatment device and no applied bias was connected to anode or cathode, providing identical water flow capacity as the active devices. The tap water source was groundwater treated with chlorine and fluoride at the source; the experiments were intended to simulate point-of-use (POU) treatment of tap water (the chlorine concentration never exceeded 0.25 mg/L).

The tanks housed a 7.8 W pump connected to 23-inch long, ½" ID x ¾" OD vinyl tubes, facilitating circulation of water at a recirculation rate of 2.9 L/min to 5.4 L/min (Figures 3-1 and 3-2). The flow then circulated back into the tank, allowing the water to re-circulate from tank to pump to POU device and back to the tank. A DC power supply source was attached to positive (anode) and negative (cathode) wires at their respective ends of the treatment device, to allow for a voltage to be applied. Although the pump had an adjustable recirculation rate, the pump was operated at a steady recirculation rate throughout the duration of each experiment.

Prior to starting an experiment, the pump was turned on while 1.0 mL of stock oocyst suspension, at approximately 2.0 x 10^7 oocysts/mL concentration, was inoculated into the tank. This inoculated water was allowed to re-circulate through the system to yield a starting concentration of approximately 5.0 x 10^6 oocysts/L in the recirculating system. The oocysts were circulated within the tank for 10 minutes before an initial sample was taken to verify the actual starting concentration. The 2 x 10^7 oocysts/mL stock concentration was selected because it is the largest quantity that could be sorted and shipped by the distributor in an individual vial. The *C. parvum* were purchased, prepared, and shipped from the Sterling Parasitology Lab in Tucson, AZ.

At t = 0 minutes, the UV lamp and applied voltage were turned on if they were part of the experiment (see Table X). The UV lamp was low pressure (9 W) and, when used, voltage was applied at 9 V. A total of 6 samples were collected for each recirculating reactor from the start of the experiment to the end of the experiment. For some experiments, samples were collected at 3-minute intervals. For other experiments, samples were collected at 15-minute intervals.

For each sampling time, including the t = 0 sample, triplicate samples of volume 1000 µL were taken from each reactor. These tubes were placed in a refrigerator at 4°C overnight, in preparation for cell culture analysis. In addition to the 1000 µL samples, a set of 300 µL triplicates were taken from each reactor and placed in individual 12x75 mm tubes vials containing 33 µL of propidium iodide (PI) and 30 µL of flow count beads. Chlorine concentration, pH, and water temperature were also measured throughout the experiment at times corresponding to sample collection times. Chlorine concentrations never exceeded 0.25 mg/L, pH was always between 6.2 and 6.3, and temperature was always between 19°C and 21°C.

Treatment of *C. parvum* by each respective reactor was independently performed, where inactivation was demonstrated by the detection/absence of the oocysts using the IFA method combined with cell culture. The data was fit using a first order reaction model (Equations 3-1 and 3-2), where the reaction rate was determined by the slope of the best-fit line; the 95% confidence interval was also determined for the inactivation rate.

$$C = C_o e^{-kt} \qquad \text{Equation 3-1}$$

$$\log \frac{C}{C_o} = -kt \qquad \text{Equation 3-2}$$

3.3.b. Hydroxyl radical experiments

An additional set of experiments was conducted to compare and characterize the rate of hydroxyl radical production by each reactor configuration. With the exception of the source water, which was changed from tap water to Milli-Q water with a resistivity of 18.2 MΩ·cm at 25°C, these experiments had identical device configuration as the inactivation experiments. Each tank was prepared with 50 mM methanol in 4 L of Milli-Q water. The recirculation rates tested were 2.88 L/min, 4.08 L/min, and 5.40 L/min. Samples were taken every 30 seconds for the first 3 minutes, and then every 3 minutes for the remaining 15 minutes. After sampling, 100 µL of 5.5 mM recrystallized dinitrophenylhydrazine (DNPH) and 50 µL of 1 N nitric acid were added to each 1 mL aliquot; the addition of DNPH converts formaldehyde to the respective hydrazone prior to HPLC analysis (Keenan, 2008).

The source water used for the hydroxyl experiments was 18.2 MΩ·cm at 25°C. This decision was made to determine the production rate of hydroxyl radicals sans inorganic carbon. The ratio of hydroxyl radical production would be similar to the *C. parvum* experiments, with all other operational parameters being identical, creating a scenario of maximum hydroxyl radical production within each system. The data was fit using a zero order reaction model (Equations 3-3 and 3-4), where the reaction rate was determined by the slope of the best-fit line; the 95% confidence interval was also determined for the inactivation rate.

$$\frac{dC}{dt} = -k \qquad \text{Equation 3-3}$$

$$C = C_0 - kt \qquad \text{Equation 3-4}$$

3.4 ANALYTICAL METHODS

3.4.a Cell Culture Analysis with Immunofluorescence Assay

Oocyst infectivity was measured by pipetting 400 µL of sample onto 4.5 x 10^4 cells/cm^2 cultures of human intestinal adenocarcinoma cells (HCT-8). After incubation for 3 days at 36°C, immunofluorescence assay (IFA) was used to assess the number of infected cells so that an estimate of infectious oocyst concentration could be determined. The method used to perform the analysis is described by Johnson (2012) and details are provided in Appendix A.

Before the experiment to inactivate the pathogen, a sample of the HCT-8 was sent to an independent lab (Bionique Testing Laboratory, Saranac Lake, NY) and tested for an intercellular gram-negative bacterium capable of self-replication, *Mycoplasma* (Bionique, 2011). Testing for *Mycoplasma* required 1-2 days. All submitted samples were negative for contamination. In that two day time frame, cell walls were established by inoculation and incubation of the HCT-8 into a 150 cm^2 flask with maintenance medium. New batches of maintenance medium allowed for the cells to be passaged twice a week. Between passages, cells were incubated in an environment of 37°C, 5% CO_2. When the cell culture was stabilized (typically 3-4 weeks after the initial HCT-8 cell inoculation), the cells were split into two flasks, in preparation for chamber slide and 16-well plate oocyst inoculation.

Each slide was viewed using a Chiu Technical Corporation Mercury 100-W microscope, with lens 480/40, DM 505, BA 535/50 FITC HYQ, using both the 100X lens and 200X lens. The quantity of oocysts was recorded using a tally counter.

3.4.b. Propidium Iodide Analysis

Propidium iodide (PI), a red/orange fluorescent dye that can stain membranes of oocysts with intact, damaged, and/or compromised walls (Hoefel, 2003), was used for tagging of the detected oocysts. PI was prepared by adding 5 mg of PI to 10 mL of reagent grade water, which was vortexed until the solid PI dissolved. A set of 300 µL triplicate samples were taken from each reactor and placed in individual 12x75 mm tubes vials containing 33 µL of propidium iodide (PI) and 30 µL of flow count beads. Quantification of cells was performed using a flow cytometer (Epics, XL, Coulter Group, Miami, FL).

3.4.c Hydroxyl Radical Analysis

A high performance liquid chromatography (HPLC) analysis was used to determine the concentration of hydroxyl radical in experiments designed to study hydroxyl radical production. A derivatization method previously described (Tai, 2004) was employed with an Agilent Technologies 1260 Infinity HPLC instrument. The HPLC was equipped with a degasser, binary pump, and diode array detector used to measure UV absorbance. The diode array detector was programmed to a 350 nm wavelength. An Agilent Poroshell 120 EC-C18 column (3.0 x 50 mm, 2.7 µm particles) was used with an Agilent EC-C18 (3.0 x 5 mm, 2.7 µm particles) guard column. To perform the isocratic elution at a recirculation rate of 0.6 mL/min, a 5 mM formic acid buffer with 10% acetonitrile was used as the aqueous phase, while acetonitrile solution was the mobile phase at a 60:40 ratio. Additional details are provided in Appendix B.

3.4.d. Other Analytes

Sample pH values were measured using pH indicator strips (Merck Millipore, Darmstadt, Germany). Typically, pH is monitored by a pH probe but concern regarding the adhesion of oocysts to the probe prompted the use of pH indicator strips instead. Chlorine concentration was measured using the DPD (N,N,-diethyl-p-phenylenediamine) standard method (Standard Method 4500 – CI G, 2013). Temperature was recorded using an infrared digital tank thermometer.

3.5. RESULTS AND DISCUSSION

3.5.a Hydroxyl Radical Production

3.5.a.1 Influence of Recirculation Rate on Hydroxyl Radical Production

Figure 3-3 shows the concentration of formaldehyde as a function of time in experiments conducted with the PECO device. As noted previously, the rate of change in formaldehyde concentration correlates with the rate of hydroxyl radical production by the device. Hydroxyl radical production has a linear dependence on time for all three of the recirculation rates evaluated, as expected (Equation 3-4).

The data for each recirculation rate was independently fit by linear regression to estimate the rate of hydroxyl radical production from the slope of the best fit. In addition, the 95% confidence interval for the slope estimate was also calculated. The results are shown in Figure 3-4, which indicates that there was no observable dependence of hydroxyl radical production rate on the recirculation rate. Because there was no observable dependence on recirculation rate, the data from all three recirculation rates were fit together and this result is shown in Figure 3-3. For this linear fit of all the PECO data, the hydroxyl radical production rate was 0.15 ± 0.02 μM/min (Table 3-2).

Although the example used in this section was for the PECO device, a similar approach was used to estimate hydroxyl radical production rate by all reactors and the results are shown in Table 3-2. This table shows that recirculation rate had no observable effect on the hydroxyl radical production rate for any of the reactor technologies evaluated in this study; this result is consistent with expectations. Total residence time within the reactor is equivalent to 1) the frequency of bulk water passing through the reactor, based on the recirculation rate, and 2) the contact time between the bulk water and the catalyst. Regardless of the recirculation rate in the recirculating batch reactor, the contact time is proportional to the frequency of passing and the residence time within the reactor (White, 1982). Thus, even though the water spends less time per pass through the reactor with increasing flow rate, the water spends the same total amount of time in the reactor because it passes through the reactor more frequently.

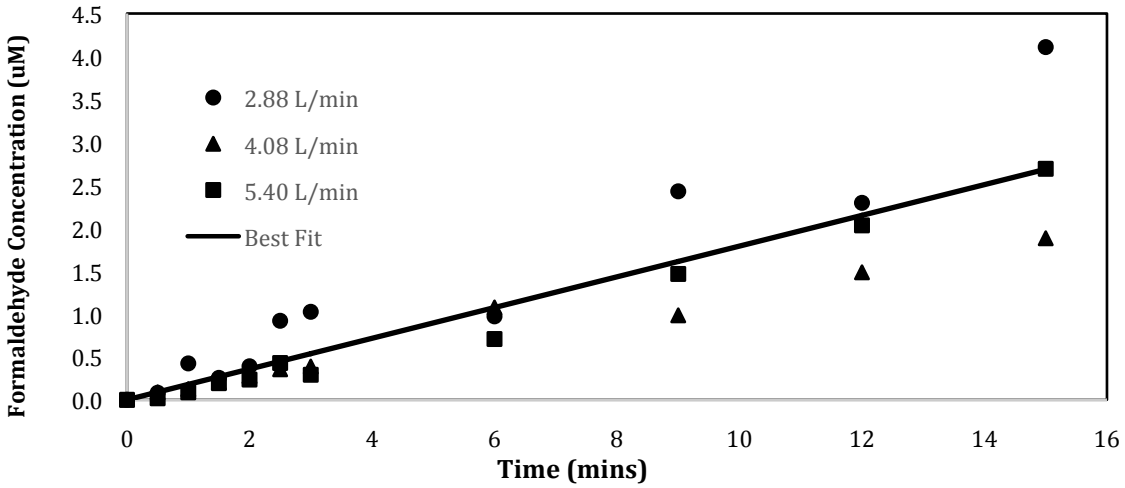

Figure 3-3. Formaldehyde production by the PECO device at different recirculation rates, with the linear fit of all data. The estimated production rate was 0.15 ± 0.02 μM/min.

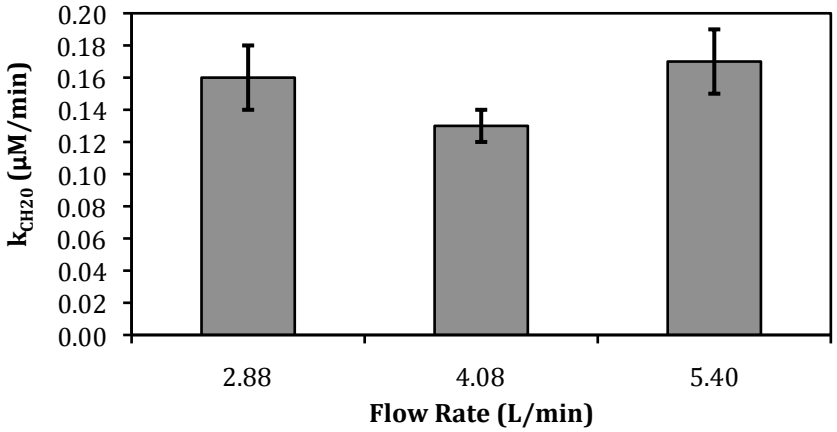

Figure 3-4: Formaldehyde production rate constant, k_{CH20}, by PECO along with the 95% confidence level for each value.

Treatment Method	Recirculation Rate			
	2.9 L/min	4.1 L/min	5.4 L/min	Combined
	CH_2O production rate constant k_{CH2O} (µM/min)	CH_2O production rate constant k_{CH2O} (µM/min)	CH_2O production rate constant k_{CH2O} (µM/min)	CH_2O production rate constant k_{CH2O} (µM/min)
Control	0	0	0	0
Electrolysis	0.006 ± 0.001	0.007 ± 0.001	0.006 ± 0.001	0.006±0.001
PCO	0.11 ± 0.01	0.05 ± 0.01	0.16 ± 0.01	0.11±0.02
PECO	0.16 ± 0.02	0.13 ± 0.01	0.17 ± 0.01	0.15±0.02
UV	0.24 ± 0.02	0.30 ± 0.01	0.29± 0.01	0.28±0.01

Table 3-2: Comparison of POU treatment devices, along with varying recirculation rate (2.9 L/min – 5.4 L/min), for the generation of hydroxyl radicals. Rate constants are the estimate ± the 95% confidence interval for the estimate.

3.5.a.2 Influence of Reactor Type on Hydroxyl Radical Production

Figure 3-5 shows the concentration of formaldehyde as a function of time in experiments conducted with different reactors. While Figure 3-5 only displays the results for the PCO and PECO reactors, the electrolysis (ELE), UV and control reactors were also analyzed using the same approach. The rate constants for all systems are shown in Table 3-2.

As expected, the reactor type had an effect on hydroxyl radical production, with electrolysis having the slowest production rate and UV radiation having the highest. The electrolysis reactor, operating without UV light irradiation to activate the titanium dioxide, had the lowest production rate of hydroxyl radicals, which was expected because the electrolysis component must 1) provide enough voltage (>1.23 V) to split water into hydrogen and water, and 2) provide enough current to transport the electrons to the cathode interface where reduction reactions occur; neither of these conditions lead to hydroxyl radicals production. Because the PCO and PECO reactors both had the TiO_2 catalyst and UV irradiation, both reactors were expected to produce hydroxyl radicals. Notably, the PCO reactor had a lower hydroxyl radical production rate compared to the PECO reactor. This was expected, as the improvement from the PCO to PECO is the applied bias that moves electrons in the conduction band from the anode to the liquid cathode interface. The movement of the electrons leaves holes in the anode's valence band, where the accumulation of electrons at the cathode react with electron acceptors to produce hydroxyl radicals (Equation 3-5). The UV reactor produced the highest rate of hydroxyl radicals of all the reactors. At a wavelength of 136 nm to 185 nm, UV is absorbed by water molecules where production of hydrogen atoms and hydroxyl radicals occurs (Crovisier 1989, Weeks

1963). The MP UV lamp housed in the reactors has a wavelength range of 185 to 480 nm, providing an opportunity for hydroxyl radicals to be generated via photodissociation (Equation 3-5).

$$H_2O \xrightarrow{h\nu} \frac{1}{2}H_2 + {}^{\bullet}OH$$

Equation 3-5

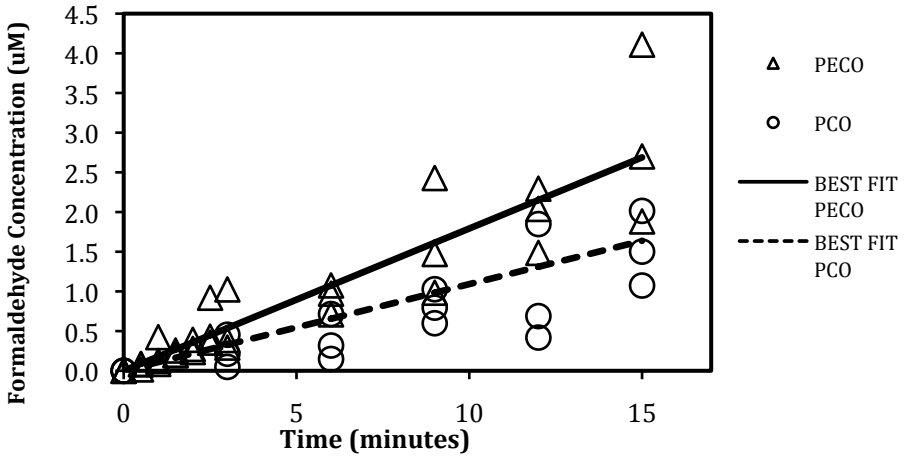

Figure 3-5: Formaldehyde production rate for PECO and PCO for all recirculation rates tested. The best fit line for each reactor, calculated using regression analysis, is also shown.

3.5.b *Cryptosporidium* Inactivation

3.5.b.1 Influence of Recirculation Rate on *Cryptosporidium* Inactivation

The PI/flow cytometer analysis was performed to quantify the total number of oocysts in the tank to assess the possibility of oocyst loss due to adhesion to reactor and/or tank surfaces. At most there was an 8.5% loss of oocysts (Figure 3-6).

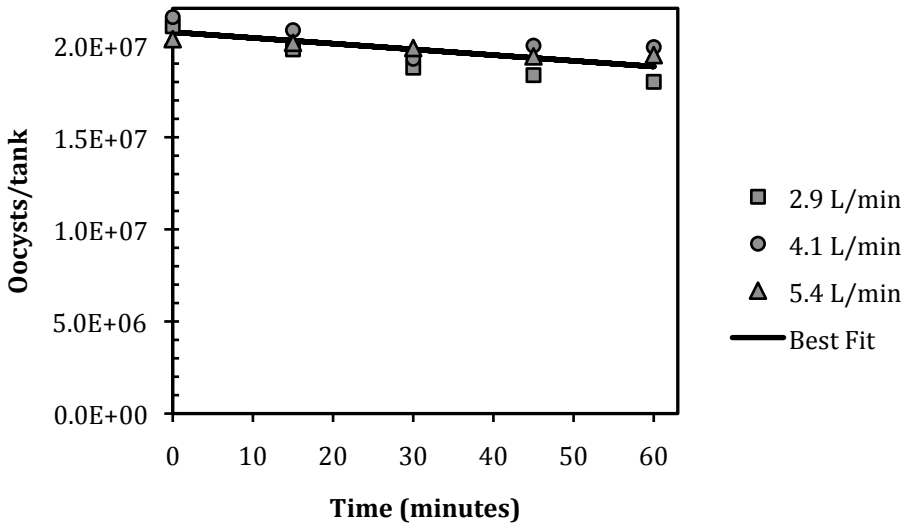

Figure 3-6: Quantification of oocysts per 4 L tank of water, seeded at 2 x 10^7 per tank. Oocyst count provided by the flow cytometer for the PECO reactor with varying recirculation rates.

Figure 3-7 shows the inactivation of *C. parvum* by PECO at the three recirculation rates tested. As shown in this figure, there was no dependence on the recirculation rate for the inactivation of *C. parvum*. The PECO device, regardless of recirculation rate, achieved 2-log inactivation by the 180-second sample point. The inactivation rate constants for the 2.9, 4.1, and 5.4 L/min recirculation rates were at least 1.2 x $10^{-2} \pm 2.8 \times 10^{-3}$ sec^{-1}, 6.5 x $10^{-3} \pm 1.9 \times 10^{-3}$ sec^{-1}, and 1.5 x $10^{-2} \pm 2.6 \times 10^{-3}$ sec^{-1}, respectively (Figure 3-8). These rate constants were based on best fit lines that included experiments that achieved a non-detectable level of infectious oocysts by the end of the experiment. These data points were assumed to have an infectious oocyst concentration equal to the limit of detection and, thus, the calculated inactivation rate constant represents the minimum possible estimate for the rate constant.

The lack of dependence on recirculation rate is consistent with the aforementioned results for hydroxyl radical production rate, where the hydroxyl radical production rates were also independent of the recirculation rate. As noted earlier, the total contact time with the catalyst is independent of the recirculation rate (White, 1982). Similar findings were obtained for other reactor types as well, shown in Table 3-3.

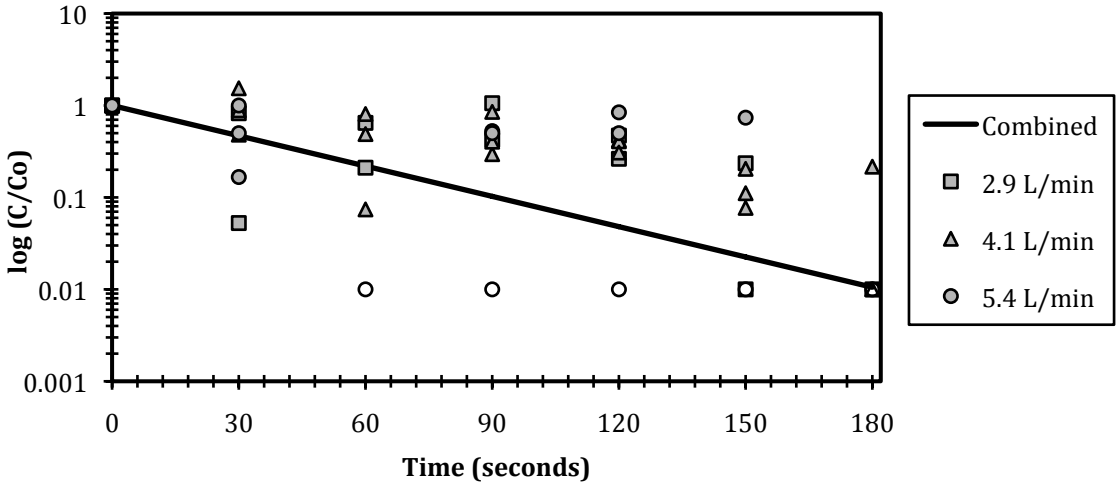

Figure 3-7: Log inactivation of *C. parvum* with PECO. Open data points represent values that were less than the quantifiable range for the experiment. For one of the reactors operated at 5.4 L/min, infectious oocyst concentration was below detection limit for all $t \geq 60$ min. For the other reactor operated at this flow rate, this occurred at $t = 180$ min. For one of the reactors operated at 4.1 L/min, this was true for all $t \geq 180$ min. For the reactors operated at 2.9 L/min, one achieved a non-detectable concentration for $t \geq 150$ min and the other achieved this at $t = 180$ min.

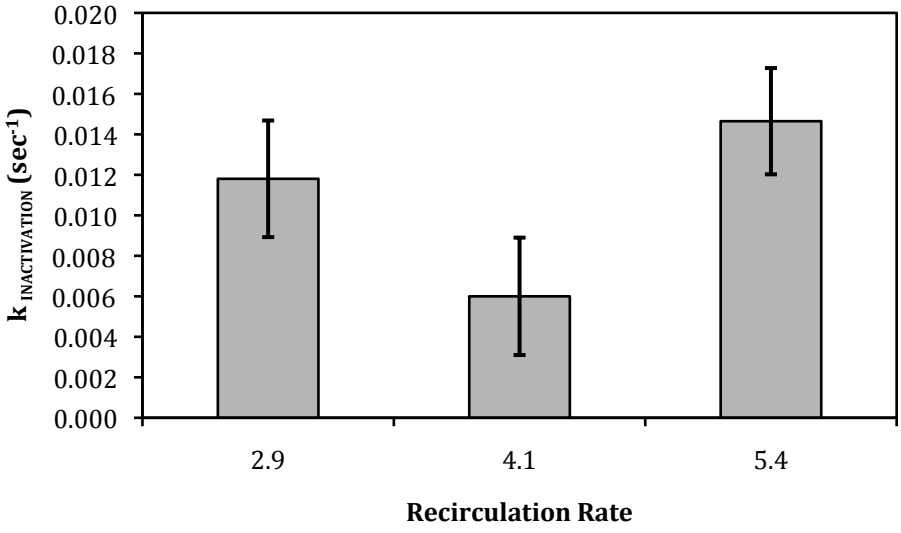

Figure 3-8: Dependence of *C. parvum* inactivation rate on the recirculation rate of the PECO reactor, along with the 95% confidence interval.

	Low (2.88 L/min)	Medium (4.08 L/min)	High (5.41 L/min)	Combined
	k_I (sec^{-1})	k_I (sec^{-1})	k_I (sec^{-1})	k_I (sec^{-1})
Control	$5.6 \times 10^{-10} \pm 1.0 \times 10^{-10}$	$6.3 \times 10^{-10} \pm 1.0 \times 10^{-10}$	$4.8 \times 10^{-10} \pm 1.0 \times 10^{-10}$	$5.6 \times 10^{-10} \pm 1.0 \times 10^{-10}$
PCO	$6.1 \times 10^{-4} \pm 1.2 \times 10^{-4}$	$6.7 \times 10^{-4} \pm 2.9 \times 10^{-4}$	$6.0 \times 10^{-4} \pm 1.4 \times 10^{-4}$	$6.3 \times 10^{-4} \pm 8.5 \times 10^{-5}$
UV	$1.7 \times 10^{-3} \pm 9.8 \times 10^{-4}$	$1.8 \times 10^{-3} \pm 4.6 \times 10^{-4}$	$1.8 \times 10^{-3} \pm 5.4 \times 10^{-4}$	$1.8 \times 10^{-3} \pm 3.2 \times 10^{-4}$
Electrolysis	*	*	$1.8 \times 10^{-3} \pm 2.6 \times 10^{-4}$	$3.3 \times 10^{-3} \pm 3.0 \times 10^{-3}$
PECO	$1.2 \times 10^{-2} \pm 2.8 \times 10^{-3}$	$6.5 \times 10^{-3} \pm 1.9 \times 10^{-3}$	$1.5 \times 10^{-2} \pm 2.6 \times 10^{-3}$	$1.1 \times 10^{-2} \pm 1.6 \times 10^{-3}$

Table 3-3: Effect of bulk water recirculation rate and reactor type on the inactivation rate of *C. parvum*. The reported values are the minimum possible inactivation rates. * Electrolysis was not tested at the low and medium recirculation rates.

3.5.b.2 Influence of Treatment Technology on *Cryptosporidium* Inactivation

Figure 3-9 shows the inactivation of *C. parvum* versus time for both PCO and PECO reactors. Although Figure 3-9 only displays the IFA results for the PCO and PECO reactors; the electrolysis, UV and control reactors were also analyzed using the same approach (see Table 3-3 for results from these reactors). The PECO reactor achieved 2-log inactivation of *C. parvum* after 3 minutes of treatment. The PCO treatment technology achieved a 1-log inactivation after 30 minutes of treatment. The control reactors were also analyzed using the IFA method, and demonstrated 0-log inactivation for the duration of the experiment.

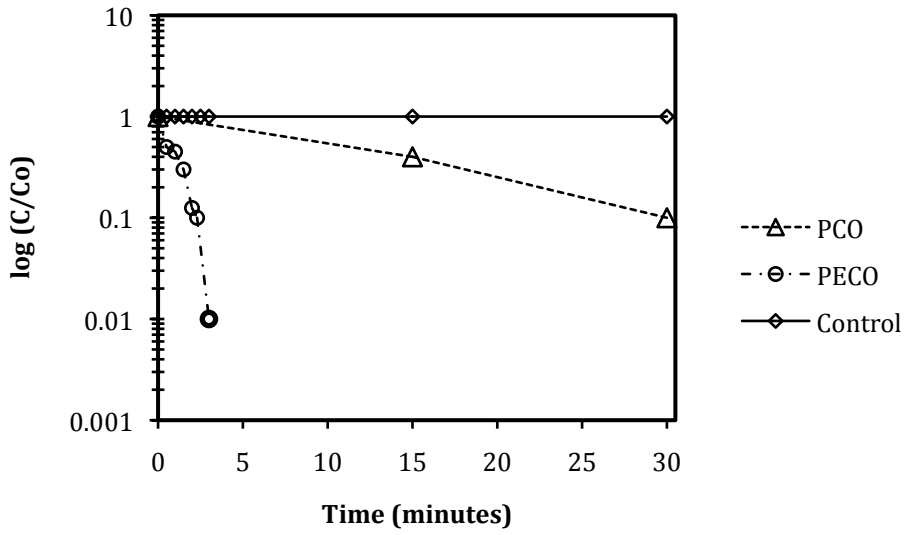

Figure 3-9: Comparison of PCO and PECO for inactivation of *C.parvum* at a recirculation rate of 5.4 L/min. The bold open data point represents a value that was less than the quantifiable range for the experiment.

As shown in Table 3-3 and Figure 3-10, the PECO device performed better than the UV and electrolysis reactors, and all three of these reactors performed better than the PCO reactor. There was no observable correlation between *C. parvum* inactivation rate and hydroxyl radical production rate. The PECO device included all three technologies (photocatalysis, electrolysis, and irradiation), although exposure of oocysts to UV radiation was largely blocked by the TiO_2 anode in the PECO reactor (see Figure 3-2). Similarly, the PCO device included photocatalysis and irradiation components but the oocysts were largely blocked from UV radiation in this reactor as well.

The PECO reactor was observed to inactivate *C. parvum* 17 times faster than PCO, but produced hydroxyl radicals at a rate that was only 1.4 times faster than the PCO reactor. The comparison of PCO and PECO demonstrates that the applied bias intended to increase the concentration of hydroxyl radicals plays a possible role in the inactivation of *C. parvum*, but the inactivation rate increased significantly more than expected, given the modest increase in hydroxyl radical production rate. This finding is consistent with previous research that hydroxyl radicals are highly reactive oxidants for treating water contaminated with *C. parvum* (Curtis 2008, Cho 2008, Ryu 2008).

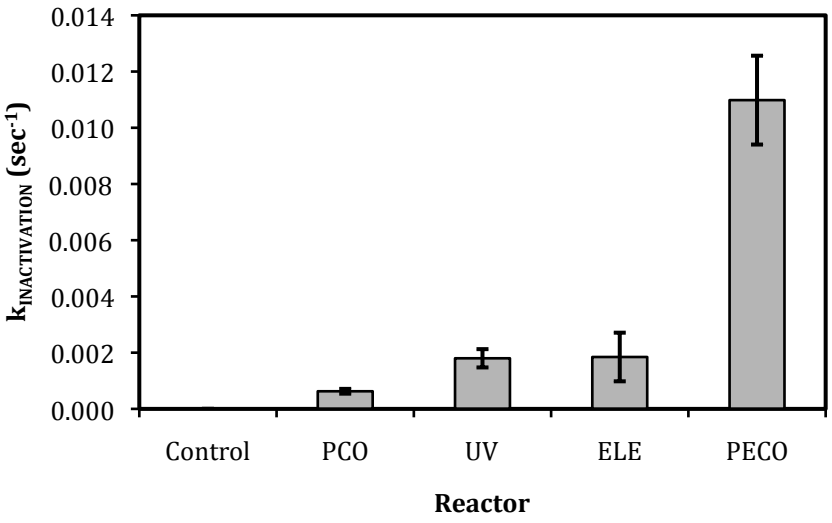

Figure 3-10: Estimated inactivation rates of *C. parvum* by alternative treatment technologies. The values are also plotted with the 95% confidence level. Oocysts were seeded at $2x10^7$ oocysts/L.

Although the PECO and PCO reactors differed with respect to hydroxyl radical production, they also differed with respect to the 9 V applied bias. This bias is sufficiently large to generate hydrogen and oxygen from water, and it is plausible that this bias is responsible for some *C. parvum* inactivation as well. The comparison of the PECO reactor with the electrolysis reactor reveals that this may be the case. When comparing these two reactors, the PECO reactor was 25 times faster for hydroxyl radical production and achieved a higher level of performance for *C. parvum* inactivation. Previous research (Curtis, 2002) compared a photocatalytic system to a photoelectrocatalytic system for the inactivation of *C. parvum*. The electric field enhancement improved the inactivation, but the improvement was attributed to the greater proportion of hydroxyl radicals on the cathode liquid surface of the catalyst. This is consistent with the results of this study, where the electrolysis component produced the lowest concentration of hydroxyl radicals when compared to the other active reactors. The comparison of PECO with both PCO and electrolysis suggests that electrolysis may play a larger role than hydroxyl radical production for *C. parvum* inactivation in the reactors tested. The mechanism by which electrolysis would achieve *C. parvum* inactivation requires further study.

As previously noted, the UV reactor used in this study (dose = 40 mJ/cm^2) achieved the highest generation rate of hydroxyl radicals ($k_{OH\text{-}UV}$ = 0.28 ± 0.01 μM/min) and, thus, that reactor likely achieved inactivation via a combination of both irradiation and hydroxyl radical

production. While the PECO was expected to have a superior performance than the other reactors for the hydroxyl radical component, previously published inactivation results for UV irradiation without hydroxyl radicals should not be ignored. In other studies, UV reactors have achieved 2-log inactivation of *C. parvum* at doses of 1 – 40 mJ/cm^2 (Amoah, 2005; Zimmer, 2003; Morita, 2002; Linden, 2001; Shin, 2001).

3.6. CONCLUSION

The rates of hydroxyl radical production and *C. parvum* inactivation had no dependence on the recirculation rate of the reactor. However, the reactor type affected the production of hydroxyl radicals within the system. When comparing PECO and electrolysis reactors, the PECO reactor was 25 times faster for hydroxyl radical production and achieved a higher level of performance for *C. parvum* inactivation. This comparison reveals that the applied bias may have a role in the inactivation of *C. parvum*. The PECO reactor did not produce the highest rate of hydroxyl radicals within a given system; the UV reactor produced hydroxyl radicals at the highest rate. Therefore, the PECO reactor was not the best method of generating hydroxyl radicals for these experiments. However, the reactor was the most efficient to inactivate *C. parvum.*

3.7 ACKNOWLEDGMENT

Support for this project was provided by AquaMost, Inc. and the National Science Foundation Integrative Graduate Education Research Traineeship Program. Martin Collins is thanked for his significant contribution to flow cytometer operation. Megan McConville is thanked for her significant contribution to DNPH preparation and HPLC operation. Matthew Russell is thanked for his contribution to hydroxyl radical experiment sampling.

3.8 REFERENCES

Amoah, K., Craik, S., Smith, D.W., and Belosevic, M. (2005) Inactivation of *Cryptosporidium* oocysts and *Giardia* cysts by ultraviolet light in the presence of natural particulate matter. Journal of Water Supply Research and Technology-Aqua 54: 165-178.

Assavasilavasukul, P., Lau, B.L.T., Harrington, G.W., Hoffman, R.M., and Borchardt, M.A. (2008) Effect of pathogen concentrations on removal of *Cryptosporidium* and *Giardia* by conventional drinking water treatment. Water Research 42: 2678-2690.

Campbell, A.T., Robertson, L.J., and Smith, H.V. (1992) Viability of *Cryptosporidium-Parvum* oocysts – Correlation of *in vitro* excystation with inclusion or exclusion of fluorogenic vital dyes. Applied and Environmental Microbiology 58: 3488-3493.

Centers for Disease Control and, P. (2013), Surveillance for waterborne disease outbreaks associated with drinking water and other nonrecreational water - United States, 2009-2010, MMWR. Morbidity and mortality weekly report, 62(35), 714-720.

Cho, E.-J., Yang, J.-Y., Lee, E.-S., Kim, S.-C., Cha, S.-Y., Kim, S.-T. (2013) A Waterborne Outbreak and Detection of *Cryptosporidium* Oocysts in Drinking Water of an Older High-Rise Apartment Complex in Seoul. Korean Journal of Parasitology 51: 461-466.

Cho, M., and Yoon, J. (2008) Measurement of OH radical CT for inactivating *Cryptosporidium* parvum using photo/ferrioxalate and photo/TiO2 systems. Journal of Applied Microbiology 104: 759-766.

Craik, S.A., Weldon, D., Finch, G.R., Bolton, J.R., and Belosevic, M. (2001) Inactivation of *Cryptosporidium* parvum oocysts using medium- and low-pressure ultraviolet radiation. Water Research 35: 1387-1398.

Curtis, T. P., Walker, G., Dowling, B.M., Christensen, P.A. (2002). Fate of *Cryptosporidium* oocysts in an immobilised titanium dioxide reactor with electric field enhancement. Water Research. 36, 2410-2413.

Dupont, H.L., Chappell, C.L., Sterling, C.R., Okhuysen, P.C., Rose, J.B., and Jakubowski, W. (1995) The infectivity of *Cryptosporidium parvum* in healthy volunteers. New England Journal of Medicine 332: 855-859.

Englehardt, J.D., and Swartout, J. (2006) Predictive Bayesian microbial dose-response assessment based on suggested self-organization in primary illness response: *Cryptosporidium parvum*. Risk Analysis 26: 543-554.

Fox, K.R., and Lytle, D.A. (1996) Milwaukee's crypto outbreak: Investigation and recommendations. American Water Works Association Journal 88: 87-94.

Harrington, G.W., Xagoraraki, I., Assavasilavasukul, P., and Standridge, J.H. (2003) Effect of filtration conditions on removal of emerging waterborne pathogens. Journal American Water Works Association 95: 95-104.

Hoefel, D., Grooby, W.L., Monis, P.T., Andrews, S., and Saint, C.P. (2003) Enumeration of water-borne bacteria using viability assays and flow cytometry: a comparison to culture-based techniques. Journal of Microbiological Methods 55: 585-597.

Hoffmann, M.R., Martin, S.T., Choi, W.Y., and Bahnemann, D.W. (1995) Environmental applications of semiconductor photocatalysis. Chemical Reviews 95: 69-96.

Johnson, A.M., Di Giovanni, G.D., and Rochelle, P.A. (2012) Comparison of assays for sensitive and reproducible detection of cell culture-infectious *Cryptosporidium parvum* and *Cryptosporidium hominis* in drinking water. Applied and Environmental Microbiology 78: 156-162.

Keenan, C. R., and D. L. Sedlak (2008), Factors affecting the yield of oxidants from the reaction of manoparticulate zero-valent iron and oxygen, Environmental Science & Technology, 42(4), 1262-1267.

Liao, C. H., Kang, S.F., Wu, F.A. (2001). Hydroxyl radical scavenging role of chloride and bicarbonate ions in the H_2O_2/UV process. Chemosphere. 44, 1193-1200.

Linden, K.G., Shin, G., and Sobsey, M.D. (2001) Comparative effectiveness of UV wavelengths for the inactivation of *Cryptosporidium parvum* oocysts in water. Water Science and Technology 43: 171-174.

Linsebigler, A.L., Lu, G.Q., and Yates, J.T. (1995) Photocatalysis of TiO_2 surfaces – Principles, mechanisms, and selected results. Chemical Reviews 95: 735-758.

Mackenzie, W.R., Hoxie, N.J., Proctor, M.E., Gradus, M.S., Blair, K.A., Peterson, D.E. (1994) A massive outbreak in Milwaukee of *Cryptosporidium* infection transmitted through the public water supply. New England Journal of Medicine 331: 161-167.

Messner, M.J., Chappell, C.L., and Okhuysen, P.C. (2001) Risk assessment for *Cryptosporidium*: A hierarchical Bayesian analysis of human dose response data. Water Research 35: 3934-3940.

Morita, S., A. Namikoshi, T. Hirata, K. Oguma, H. Katayama, S. Ohgaki, N. Motoyama, and M. Fujiwara (2002), Efficacy of UV irradiation in inactivating *Cryptosporidium parvum* oocysts, Applied and Environmental Microbiology, 68(11), 5387-5393.

Peeters, J. E., E. A. Mazas, W. J. Masschelein, I. V. M. Dematurana, and E. Debacker (1989), Effect of disinfection of drinking water with ozone or chloride dioxide on survival of Cryptosporidium parvum oocysts. Applied and Environmental Microbiology, 55(6), 1519-1522.

Rennecker, J.L., Corona-Vasquez, B., Driedger, A.M., Rubin, S.A., and Marinas, B.J. (2001) Inactivation of *Cryptosporidium parvum* oocysts with sequential application of ozone and combined chlorine. Water Science and Technology 43: 167-170.

Ryu, H., Gerrity, D., Crittenden, J.C., and Abbaszadegan, M. (2008) Photocatalytic inactivation of *Cryptosporidium parvum* with TiO_2 and low-pressure ultraviolet irradiation. Water Research 42: 1523-1530.

Shin, G.A., Linden, K.G., Arrowood, M.J., and Sobsey, M.D. (2001) Low-pressure UV inactivation and DNA repair potential of *Cryptosporidium parvum* oocysts. Applied and Environmental Microbiology 67: 3029-3032.

Tai, C., Peng, J.F., Liu, J.F., Jiang, G.B., and Zou, H. (2004) Determination of hydroxyl radicals in advanced oxidation processes with dimethyl sulfoxide trapping and liquid chromatography. Analytica Chimica Acta 527: 73-80.

White, M.G., Bensalem, O., and Ernst, W.R. (1982) The mathematical modeling of batch reactors for kinetics studies. Chemical Engineering Journal and the Biochemical Engineering Journal 25: 223-227.

Xagoraraki, I., Harrington, G.W., Assavasilavasukul, P., and Standridge, J.H. (2004) Removal of emerging waterborne pathogens and pathogen indicators by pilot-scale conventional treatment. Journal American Water Works Association 96: 102-113.

Xiao, S., An, W., Chen, Z., Zhang, D., Yu, J., and Yang, M. (2012) Occurrences and genotypes of *Cryptosporidium* oocysts in river network of southern-eastern China. Parasitology Research 110: 1701-1709.

Zanoni, M.V.B., Sene, J.J., Selcuk, H., and Anderson, M.A. (2004) Photoelectrocatalytic production of active chlorine on nanocrystalline titanium dioxide thin-film electrodes. Environmental Science & Technology 38: 3203-3208.

Zimmer, J.L., Slawson, R.M., and Huck, P.M. (2003) Inactivation and potential repair of *Cryptosporidium parvum* following low- and medium-pressure ultraviolet irradiation. Water Research 37: 3517-3523.

4. PRIMARY DEGRADATION OF TARTRAZINE USING PHOTOELECTROCATALYTIC OXIDATION

Kyana R.L. Young[a], Christina K. Remucal[a,b], Gregory W. Harrington[a]
[a]University of Wisconsin – Madison, Civil and Environmental Engineering, Madison, WI
[b] University of Wisconsin – Madison, Environmental Chemistry and Technology, Madison, WI

4.1. ABSTRACT

Advanced oxidation processes (AOP) are beneficial for treating contaminants that are typically not removed or inactivated using conventional biological or physical-chemical technologies. The effective component of AOP is the generation of hydroxyl radicals. There are a number of technologies that can generate hydroxyl radicals, where under the illumination of titanium dioxide by ultraviolet irradiation, electrons are moved into a higher energy state that leaves a hole capable of oxidation reactions. This hole can generate hydroxyl radicals but only if the rate of radical generation is faster than the rate at which the electron recombines with the hole. By applying a voltage bias to the titanium dioxide, the electrons are prevented from recombining with the hole, allowing for greater generation of hydroxyl radicals. This technique is known as photoelectrocatalytic oxidation (PECO). PECO has proven to be a more effective AOP technology for some applications.

This chapter investigates the degradation of tartrazine (FD&C Acid Yellow No. 23), by comparing operational parameters of recirculation rate, tartrazine concentration, chloride ion concentration, and applied bias voltage by treatment with PECO. Experiments were conducted in a recirculating batch reactor with tartrazine spiked in at an initial concentration of 2 to 12 mg/L per liter. Absorbance of tartrazine was measured using a spectrophotometer; the concentration was calculated using Beer's Law.

The first order inactivation rate constants were analyzed for tartrazine degradation, with independent variables of recirculation rate, tartrazine concentration, chloride ion concentration, and voltage. The concentration of tartrazine had no effect on the first-order rate constant. Similarly, there was no dependence of the degradation rate constant on recirculation rate. There was dependence of the first order reaction rate on chloride concentration. However, as the chloride ion concentration increased, performance eventually leveled off. The degradation rate constant increased as the voltage increased; this was observed when the electric potential was greater than 8V.

4.2. INTRODUCTION

The conjugated use of titanium dioxide and ultraviolet irradiation, UV/TiO_2, has shown promising results in the removal of pharmaceuticals, endocrine disrupting compounds, and industrial dyes from water (Wang 2010, Rajkumar 2006, Abou-Elela 2009). When the semiconductor TiO_2 is excited by ultraviolet (UV) light, electrons (e^-) move from the valence band to the conduction band, leaving holes (h^+) in the valence band. The holes can then oxidize substances dissolved in the bulk water of the system. These electrons require sufficient energy from photons (>3.2 eV) to move across the band gap and initiate redox reactions that are vital for the generation of hydroxyl radicals; the electrons on the surface of the TiO_2 move from the anode to the liquid-cathode interface. If the hydroxyl radicals do not participate in reactions within nanoseconds of electron promotion to the conduction band, recombination of the electron back to the hole occurs (Hoffmann, 1995). The powerful oxidizing capability of hydroxyl radicals makes UV/TiO_2 appealing to be implemented for water treatment, as it can contribute to the degradation of tartrazine and other target contaminants.

The limiting step in this advanced oxidation process is the availability of constant applied energy (i.e. UV light), which encourages e^-/h^+ separation. While the current process of UV/TiO_2 has been successful at treating a host of contaminants, further exploration into the development of improved technologies continues to be investigated. This exploration motivated the development for uses of electrical currents to supplement the e^-/h^+ separation. The inclusion of the electrical current is known as photoelectrocatalytic oxidation (PECO).

Zanoni (2004) reported that use of electrical current bends the valence band away from the conduction band, therefore increasing the distance the electron has to travel to recombine with the hole-pair. This increased distance allows for sufficient time for redox reactions to occur, thus increasing the availability of hydroxyl radicals that contribute to treatment efficiency.

The efficiency of the reactor is subjected to the operational configuration of PECO, the ability to activate titanium-dioxide by UV irradiation, and the implementation of the photoactive electrode to generate two powerful oxidants within the bulk water: free chlorine and hydroxyl radicals. For example, free chlorine species (HOCl, OCl^-, and Cl_2) are produced by oxidation of dissolved chloride ions, added as sodium chloride (NaCl) in water. These free chlorine species can assist in the oxidation of substances dissolved in the bulk water.

The treatment of water containing tartrazine is categorized by three components: the degradation of tartrazine color, the mineralization of the tartrazine, and the by-product formation of the carbon bond destruction (Ghaly, 2013). These three components are referred to as primary, secondary, and tertiary degradation, respectively. This study analyzed the primary degradation of tartrazine, based on four operational parameters: initial tartrazine concentration, recirculation rate through the device, chloride concentration (added as NaCl), and applied voltage.

4.3 MATERIALS

Analytical grade tartrazine (Acid Yellow No. 23, $C_{16}H_9N_4Na_3O_9S_2$, molecular weight = 534.3 g/mol, water solubility = 140 g/L at 25°C, λ_{max} = 425nm) was obtained from Alfa Aesar, and used as received in powder form. Analytical grade sodium chloride (NaCl, molecular weight = 58.44 g/mol, water solubility = 35.65 g/l at 25°C) was obtained from Sigma Aldrich and used as received. Milli-Q water 18.2 MΩ·cm at 25ºC was used as the water source for tartrazine preparation, as well as the bulk water volume for the experiments.

The reactor, containing a UV light, an anode with TiO_2 immobilized film, and a titanium cathode, was designed, manufactured, and prepared by AquaMost, Inc, in Madison, WI. A more complete description of the reactor is provided elsewhere (Young, 2014). The method used to manufacture the immobilized film is considered proprietary.

4.4 EXPERIMENTAL METHODS

4.4.a. Hydroxyl Radical Experiments

Refer to Chapter 3 regarding Hydroxyl Radical Experiments, where the production rates of hydroxyl radicals within the PCO and PECO reactor was analyzed using HPLC. Recirculation rates of 2.8, 4.1, and 5.4 L/min were chosen as the operational parameter.

4.4.b. Chlorine Concentration Experiments

Experiments for chlorine generation were performed at the Water Science and Engineering Laboratory at the University of Wisconsin – Madison. All experiments used a 7.0-L capacity closed container aquarium tanks filled with 4.0 L of Milli-Q water at 25ºC. Each tank housed a 7.8-W Mini Jet MN404 pump (Max Q = 6.7 L/min), connected to two 23-inch long, ½” ID x ¾” OD vinyl tubes, that was operated at a recirculation rate of 4.1 L/min (Young, 2014). A

DC power supply (Atten Instruments, APS3005S, Regulated DC Power Supply) source was used to apply a potential 9V to the PECO reactor. The chloride ion concentration ranged from 50 mg/L – 500 mg/L.

4.4.c. Tartrazine Degradation Experiments

Experiments for tartrazine degradation were performed at the Water Science and Engineering Laboratory at the University of Wisconsin – Madison. All experiments used six 7.0-L capacity closed container aquarium tanks filled with 4.0 L of Milli-Q water at 25ºC. The nascent stage of the experimental process began with the identification of four independent operational parameters: applied voltage (0 V to 12 V), recirculation rate through the device (2.9 L/min to 5.4 L/min), initial chloride concentration (20.8 mg/L to 250.0 mg/L), and initial tartrazine concentration (3.0 mg/L to 12.0 mg/L). Five separate PECO units were operated with identical experimental operational conditions to quantify variability in anode production, while the sixth PECO unit served as the control. Each tank housed a 7.8-W Mini Jet MN404 pump (Max Q = 6.7 L/min), connected to two 23-inch long, ½" ID x ¾" OD vinyl tubes, that was operated at a recirculation rate of 2.9 to 5.4 L/min (Young, 2014). Although the pump had an adjustable recirculation rate, the pump was operated at a steady recirculation rate throughout the duration of each experiment. A DC power supply (Atten Instruments, APS3005S, Regulated DC Power Supply) source was used to apply a potential (0 V to 12 V) to the PECO reactor.

Prior to turning on the UV lamp, the 4.0 L of water were dosed with a specified mass of tartrazine and NaCl, and the resulting mixture was allowed to recirculate through the system for ten minutes. This pre-sampling recirculation established a homogenous concentration throughout the entire system. Both the tartrazine concentration and pH were monitored and recorded before the PECO device was used and throughout the duration of each experiment. The initial free chlorine concentration was 0 mg/L, as the device was used to generate chlorine by oxidation of chloride.

4.5 ANALYTICAL METHODS

4.5.a. Hydroxyl Radical Analysis

Refer to Chapter 3 regarding Hydroxyl Radical Analysis, where the data was fit using a zero order reaction model. The reaction rate was determined by calculating the slope of the best-fit line, and the 95% confidence interval was also determined for the inactivation rate.

4.5.b. Chlorine Concentration

Temperature was recorded using an infrared digital thermometer. Ten mL samples were collected at specified time intervals. Chlorine concentration was measured using the DPD (N,N,-diethyl-p-phenylenediamine) standard method (Standard Method 4500 – CI G, 2013).

4.5.c. Tartrazine Concentration

To determine the concentration of tartrazine within the system, absorbance values were measured with a HACH DR/820 * DR/850 Datalogging Colorimeter. The spectrophotometer readings were converted to concentration through use of Beer's Law (Equations 4-1 and 4-2) (Pfeiffer, 1951):

$$A = \varepsilon \times l \times c \qquad \text{Equation 4-1}$$

$$c = \frac{A}{\varepsilon l} \qquad \text{Equation 4-2}$$

where A is the absorbance of the solution at λ_{max} = 425nm, ε is the molar absorptivity (3.64 x 10^4 M^{-1} cm^{-1}), l is the path length of the sample that the light passes through (1 cm), and c is the analyte concentration of the sample (mol L^{-1}). The primary degradation (color) of tartrazine was measured using the spectrophotometer, and graphed using a first-order reaction rate model (Equations 4-3 and 4-4), as a natural log of the final concentration and initial concentration versus time.

$$\frac{dC}{dt} = -kC \qquad \text{Equation 4-3}$$

$$C = C_0 e^{-kt} \qquad \text{Equation 4-4}$$

4.6 RESULTS

4.6.a. Hydroxyl Radicals

Refer to Chapter 3 regarding Hydroxyl Radical Results, where the hydroxyl radical production rates for the PCO and PECO reactors were presented. The PECO combined production rate for the three respective recirculation rates was 0.015 ± 0.002 μM/min, while the PCO reactor had a combined production rate of 0.011 ± 0.002 μM/min.

4.6.b Tartrazine Degradation

4.6.b.1 Effect of initial tartrazine concentration on tartrazine degradation

Figure 4-1 shows the primary degradation of tartrazine over a time period of 1.2 days. The operational conditions for the experiment were [Cl^-] = 100 mg/L, voltage = 9 V, and recirculation rate = 4.1 L/min. The primary degradation followed a first order reaction rate as demonstrated by fits with several rate laws. To confirm this, the recirculating batch reactor was spiked with tartrazine at several initial concentrations to see if the rate constant was independent of initial concentration. As shown in Figure 4-2, the increasing initial concentration of tartrazine had little effect on the first-order rate constant. Because the first-order rate constant estimates were independent of initial concentration and models with other orders of reaction showed such a dependence, a first-order model was deemed appropriate for primary degradation of tartrazine. These results also suggest that the finite number of active sites on the surface of the TiO_2 were sufficient in number to manage the increased dye concentration (Daneshvar 2006, Lhomme 2005, Jain, 2008, Krishnakumar, 2011, Vautier, 2001). Based on these results, first–order reaction kinetics were applied to all degradation experiments including those run over shorter time durations.

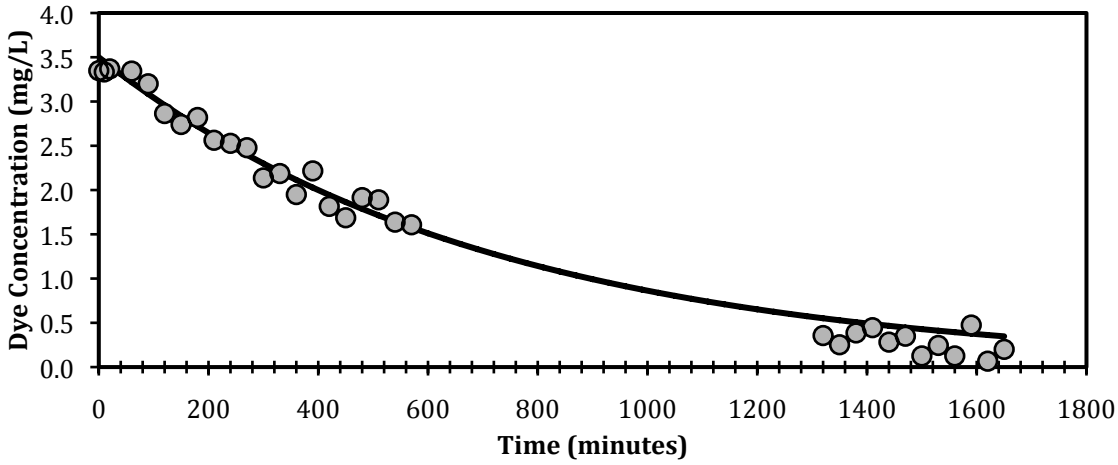

Figure 4-1: Tartrazine dye degradation for initial tartrazine concentration = 3.5 mg/L, [Cl^-] = 100 mg/L, voltage = 9.0 V, and recirculation rate = 4.1 L/min.

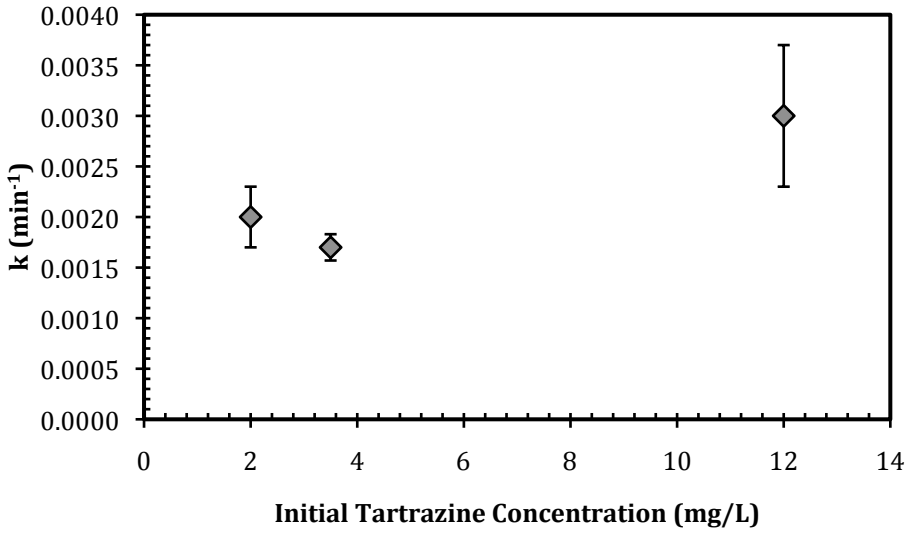

Figure 4-2: Influence of initial tartrazine concentration on the degradation rate of tartrazine dye, with the 95% confidence interval. Operational parameters: recirculation rate = 4.1 L/min, voltage = 9 V, chloride concentration = 100 mg/L.

4.6.b.2 Effect of recirculation rate of bulk water on the degradation of tartrazine

Figure 4-3 shows the influence of recirculation rate on the estimated tartrazine degradation rate constant. There was no statistically significant dependence of the degradation rate constant on increasing recirculation rate. The increase of flow through the reactor was expected to decrease the residence time for each pass through the reactor, but total residence time

within the recirculating batch reactor is equal regardless of recirculation rate (White, 1982). Thus, the result was consistent with expectation.

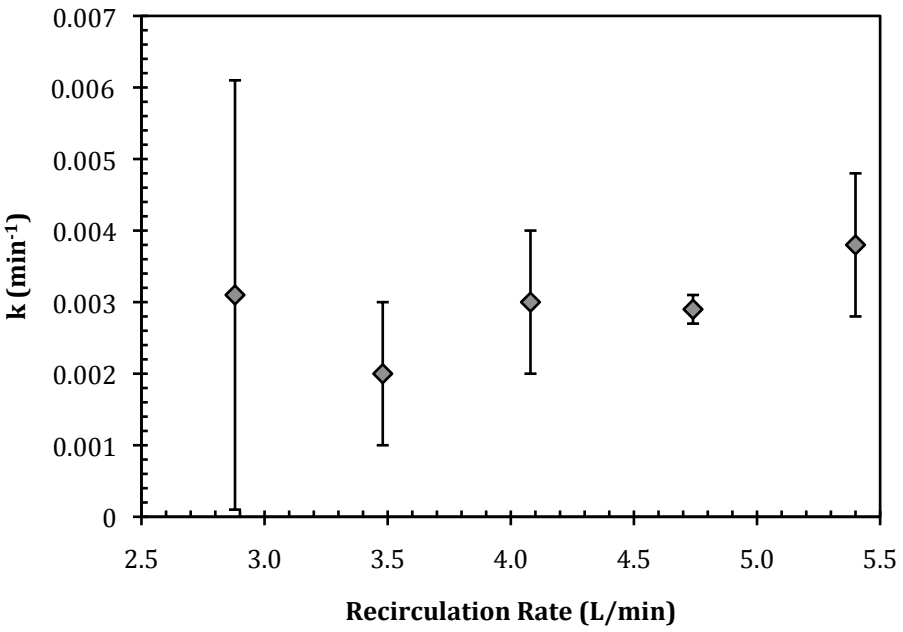

Figure 4-3: Effect of recirculation rate on primary degradation rate of tartrazine. Error bars show 95% confidence interval. Initial tartrazine concentration = 12 mg/L, [Cl^-] = 100 mg/L, voltage = 9.0 V.

4.6.b.3 Effect of chloride concentration on tartrazine degradation

The estimates for the reaction rate constants are shown in Figure 4-4, where the degradation rate of tartrazine increased with increasing chloride concentration for chloride concentrations less than 62 mg/L. However, there was no observable effect of chloride concentration for chloride concentrations greater than 124 mg/L. Because there is little degradation of tartrazine at small chloride concentration, it appears that chlorine generation is the primary route of tartrazine degradation.

The asymptotic shape for the data in Figure 4-4 is expected. With the irradiation of the TiO_2 by UV, the TiO_2 surface becomes more cationic making it more likely that the holes would attract the chloride ions (Wang, 2006). When the concentrations of chloride ions in a system are increased, increasing numbers of ions adsorb to the surface of the catalyst and prevent

recombination of hole-pair (Zanoni, 2004). This stunted recombination increases production of free chlorine and hydroxyl radicals, leading to an increasing likelihood for tartrazine degradation (Wang, 2011; Zanoni, 2004). In addition, the flow of electrical charge, current, also increases as the chloride ion increases, providing an increased opportunity for oxidation reactions of chloride ions to produce chlorine (Figure 4-5, 4-6).

As the chloride ion concentration continues to increase, the ions may occupy the catalyst surface and prevent the dye reacting with the surface (Yuan, 2012).

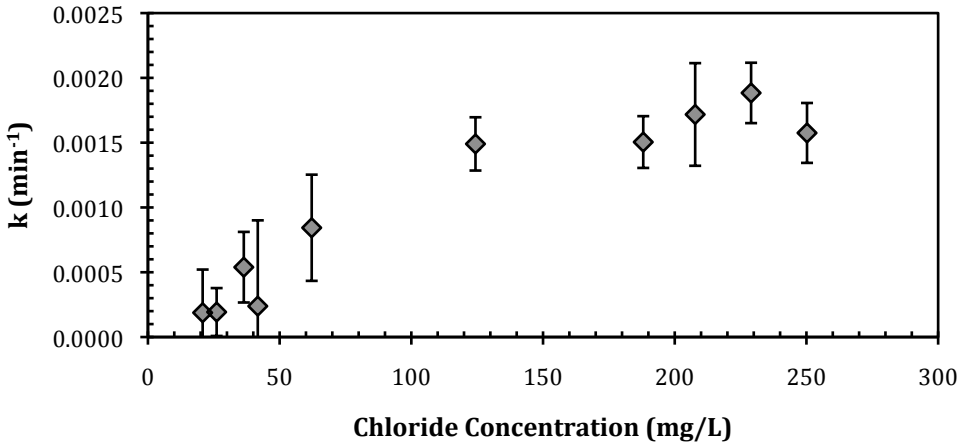

Figure 4-4: Effect of chloride concentration on tartrazine degradation kinetics. Error bars show 95% confidence interval. Recirculation rate = 4.1 L/min, initial tartrazine concentration = 12 mg/L, and voltage = 9 V.

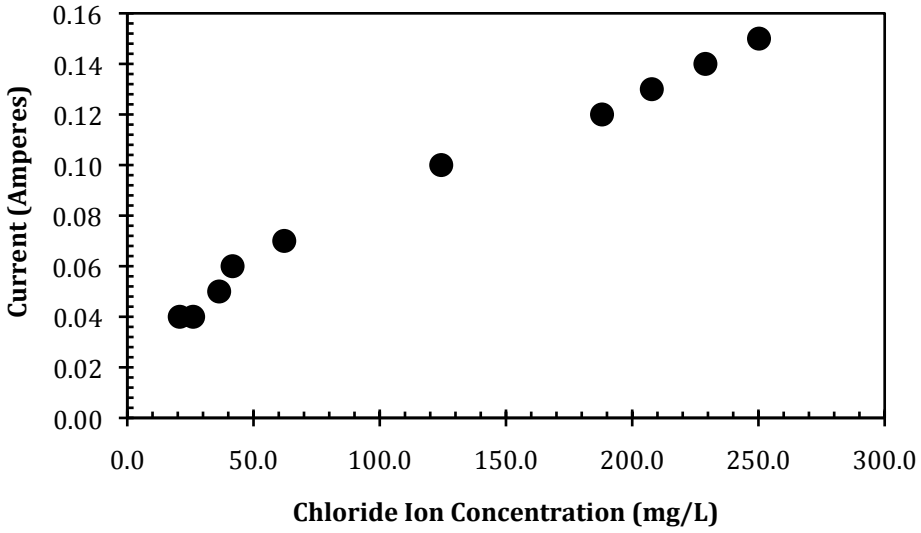

Figure 4-5: Effect of chloride concentration on current within a PECO reactor. Recirculation rate = 4.1 L/min, initial tartrazine concentration = 12 mg/L, and voltage = 9 V.

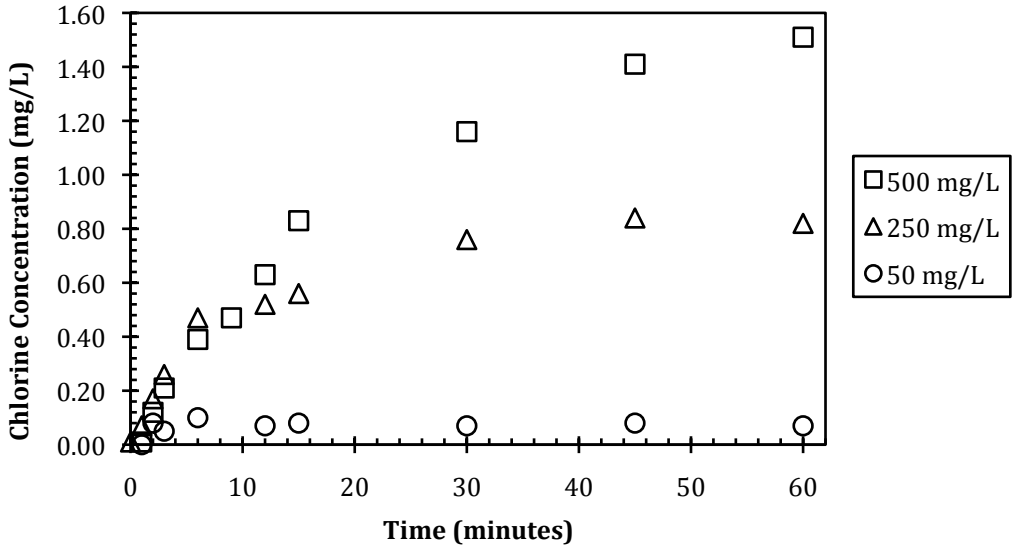

Figure 4-6: Effect of chloride concentration on chlorine production within a PECO reactor. Chloride ion concentration = 50 mg/L – 500 mg/L, recirculation rate = 4.1 L/min, voltage = 9V.

4.6.b.4 Effect of voltage on tartrazine degradation

As the voltage increases, the degradation rate increases but this observation is only apparent at electric potentials higher than 8 V (Figure 4-7). At potentials less than 8 V, there was

no significant difference between applied voltages. The highest degradation rate occurred at the highest applied voltage, 12V: $k_{12V} = 0.0033\ min^{-1}$.

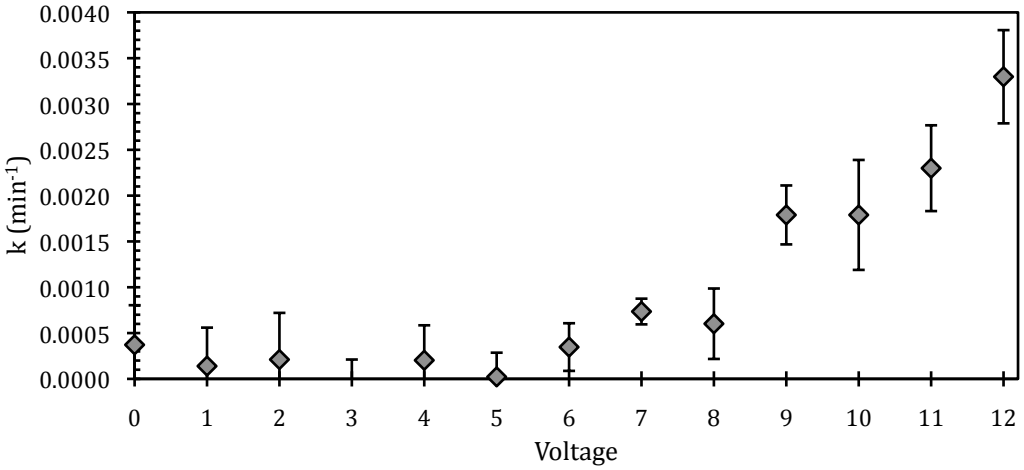

Figure 4-7: Effect of applied voltage on tartrazine decolorization. Error bars show 95% confidence interval. [Cl^-] = 100 mg/L, initial tartrazine concentration = 12 mg/L, and recirculation rate = 4.1 L/min.

Increasing the applied voltage reduces electron-hole recombination, allowing for increased chlorine and/or hydroxyl radical production (Zanoni, 2004). The electrode, connected to the semiconductor, is responsible for bending the valence band away from the conduction band, increasing the distance between the electron and the hole pair. Also, the electrons are now attracted to the increased positive potential of the anode. This deficiency in recombination assists with more holes to 1) react with H_2O, generating hydroxyl radicals on the surface of the TiO_2 surface and 2) participate in the oxidation of chloride to chlorine. The chlorine and hydroxyl radicals then oxidize the dye, to degrade the dye over time. However, as per notification from AquaMost, Inc, degradation of anodes over serial use of the PECO may decrease the voltage performance; the reactor required higher voltages over time to achieve similar current as when the anodes were newer. This aging is due to passivation of the anode, where the titanium metal becomes oxidized at the surface and no photocatalytic activity can take place on the TiO_2 surface. To counteract the passivation, the electrodes may be heated at high temperature to produce anatase or rutile crystals forms of TiO_2. These crystallized forms are suitable for photocatalytic activity. Heating of the electrodes was not performed for the aforementioned experiments.

4.7 CONCLUSIONS

Neither hydroxyl radical production, nor dye degradation, had dependence on the recirculation rate of the reactor. However, increasing applied voltage and chloride ion concentration demonstrated the greatest increase in degradation rates. For chloride ion concentration, holes within the device generate chlorine through oxidation of chloride ions; the chlorine serves as the main component of the tartrazine color removal. For the applied voltage, the electrode connected to the semiconductor is responsible for bending the valence band away from the conduction band, increasing the distance between the electron and the hole pair. This deficiency in recombination assists with more holes to react with H_2O, to generate hydroxyl radicals on the surface of the TiO_2 catalyst which then oxidizes the dye over time. Both the applied voltage and chloride ion concentration are effective and provide the best operational improvement for the overall tartrazine concentration degradation.

4.8 ACKNOWLEDGMENTS

Support for this project was provided by AquaMost, Inc, the National Science Foundation Integrative Graduate Education Research Traineeship Program, and Graduate Engineering Research Scholars Program. Megan McConville is thanked for her significant contribution to DNPH preparation, and HPLC operation. The contributions of Matthew Russell, Keiva Coppage, YiFan Li, and Nelson Chan, for sampling and data analysis, were superior for undergraduate participation; their involvement is greatly appreciated.

4.9 REFERENCES

Abou-Elela, S. I., and M. A. El-Khateeb (2009), Treatment of ink wastewater via heterogeneous photocatalytic oxidation, Desalination and Water Treatment, 7(1-3), 1-5.

Banerjee, A. N., S. W. Joo, and B.-K. Min (2012), Photocatalytic Degradation of Organic Dye by Sol-Gel-Derived Gallium-Doped Anatase Titanium Oxide Nanoparticles for Environmental Remediation, Journal of Nanomaterials.

Daneshvar, N., D. Salari, A. Niaei, and A. R. Khataee (2006), Photocatalytic degradation of the herbicide erioglaucine in the presence of nanosized titanium dioxide: Comparison and modeling of reaction kinetics, Journal of Environmental Science and Health Part B-Pesticides Food Contaminants and Agricultural Wastes, 41(8), 1273-1290.

Ghaly, M. Y., J. Y. Farah, and A. M. Fathy (2007), Enhancement of decolorization rate and COD removal from dyes containing wastewater by the addition of hydrogen peroxide under solar photocatalytic oxidation, Desalination, 217(1-3), 74-84.

Hoffmann, M. R., S. T. Martin, W. Y. Choi, and D. W. Bahnemann (1995), Environmental Applications of Semiconductor Photocatalysis, Chemical Reviews, 95(1), 69-96.

Jain, R., and S. Sikarwar (2008), Photodestruction and COD removal of toxic dye erioglaucine by TiO(2)-UV process: influence of operational parameters, International Journal of Physical Sciences, 3(12), 299-305.

Jain, R., and S. Sikarwar (2010), Adsorptive and Desorption Studies on Toxic Dye Erioglaucine Over Deoiled Mustard, Journal of Dispersion Science and Technology, 31(7), 883-893.

Jones, A. P., and R. J. Watts (1997), Dry phase titanium dioxide-mediated photocatalysis: Basis for in situ surface destruction of hazardous chemicals, Journal of Environmental Engineering-Asce, 123(10), 974-981.

Krishnakumar, B., and M. Swaminathan (2011), Influence of operational parameters on photocatalytic degradation of a genotoxic azo dye Acid Violet 7 in aqueous ZnO suspensions, Spectrochimica Acta Part a-Molecular and Biomolecular Spectroscopy, 81(1), 739-744.

Lhomme, L., S. Brosillon, and D. Wolbert (2008), Photocatalytic degradation of pesticides in pure water and a commercial agricultural solution on TiO2 coated media, Chemosphere, 70(3), 381-386.

Pfieffer, H.G., Liebhafsky, H. A. (1951),The origins of Beer's law, Journal of Chemical Education 28(3), 123.

Rajkumar, D., and J. Guk Kim (2006), Oxidation of various reactive dyes with in situ electro-generated active chlorine for textile dyeing industry wastewater treatment, Journal of Hazardous Materials, 136(2), 203-212.

Vautier, M., C. Guillard, and J. M. Herrmann (2001), Photocatalytic degradation of dyes in water: Case study of indigo and of indigo carmine, Journal of Catalysis, 201(1), 46-59.

Wang, W.-Y., M.-L. Yang, and Y. Ku (2010), Photoelectrocatalytic decomposition of dye in aqueous solution using Nafion as an electrolyte. Chemical Engineering Journal, 165(1), 273-280.

Wang, X.-K., Y.-C. Wei, C. Wang, W.-L. Guo, J.-G. Wang, and J.-X. Jiang (2011), Ultrasonic degradation of reactive brilliant red K-2BP in water with CCl4 enhancement: Performance optimization and degradation mechanism, Separation and Purification Technology, 81(1), 69-76.

White, M. G., O. Bensalem, and W. R. Ernst (1982), The mathematical-modeling of batch recirculation reactors for kinetics studies, Chemical Engineering Journal and the Biochemical Engineering Journal, 25(2), 223-227.

Young, K.R.L., Remucal, C.K., Harrington, G.W. (2014), Primary degradation of tartrazine using photoelectrocatalytic oxidation [In preparation for submission]

Zanoni, M. V. B., J. J. Sene, H. Selcuk, and M. A. Anderson (2004), Photoelectrocatalytic production of active chlorine on nanocrystalline titanium dioxide thin-film electrodes, Environmental Science & Technology, 38(11), 3203-3208.

5. PRIMARY DEGRADATION OF ERIOGLAUCINE USING PHOTOELECTROCATALYTIC OXIDATION

Kyana R.L. Young[a], Christina K. Remucal[a,b], Gregory W. Harrington[a]
[a]University of Wisconsin – Madison, Civil and Environmental Engineering, Madison, WI
[b] University of Wisconsin – Madison, Environmental Chemistry and Technology, Madison, WI

5.1. ABSTRACT

Advanced oxidation processes (AOP) are beneficial for treating contaminants that are typically not removed or inactivated using conventional biological or physical-chemical technologies. The effective component of AOP is the generation of hydroxyl radicals. There are a number of technologies that can generate hydroxyl radicals, where under the illumination of titanium dioxide by ultraviolet irradiation, electrons are moved into a higher energy state that leaves a hole capable of oxidation reactions. This hole can generate hydroxyl radicals but only if the rate of radical generation is faster than the rate at which the electron recombines with the hole. By applying a voltage bias to the titanium dioxide, the electrons are prevented from recombining with the hole, allowing for greater generation of hydroxyl radicals. This technique is known as photoelectrocatalytic oxidation (PECO). PECO has proven to be a more effective AOP technology for some applications.

This chapter investigates the degradation of erioglaucine (FD&C Acid Blue No. 5), by comparing operational parameters of recirculation rate, erioglaucine concentration, and applied bias voltage by treatment with PECO. Experiments were conducted in a recirculating batch reactor with erioglaucine spiked in at an initial concentration of about 20 mg/L per liter. Absorbance of erioglaucine was measured using a spectrophotometer; the concentration was calculated using Beer's Law.

The first order inactivation rate constants were analyzed for erioglaucine degradation, with independent variables of recirculation rate, erioglaucine concentration, and voltage. The recirculation rate of 4.1 L/min, applied voltage = 9V, chloride ion concentration = 100.0 mg/L, and 10.0 mg/L concentration of the erioglaucine achieved the highest degradation rate, k = 0.0173± 0.00004 min^{-1}, of all the respective experiments.

5.2. INTRODUCTION

The conjugated use of titanium dioxide and ultraviolet irradiation, UV/TiO_2, has shown promising results in the removal of pharmaceuticals, endocrine disrupting compounds, and industrial dyes from water (Wang 2010, Rajkumar 2006, Abou-Elela 2009). When the semiconductor TiO_2 is excited by ultraviolet (UV) light, electrons (e^-) move from the valence band to the conduction band, leaving holes (h^+) in the valence band. The holes can then oxidize contaminants found in the bulk water of the system. These electrons require sufficient energy from photons (>3.2 eV) to move across the band gap and initiate redox reactions that are vital for the generation of hydroxyl radicals; the electrons on the surface of the TiO_2 move from the anode to the liquid-cathode interface. If the hydroxyl radicals do not participate in reactions within nanoseconds of electron promotion to the conduction band, recombination of the electron back to the hole occurs (Hoffmann, 1995). The powerful oxidizing capability of hydroxyl radicals makes UV/TiO_2appealing to be implemented for water treatment, as it can contribute to the degradation of erioglaucine and other target contaminants.

The limiting step in this advanced oxidation process is the availability of constant applied energy, which encourages the e^-/h^+ separation. While the current process of UV/TiO_2 has been successful at treating a host of contaminants, further exploration into the development of improved technologies continues to be investigated. This exploration motivated the development for uses of electrical currents to supplement the e^-/h^+ separation. The inclusion of the electrical current is known as photoelectrocatalytic oxidation (PECO).

Other electrolysis experiments have shown degradation of dispersed dyes up to 90% compared to that of photocatalysis (UV/TiO_2), or electrolysis (1 V) (Banerjee, 2012). Zanoni (2004) reported that use of electrical current bends the valence band away from the conduction band, therefore increasing the distance the electron has to travel to recombine with the hole-pair. This increased distance allows for sufficient time for redox reactions to occur, thus increasing the availability of hydroxyl radicals that contribute to treatment efficiency.

The efficiency of the reactor is subjected to the operational configuration of PECO, the ability to activate titanium-dioxide by UV irradiation, and the implementation of the photoactive electrode to generate two powerful oxidants within the bulk water: free chlorine and hydroxyl radicals. For this paper, the free chlorine species (HOCl, OCl^-, and Cl_2) are produced by oxidation of dissolved chloride ions, added as sodium chloride (NaCl) in water.

The treatment of water containing erioglaucine is categorized by three components: the degradation of erioglaucine color, the mineralization of the erioglaucine, and the by-product formation of the carbon bond destruction (Ghaly, 2013). These three components are referred to as primary, secondary, and tertiary degradation, respectively. This study analyzed the primary degradation of erioglaucine, based on three operational parameters: initial erioglaucine concentration, recirculation rate through the device, and applied voltage.

5.3. EXPERIMENTAL APPROACH

5.3.a. Materials

Erioglaucine (Acid Blue No. 5, $C_{37}H_{34}Na_2N_2O_9S_3$, Molecular Weight = 792.85 g/mol, water solubility = 50 g/L, LD_{50} = 4600 mg/kg, λ_{max} = 629nm) was purchased from Aldrich and used as received, in powder form. Sodium chloride (NaCl), ACS grade (Molecular Weight = 58.44 g/mol, water solubility = 359 g/L, LD_{50} = 3550 mg/kg) was purchased from Sigma-Aldrich and used as received. Milli-Q water 18.2 MΩ·cm at 25ºC was used as the water source for erioglaucine preparation, as well as the bulk water volume for the experiments.

The reactor, containing a UV light, an anode with TiO_2 immobilized film, and a titanium cathode, was designed, manufactured, and prepared by AquaMost, Inc, in Madison, WI. A more complete description of the reactor is provided elsewhere (Young, 2014). The method used to manufacture the immobilized film is considered proprietary.

5.4 EXPERIMENTAL METHODS

5.4.a Hydroxyl Radical Experiments

Refer to Chapter 3 regarding Hydroxyl Radical Experiments, where the production rate of hydroxyl radicals within the PCO and PECO reactor is analyzed using HPLC. Recirculation rates of 2.8, 4.1, and 5.4 L/min were chosen as the operational parameter.

5.4.b. Erioglaucine Degradation Experiments

These experiments focused on the optimization of the PECO device for dye degradation, using erioglaucine as the target dye. The nascent stage of the experimental process began with the identification of five independent variables: applied voltage, water recirculation rate through the device, and dye concentration. Experiments were performed at the Water Science and

Engineering Laboratory at the University of Wisconsin – Madison. All experiments used six 7.0-L capacity closed container aquarium tanks filled with 4.0 L of Milli-Q water (18.2 MΩ·cm) at 25ºC. Five separate PECO units were operated with identical experimental conditions (recirculation rate, dye concentration, and voltage), while the sixth PECO unit served as the control. Each tank housed a 7.8 W Mini Jet MN404 106 GPH pump, connected to two 23-inch long, ½" ID x ¾" OD vinyl tubes, which facilitated the recirculation of water at a rate of 2.9 to 5.4 L/min (Young, 2014). Although the pump has an adjustable recirculation rate, the pump was operated at a steady recirculation rate throughout the duration of each experiment. A DC power supply (Atten Instruments, APS3005S, Regulated DC Power Supply) source has attached positive (anode) and negative (cathode) wires to their respective ends of the reactor, allowing a potential (0 V to 12 V) to be applied to the respective reactor.

A specified mass (0.12 g to 0.80 g) of dye, and 100 mg/L of chloride, were dosed into 4.0 L of Milli-Q with 18.2 MΩ·cm at 25ºC. The dye-water mixture was allowed to recirculate throughout the system for ten minutes; this pre-sampling recirculation established a homogenous solution concentration throughout the entire system. Both the dye concentration and pH were monitored and recorded before the PECO device was used. Ten (10) mL of sample, taken every 10 minutes for an hour, was analyzed for absorbance values.

5.5 ANALYTICAL METHODS

5.5.a. Erioglaucine Concentration

To determine the concentration of erioglaucine within the system, the absorbance values were measured with a HACH DR/820 * DR/850 Datalogging Colorimeter. The spectrophotometer readings were converted to concentration through use of Beer's Law (Equations 5-1 and 5-2) (Pfeiffer, 1951):

$$A = \varepsilon \times l \times c \qquad \text{Equation 5 - 1}$$

$$c = \frac{A}{\varepsilon l} \qquad \text{Equation 5 - 2}$$

where A is the absorbance of the solution, ε is the molar absorptivity (9.8 x 10^4 L mol^{-1} cm^{-1}), l is the path length of the sample that the light passes through (1 cm), and c is the analyte concentration of the sample (mol L^{-1}). The primary degradation (color) of erioglaucine was

measured using the spectrophotometer, and graphed using a first-order reaction rate model (Equations 5-3 and 5-4), as a natural log of the final concentration and initial concentration versus time.

$$\frac{dC}{dt} = -kC \qquad \text{Equation 5-3}$$

$$C = C_0 e^{-kt} \qquad \text{Equation 5-4}$$

5.5.b. Hydroxyl Radical Analysis

Refer to Chapter 3 regarding Hydroxyl Radical Analysis, where the data was fit using a zero order reaction model. The reaction rate was determined by calculating the slope of the best-fit line, and the 95% confidence interval was also determined for the inactivation rate.

5.6 RESULTS

5.6.a. Hydroxyl Radicals

Refer to Chapter 3 regarding Hydroxyl Radical Results, where the hydroxyl radical production rates for the PCO and PECO reactors were presented. The PECO combined production rate for the three respective recirculation rates was 0.015 ± 0.002 μM/min, while the PCO reactor had a combined production rate of 0.011 ± 0.002 μM/min.

5.6.b Erioglaucine degradation

5.6.b.1 Effect of initial erioglaucine concentration on erioglaucine degradation

Figure 5-1 shows the primary degradation of erioglaucine for a time period of 26 hours, where the operational parameters for the experiment were initial dye concentration = 10.0 mg/L. [Cl^-] = 100.0 mg/L, voltage = 9.0 V, and recirculation rate = 4.1 L/min. The primary degradation followed a first order reaction rate as demonstrated by fits with several rate laws. The system was monitored for dye degradation at concentrations of 3.0, 3.5, and 10 mg/L, to determine if the rate constant was independent on initial concentration of erioglaucine. The first order model estimates were independent of the initial concentration, and thus deemed appropriate to model the subsequent erioglaucine experiments with the same rate model.

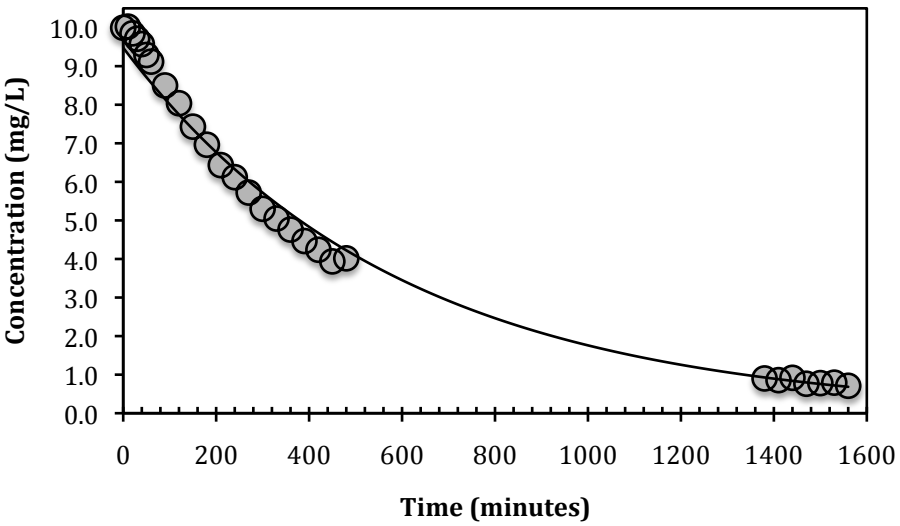

Figure 5-1: Erioglaucine dye concentration degradation for initial dye concentration = 10.0 mg/L. [Cl^-] = 100.0 mg/L, voltage = 9.0 V, and recirculation rate = 4.1 L/min.

The increasing concentration of erioglaucine did not affect the overall degradation rate – the rate constants lie within the range for the 95% confidence level (Figure 5-2). For this experiment, the degradation of the dye is dependent on the rate constant of the initial concentration of the dye. The results suggest that the finite number of active sites on the surface of the TiO_2 were sufficient in number to manage the increase in dye concentration (Daneshvar 2006, Lhomme 2005, Jain 2008, Krishnakumar 2011, Vautier 2001), and that the there was not a carrying capacity for PECO reactor to treat a range of dye concentration.

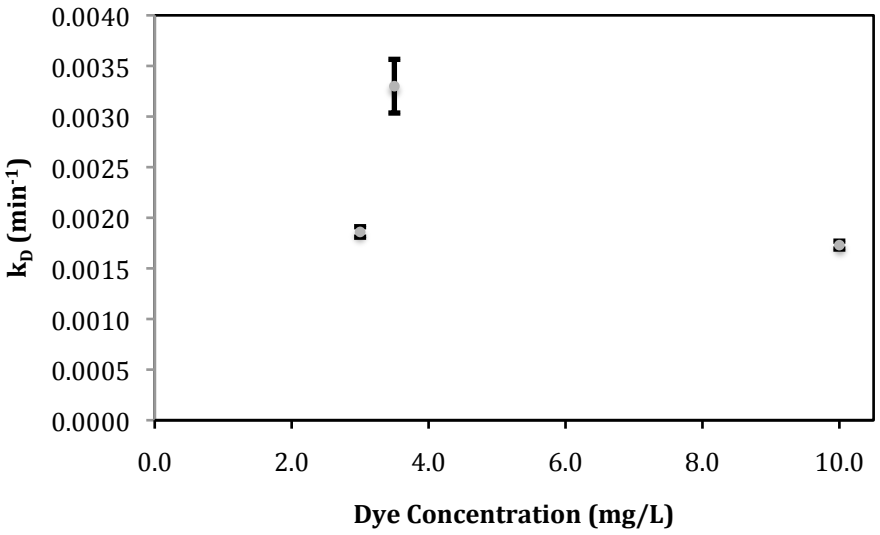

Figure 5-2: Degradation rate of erioglaucine, k_D, for varying dye concentration, showing 95% confidence level in the parameter estimate. [Cl^-] = 100.0 mg/L, voltage = 9.0 V, and recirculation rate = 4.1 L/min

5.6.b.2 Effect of recirculation rate of water on the removal of dye

The influence of recirculation rate on the estimated erioglaucine degradation rate constant was not significant (Figure 5-3). The combined degradation rate constant for this set of experiments was 0.0027 ± 0.002 min^{-1}.

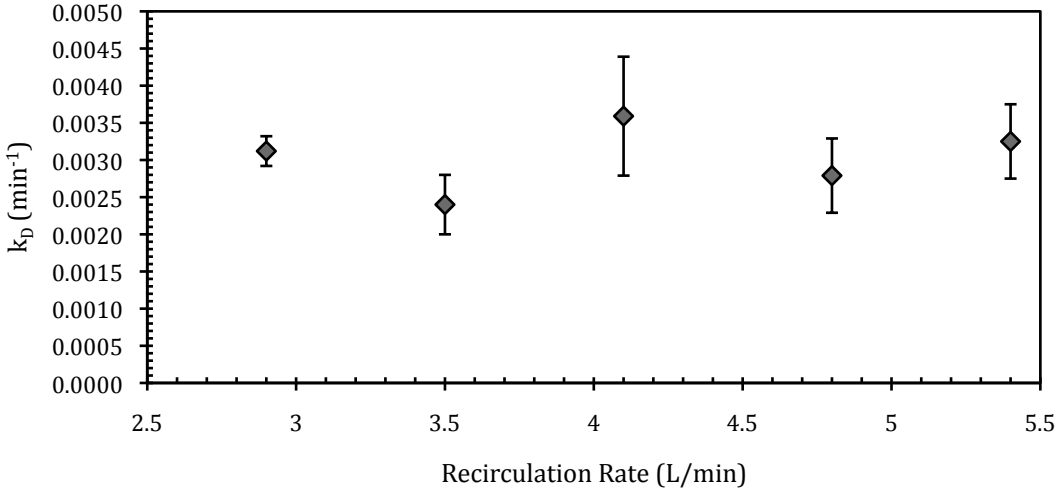

Figure 5-3: Degradation rate of erioglaucine, k, for varying recirculation rate, showing 95% confidence level in the parameter estimate. [Cl^-] = 100.0 mg/L, voltage = 9.0 V, dye concentration = 20 mg/L.

The recirculation component in degradation also occurs in systems using a circulating upflow reactor TiO_2 anatase (Saien, 2007), and is not reserved for the horizontal recirculation configuration to achieve desired degradation from pass through the reactor. The degradation within the reactor is a factor of 1) the frequency of water passing through the reactor, based on the recirculation rate, and 2) the contact time between the bulk water and the catalyst. Regardless of the recirculation rate in the recirculating batch reactor, the contact time is proportional to the frequency of passing and the residence time within the reactor (White, 1982). Thus, even though the water spends less time per pass through the reactor with increasing flow rate, the water spends the same total amount of time in the reactor because it passes through the reactor more frequently.

5.6.b.3 Effect of voltage on dye degradation

The effect of applied voltage potential on the degradation of dye from the recirculating batch reactor PECO system was analyzed, having a recirculation rate = 4.1 L/min, and a chloride ion concentration = 100.0 mg/L. The applied voltage provided DC potential from 0 V to 12 V. At potentials less than 4 V, there was no significant effect of increasing potential on erioglaucine degradation. It is apparent that as the voltage increased above 4 V, the degradation rate increased as well; the electron hole-pair recombination is minimized with an increase in the voltage (Zanoni, 2004) (Figure 5-4). The highest degradation rate occurred at a voltage of 10V: k_{10V} = 0.0017 min^{-1}. This process is beneficial to the treatment of water as the anodic bias on the semi conductor could accelerate the oxidation of organic materials (Zhang, 2003), thus aiding in the removal of target contaminants.

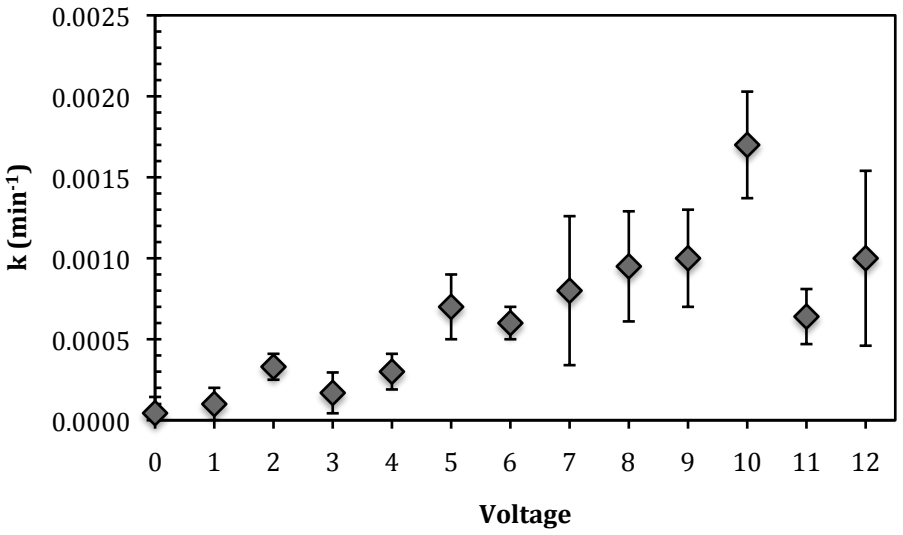

Figure 5-4: Degradation rate of erioglaucine, k, for varying voltage (0V – 12V), showing 95% confidence level in the parameter estimate. $[Cl^-]$ = 100.0 mg/L, dye concentration = 20 mg/L, and recirculation rate = 4.1 L/min

The electrode, connected to the semiconductor, is responsible for bending the valence band away from the conduction band, increasing the distance between the electron and the hole pair. Also, the electrons are now attracted to the increased positive potential of the anode. This deficiency in recombination assists by allowing more holes to 1) react with H_2O, generating hydroxyl radicals on the surface of the TiO_2 surface and 2) participate in the oxidation of chloride to chlorine. The chlorine and hydroxyl radicals then oxidize the dye over time (Table 5-3). However, as per notification from AquaMost, Inc, degradation of anodes over serial use of the PECO may decrease the voltage performance; the reactor required higher voltages over time to achieve similar current as when the anodes were newer. This aging is due to passivation of the anode, where the titanium metal becomes oxidized at the surface to a form of TiO_2 that cannot absorb UV light and, therefore, no photocatalytic activity can take place on the TiO_2 surface.

5.7 CONCLUSIONS

Neither the hydroxyl radical production, nor the dye degradation, had dependence on the recirculation rate of the reactor. However, increasing applied voltage demonstrated an increase in degradation rates. With the applied voltage, the electrode connected to the semiconductor is responsible for bending the valence band away from the conduction band, increasing the distance

between the electron and the hole pair. This deficiency in recombination assists with more holes to react with H_2O, to generate hydroxyl radicals on the surface of the TiO_2 catalyst which then oxidizes the dye to degrade the dye over time. The applied voltage and is effective at providing the best operational improvement for the overall erioglaucine dye degradation.

5.8 ACKNOWLEDGEMENTS

Support for this project was provided by AquaMost, Inc, the National Science Foundation Integrative Graduate Education Research Traineeship Program, and Graduate Engineering Research Scholars Program. Megan McConville is thanked for her significant contribution to DNPH preparation, and HPLC operation. I am thankful for contributions of Matthew Russell for sampling and data analysis is superior for undergraduate participation; his involvement is greatly appreciated.

5.9 REFERENCES

Abou-Elela, S. I., and M. A. El-Khateeb (2009), Treatment of ink wastewater via heterogeneous photocatalytic oxidation, Desalination and Water Treatment, 7(1-3), 1-5.

Banerjee, A. N., S. W. Joo, and B.-K. Min (2012), Photocatalytic Degradation of Organic Dye by Sol-Gel-Derived Gallium-Doped Anatase Titanium Oxide Nanoparticles for Environmental Remediation, Journal of Nanomaterials.

Daneshvar, N., D. Salari, A. Niaei, and A. R. Khataee (2006), Photocatalytic degradation of the herbicide erioglaucine in the presence of nanosized titanium dioxide: Comparison and modeling of reaction kinetics, Journal of Environmental Science and Health Part B-Pesticides Food Contaminants and Agricultural Wastes, 41(8), 1273-1290.

Ghaly, M. Y., J. Y. Farah, and A. M. Fathy (2007), Enhancement of decolorization rate and COD removal from dyes containing wastewater by the addition of hydrogen peroxide under solar photocatalytic oxidation, Desalination, 217(1-3), 74-84.

Hoffmann, M. R., S. T. Martin, W. Y. Choi, and D. W. Bahnemann (1995), Environmental application of semiconductor photocatalysis, Chemical Reviews, 95(1), 69-96.

Jain, R., and S. Sikarwar (2008), Photodestruction and COD removal of toxic dye erioglaucine by TiO(2)-UV process: influence of operational parameters, International Journal of Physical Sciences, 3(12), 299-305.

Jain, R., and S. Sikarwar (2010), Adsorptive and Desorption Studies on Toxic Dye Erioglaucine Over Deoiled Mustard, Journal of Dispersion Science and Technology, 31(7), 883-893.

Jones, A. P., and R. J. Watts (1997), Dry phase titanium dioxide-mediated photocatalysis: Basis for in situ surface destruction of hazardous chemicals, Journal of Environmental Engineering-Asce, 123(10), 974-981.

Krishnakumar, B., and M. Swaminathan (2011), Influence of operational parameters on photocatalytic degradation of a genotoxic azo dye Acid Violet 7 in aqueous ZnO suspensions, Spectrochimica Acta Part a-Molecular and Biomolecular Spectroscopy, 81(1), 739-744.

Lhomme, L., S. Brosillon, and D. Wolbert (2008), Photocatalytic degradation of pesticides in pure water and a commercial agricultural solution on TiO2 coated media, Chemosphere, 70(3), 381-386.

Pfieffer, H.G., Liebhafsky, H. A. (1951),The origins of Beer's law, Journal of Chemical Education 28(3), 123.

Rajkumar, D., and J. Guk Kim (2006), Oxidation of various reactive dyes with in situ electro-generated active chlorine for textile dyeing industry wastewater treatment, Journal of Hazardous Materials, 136(2), 203-212.

Saien, J., and A. R. Soleymani (2007), Degradation and mineralization of Direct Blue 71 in a circulating upflow reactor by UV/TiO2 process and employing a new method in kinetic study, Journal of Hazardous Materials, 144(1-2), 506-512.

Vautier, M., C. Guillard, and J. M. Herrmann (2001), Photocatalytic degradation of dyes in water: Case study of indigo and of indigo carmine, Journal of Catalysis, 201(1), 46-59.

Wang, W.-Y., M.-L. Yang, and Y. Ku (2010), Photoelectrocatalytic decomposition of dye in aqueous solution using Nafion as an electrolyte, Chemical Engineering Journal, 165(1), 273-280.

Wang, X.-K., Y.-C. Wei, C. Wang, W.-L. Guo, J.-G. Wang, and J.-X. Jiang (2011), Ultrasonic degradation of reactive brilliant red K-2BP in water with CCl4 enhancement: Performance optimization and degradation mechanism, Separation and Purification Technology, 81(1), 69-76.

White, M. G., O. Bensalem, and W. R. Ernst (1982), The mathematical-modeling of batch recirculation reactors for kinetics studies, Chemical Engineering Journal and the Biochemical Engineering Journal, 25(2), 223-227.

Yuan, R., S. N. Ramjaun, Z. Wang, and J. Liu (2012), Photocatalytic degradation and chlorination of azo dye in saline wastewater: Kinetics and AOX formation, Chemical Engineering Journal, 192, 171-178.

Young, K.R.L., Remucal, C.K., Harrington, G.W. (2014). Primary degradation of erioglaucine using photoelectrocatalytic oxidation [In preparation for submission]

Zanoni, M. V. B., J. J. Sene, H. Selcuk, and M. A. Anderson (2004), Photoelectrocatalytic production of active chlorine on nanocrystalline titanium dioxide thin-film electrodes, Environmental Science & Technology, 38(11), 3203-3208.

6. CONCLUSIONS AND RECOMMENDATIONS

This chapter summarizes the findings from the research presented in this dissertation and discusses the significance in understand the use of photoelectrocatalytic oxidation to treat target contaminants. This chapter will also include recommendations for further research and implementation of the photoelectrocatalytic oxidation reactor.

6.1 OVERALL CONCLUSIONS

The rates of hydroxyl radical production and *C. parvum* inactivation had no dependence on the recirculation rate of the reactor. However, the reactor type affected the production of hydroxyl radicals within the system. When comparing PECO and electrolysis reactors, the PECO reactor was 25 times faster for hydroxyl radical production and achieved a higher level of performance for *C. parvum* inactivation. This comparison revealed that the applied bias may have a role in the inactivation of *C. parvum*. The PECO reactor did not produce the highest rate of hydroxyl radicals within a given system; the UV reactor produced hydroxyl radicals at the highest rate. Therefore, the PECO reactor was not the superior method of generating hydroxyl radical for these experiments. However, the reactor was the most efficient to inactivate *C. parvum*.

For both tartrazine and erioglaucine dye, neither hydroxyl radical production, nor dye degradation, had dependence on the recirculation rate of the reactor. However, for the tartrazine dye, increasing applied voltage and chloride ion concentration demonstrated the greatest increase in degradation rates; the chlorine served as the main component of the tartrazine color removal. For erioglaucine, increasing applied voltage demonstrated an increase in degradation rates. For the applied voltage, the electrode connected to the semiconductor is responsible for bending the valence band away from the conduction band, increasing the distance between the electron and the hole pair. This deficiency in recombination assists with more holes to react with H_2O, to generate hydroxyl radicals on the surface of the TiO_2 catalyst which then oxidizes the dye over time.

6.2 RECOMMENDATIONS

6.2.1 Recommendations for further research

With the current recirculation batch reactor system, PECO can be explored for use within a finite body of water, to be continually treated over time (i.e. pond, swimming pool). An analysis for the volume of water or time required for treatment would affect the capacity of the reactor. In this scenario, a scale up of the PECO reactor may be required.

Due to the independence of *C. parvum* inactivation on the recirculation rate, future research should focus on a plug flow reactor treatment option for *C. parvum*, with a variety of reactor configurations (i.e. PECO, PCO, electrolysis, UV) as a variable. As this approach would eliminate the need for exploration of an ideal recirculation rate, a plug flow reactor is also more practical from a water quality production perspective. Additionally, the role of electrolysis clearly is a technological improvement to the traditional photocatalyic system. Within the research to explore a plug flow reactor, analysis of the ideal applied voltage should be explored as well. This study can be performed at the Water Science and Engineering Laboratory, with the opportunity to connect the device to the pilot scale conventional water treatment plant.

The PECO reactor has now been shown to treat bacteria, spores, and protozoa, the focus of future research could be directed towards virus inactivation (e.g. adenovirus). Additionally, research exploring the effectiveness of the PECO device when treating other pathogens, or a heterogeneous mix of contaminants, would be beneficial; there is rarely only one contaminant present in drinking water.

One portion of the research in this dissertation focused on the primary degradation (decolorization) of dye. Assessment of the remaining two tiers, secondary and tertiary, can be explored for mineralization and toxic chemical formation post treatment via the PECO reactor. There may also be opportunities in research to treat a heterogeneous mix of dye within a source water sample.

The research described in this dissertation focused on the use of a PECO reactor to treat target contaminants. The research also explored the new territory of measuring hydroxyl radical generation using a PECO reactor and how these radicals contribute to the treatment of *Cryptosporidium*, tartrazine and erioglaucine. Investigation into the use of recirculation rate as an operational parameter, demonstrated that the parameter had no significant influence on *Cryptosporidium* inactivation or dye degradation rates.

6.2.2 Recommendations for implementation

Exploration in to the use of solar energy to power the PECO system would be beneficial, and allow for widespread implementation in regions of the world where power supply is not readily available. With the current requirement of three power source outlets to operate one PECO unit, unintentional exclusion of a particular water treatment market may diminish wide scale implementation of a powerful treatment technology.

With the ease of use, and minimal operational requirements, the device may have useful applications in supplying the highest water quality for populations of people susceptible to minor environmental changes (i.e immunocompromised, post-surgery patients, etc.). Additionally, use of the high quality of water may be implemented for medical care facilities who require sterile tools and materials to be rinsed while in use.

Appendix A
CELL CULTURE AND IMMUNOFLUORESCENCE ASSAY

A.1 Introduction

Recent studies have investigated the use of a primary antibody specific for reproductive stages and a secondary fluorescein isothiocyanate-conjugated (FITC) anti-body, to detect infected foci (Slifko, 1997). Other studies (Schets, 2005, Bukhari 2007) investigated IFA's ability to detect infectious *C. parvum* oocysts grown in cell culture. IFA is a procedure developed for the detection of *C. parvum* oocysts in humans, animals, and bovine fecal smears (Stibbs, 1986). Subsequently, the method was modified to detect *C. parvum* in bodies of water (Ongerth, 1987). The current assay requires use of HCT-8 monolayers to support the treated oocysts (Upton, 1995). Sterilized oocysts were applied on the monolayers of HCT-8 cells, with the intention of determining the best medium supplements to support *C. parvum* development on the HCT-8 cells. The growth of the parasite, on the HCT-8 cell with the specified supplement, is determined by counting the stages under a microscope. The ideal medium contains RPMI 1640, 10% fetal bovine serum, HEPES, glucose, ascorbic acid, folic acid, aminobenzoic acid, calcium pantothenate, insulin, penicillin, streptomycin, and amphotericin. This method was developed as a simple and reproducible method for viable and surface sterilized oocysts *in vitro*. The following appendix details the cell culture protocol for the IFA.

A.2 Cell Maintenance and Splitting

All cell culture maintenance was performed under a sterilized hood at WSLH. The HCT-8 cells were obtained from American Type Culture Collection (ATCC®, Manassas, VA). Cells were shipped in a liquid nitrogen storage container, with the temperature maintained at -80°C. The cells were stored in a -80°C freezer at WSLH. When ready for use, the vial containing the cells was thawed in a 37°C bath. Once the visual thawing began, the vial was removed from the bath and placed in the operator's hands to carefully perform the remaining thawing; it is important that the transfer of cells from the vial be performed at the exact time when all thawing has occurred. Once complete thawing has occurred, the exterior of the vial was doused in sprays of 70% ethanol, to decrease the probability of contamination. After spraying, the vial was placed

under the hood, in an aseptic environment, and the contents were transferred from the vial to a 50 mL sterile conical tube containing 9.0 mL of the maintenance medium. The tube was placed in a centrifuge at 126 x *g* for 6 minutes. After centrifugation, 10 mL of supernatant were removed, via pipette, without disturbing the HCT-8 beads at the bottom of the tube, using a 10 mL pipette. Twenty-five milliliters of the cell maintenance medium were pipetted into the tube containing the HCT-8 cells, and vortexed for 10-15 seconds to suspend the cells. The suspended cells were then transferred to a 150 cm^2 capped cell culture flask (Corning®, St. Louis, MO). The flask was stored in a 37°C incubator with 5% CO_2. For the first 2-3 days of incubation, the cells were monitored for growth, using a microscope to observe an increase in confluency of the monolayer. When the confluency reached 80%, the cells were split to ensure that sufficient maintenance medium and surface area remained in the flask, providing an environment conducive for cell growth. When the cells were split, or passed, a tally was kept; passage must not exceed 30 times. At the 30^{th} passage, a new vial of HCT-8 was thawed and used for a fresh cell culture.

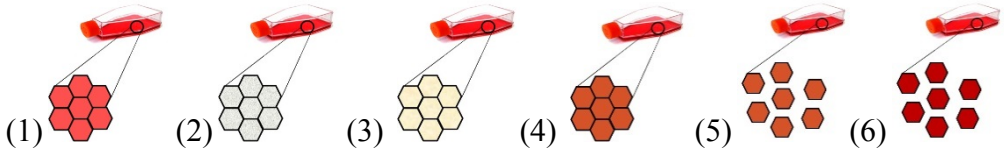

Figure A2-1: Schematic of cell maintenance

Figure A2-1 shows an illustration of the maintenance and splitting process:

(1) The cell culture medium was aspirated from the flask, without disturbing the monolayer. At this stage, the cells are red in color and remain in a confluent monolayer as shown in (Figure A2-1).

(2) The flask was gently inoculated with 10 mL of 1X phosphate buffered saline (PBS) solution, to remove the residual red maintenance medium color in the cell culture medium. Capped and gently rocked, the PBS then covered the entire monolayer on the flasks bottom (Figure A2-1).

(3) The 1X PBS was aspirated from the vial, and disposed, revealing only the rinsed monolayer (Figure A2-1).

(4) Ten mL of 0.25% trypsin (orange in hue) was inoculated into the flask, capped, and placed in a 37°C incubator for 5-7 minutes, to allow the cells to loosen from the surface

of the flask. While the flask was incubating, 50 µL of flow count beads (Flow Check, Coulter Group, Miami, FL) were added to a 12x75 mm tube, in preparation for cell count via flow cytometry.

(5) After incubation, the flask was gently tapped, to loosen the cells on the monolayer, creating cell suspension. If the cells were not loose from the surface area, the flask was returned to the incubator for one minute; the total incubation time must not exceed 8 minutes.

(6) Ten mL of fresh maintenance medium, red in color, were then added to the flask. The maintenance medium, along with the cells, was transferred from the flask, via pipetting, to a 50 mL conical centrifuge tube. The conical tube was then vortexed for 45 seconds to 1 minute. Two hundred microliters of the cell suspension were then added to the 12x75 mm tube containing the flow count beads. The tubes were then vortexed for 5 seconds and placed in the flow cytometer (Epics, XL, Coulter Group, Miami FL). The flow cytometer provided a print out of the quantity of the cells for each tube.

The quantity of cells in the suspension was used in the following calculation to determine the volume of the cell suspension to be used for further cell splitting.

$$\frac{\left(\frac{HCT8_{cells} + HCT8_{cells}}{2}\right)}{1000_{count}} \times \frac{987_{beads}}{1\mu L} \times \frac{1_{count}}{4_{beads}} \times \frac{1000\mu L}{1mL} = HCT8\frac{cells}{mL}$$

Where $HCT8_{cells}$ are the duplicate counted cells, by the flow cytometer, from the 200 µL cell suspension.

Four day passage: 3.75×10^6 cells

Three day passage: 5.25×10^6 cells

Two day passage: 6.75×10^6 cells

If the splitting was prepared for a two day split, the following equation was applied:

$$\frac{6.75 \times 10^6 \text{ cells}}{HCT\,8\frac{cells}{mL}} = mL$$

of suspension to be added to the new flask.

Each day had a cell value associated with the particular day of splitting, to allow for sufficient quantity of cells to be maintained through the splitting. Since the value for the two day passage was used, the cells were split two days from last passage. The schedule for passage was as follows:

Day1 (Monday)	Day 2 (Tuesday)	Day 3 (Wednesday)	Day 4 (Thursday)	Day 5 (Friday)	Day 6 (Saturday)	Day 7 (Sunday)	Day 8 (Monday)
Split Cells			**Split Cells**				**Split Cells**

Once the volume of cell suspension to be added to a new flask was calculated, the suspension was then added to the flask and incubated in a 37°C, 5% CO_2 incubator for the calculated days.

The cell quantity read-out provided a base for determining the quantity of cells to split, and/or to be used for future 8-chamber well preparation. Determination of cells to be split was then calculated as the quantity of cells in the current flask, cells that must be split, and the new quantity to be added to a new flask for growth; this value was $4x10^6$ cells/flask (Johnson, 2012).

A.3 8-Well Chamber Preparation

The preparation for 8-chamber wells (LAB Tek II Chamber Slide, Asheville, NC) was identical to cell splitting. However, instead of vortexing after contents are placed in 50 mL conical tube, the conical tube was centrifuged at 750 rpm for 7 minutes. The supernatant was aspirated out, leaving the pellets undisturbed. Five milliliters of maintenance medium were added to the undisturbed pellets and vortexed for 45 seconds. Two hundred microliters of the suspension were pipetted in a 12x75 mm tube, containing the 50 µL of flow count beads. The tubes were then vortexed for 5 seconds and placed in the flow cytometer.

In preparation for inoculating the well with oocysts, the cell suspensions were transferred to an 8-well chamber slide. Each chamber of the 8-well chamber slide required 500 µL of 5 mL of $4x10^4$ cells/mL previously split. The wells were set up the day before a POU device experiment was performed.

Day1 (Monday)	Day 2 (Tuesday)	Day 3 (Wednesday)	Day 4 (Thursday)	Day 5 (Friday)	Day 6 (Saturday)	Day 7 (Sunday)	Day 8 (Monday)
Split Cells		**Set up wells**	*POU run* and Split Cells				Split Cells

The quantity of cells and medium per chamber was as follows:

$$\frac{\left(\frac{HCT8_{cells} + HCT8_{cells}}{2}\right)}{1000_{count}} \times \frac{987_{beads}}{1\mu L} \times \frac{1_{count}}{4_{beads}} = HCT8\frac{cells}{\mu L}$$

$$HCT8\frac{cells}{\mu L} \times X = 4 \times 10^4 cells$$

$$X = \frac{4 \times 10^4 cells}{HCT8\frac{cells}{\mu L}} = \forall_{\mu L}$$

$$500\mu l_{cells+media} - \forall_{\mu Lcells} = \forall_{\mu L_{media}}$$

$$\forall_{\mu Lcells} \times 104_{wells} = \forall_{\mu Lcells,2} \text{of cell suspension prepared}$$

$$\forall_{\mu L_{media}} \times 104_{wells} = \forall_{\mu L_{media,2}} mL \text{ of inoculation media prepared}$$

Each chamber had $\forall_{\mu Lcells,2} + \forall_{\mu L_{media},2}$, bringing the total volume in the well to 500 $\mu L_{cells+media}$. After each chamber was inoculated with the total volume of 500 µL, the slides were placed in a sterilized plastic bag, and placed in a 37°C, 5% CO_2 incubator for 40-48 hours.

A.4 Pre-Treatment of Oocysts and Inoculation for IFA Method

Day1 (Monday)	Day 2 (Tuesday)	Day 3 (Wednesday)	Day 4 (Thursday)	Day 5 (Friday)	Day 6 (Saturday)	Day 7 (Sunday)	Day 8 (Monday)
Split Cells (2 flasks)		Set up Wells	POU run and Split Cells	**Pre-Treatment**			Split Cells

After 24 hours of incubation in a 4°C refrigerator, the 1000 µL aliquot samples were prepared for immunofluorescence assay. However, only 150 µL were needed for analysis. Two of the three tubes (capped) for each time step were placed in a centrifuge at 14,000 rpm for 2 minutes. The 850 µL of supernatant were carefully removed by tilting the tube at a 30° to 45° angle and pipetting simultaneously. The third tube was vortexed for 15 sec, before being used for serial dilutions of 1:10 and 1:100. For the 1:10 dilution, 15 mL of sample were added to 135mL of tap water. For the 1:100 dilution, 1.5 mL of sample were added to 148.5 mL of tap water.

There were 14 controls for the experiment. Duplicates of seeded oocysts were sorted into a 1.7 mL capped vial, with enumerated quantities of 1000, 750, 500, 100, and 10 oocysts. Four additional controls, Live (1), Heat Inactivated (2), and a Blank (1), were selected for the experiment. The combined quantity of vials for the experiment and control was 104.

$$5_{Time} \times 6_{Dilutions} \times 3_{PecoUnits} = 90$$

With the addition of:

$$1_{Blank} + 2_{HeatInactivated} + 1_{Live} + 2_{1000OOcysts} + 2_{750OOcysts} + 2_{500OOcysts} + 2_{100OOcysts} + 2_{10OOcysts} = 14$$

A.5 8-Chamber Well Slide Inoculation

After the total volume of the tube was prepared with 400 µL of inoculation medium and oocysts, the 8-well chamber slide was carefully removed from the incubator. The maintenance medium in each chamber was aspirated without disturbing, tearing, or damaging the monolayer. One hundred milliliters of IFA method inoculation medium were added to each chamber. The chamber slides were incubated in 36°C, 5% CO_2 for 65-72 hours.

Without disturbing the monolayers, the inoculation medium was aspirated from each chamber. Five hundred milliliters of methanol were added to each chamber to prevent the cells from continuing to grow. After 10 minutes, the methanol was aspirated off and the monolayer air-dried. While the methanol was air drying, a blocking buffer was prepared for the monolayer. The blocking buffer consisted of 49.0 mL of phosphate buffered saline (PBS), 1 mL of goat serum, and 1.0 µL of Tween 20. Upon achieving a dry monolayer, 500 µL of the blocking buffer were added to each chamber and placed on a rocker for 30 minutes. This period of time allowed for the blocking buffer to completely cover the monolayer, all the while providing sufficient time to prepare the anti-sporozoite antibody. Fifteen mL of 0.008 mg/mL of primary rat anti-sporozoite antibody (Sporo-Glo, New Orleans, LA) were prepared at 1:100 of primary anti-sporozoite antibody to PBS. The blocking buffer was then aspirated using a pipette, with close attention not to tear or damage the cell monolayer. At this point, 150 µL primary antibody of anti-sporozoite were added to each chamber, and placed on the rocking platform for 1 hour. The tray containing 8-chamber well slides was covered with aluminum foil, to prevent natural light from reacting with the antibody. After the 1-hour rocking platform time expired, 30 µL secondary goat anti rat IgG FITC labeled antibody (Sigma, St. Louis, MO) were diluted in 10 mL of 1x PBS, and added to each chamber. The stain was aspirated and washed twice with 500 µL of 1X PBS, each time with no damage to the monolayer.

After twice washing the monolayer, the chamber was removed from each slide by gently forcing a spatula between the chamber and the slide. Once separation between chamber and slide occurred, two drops of Method 1623 DABCO mounting medium were placed on top of each slide. A 22 x 50 mm coverslip was applied to each slide and stored in a 4°C refrigerator until ready for microscopy.

Each slide was viewed using a microscope with a Chiu Technical Corporation Mercury 100-W bulb, with lens fluorescein filter (480/40, DM 505, BA 535/50 FITC HYQ) to detect the

fluorescent stained oocysts. Each slide was viewed using both the 100X lens and 200X lens. All oocyst quantities were tallied with a tally counter and graphed for log removal analysis.

A.6 Flow Cytometry

Vesey (1991) was the earliest to document the use of flow cytometry to detect *C. parvum.* Vesey improved the detection, by using flocculation concentration, where large volumes of water were filtered and analyzed using flow cell cytometry and cell sorting. This method was developed to accommodate the lack of comparability of cell cultures using heterotrophic plate counts, and to allow for detection of treated sewage water where the concentrations of oocysts were 1000 oocysts/L or higher (Vesey, 1994). Recoveries for this improved method were documented at 92%. Currently the flow cytometer is used for detection, recovery, and enumeration (Hammes, 2005). Flow cytometry, combined with fluorescence of a sample and using flow count beads (Flow Check, Coulter Group, Miami, FL), can sort and count the concentration of the target protozoa, through use of forward and side scatter of the oocysts. This scatter analysis allows for a quantification of cells within a given sample.

A live sample of oocysts was used as the positive control for the detection methods. An advanced microbiologist at WSLH performed the enumeration of the oocysts. Heat inactivated, gamma irradiated (0.5 kGY), and UV irradiated (60 mJ/cm^2) oocysts, prepared by WSLH, served as negative controls. Propidium iodide (PI), a red/orange dye fluorescent dye that can stain membranes of all oocysts including those with damaged or compromised walls (Hoefel, 2003), can be detected by a flow cytometer (Epics, XL, Coulter Group, Miami FL) to quantify oocysts within a specified sample. The integration of flow cytometry with PI is a significant improvement to the IFA method (Berney, 2007; Bukhari, 2007; Campbell, 1992; Cozon 1992). For this study, the use of PI was used for enumeration of total oocysts (live + dead) detected. PI was prepared by adding 5 mg of PI to 10 mL of reagent grade water. Each vial received identical treatment through the process, regardless of whether the sample was a control or reactor treated sample.

Each vial was inoculated with a 150 µL of Acidified Hanks Balanced Salt Solution (AHBSS), to maintain the system pH. The AHBSS/2% trypsin was prepared with 0.40 g of trypsin to 19.60 mL of HBSS and 400 µL of 0.1 M hydrochloric acid (HCl). The AHBSS/2%

trypsin was vortexed for 30 sec and 10 µL were extracted to test for the desired pH of 2, using pH test paper strips (Edmund Scientifics, Tonawanda, NY).

After the addition of AHBSS, each tube was incubated for 60 minutes at 37°C, and vortexed for 10 seconds every 15 minutes. Upon completion of the 60-minute incubation, 300 µL of the IFA Method Inoculation Medium was added to each tube. Each tube was centrifuged at 14,000 rpm for two minutes. Five hundred microliters of the supernatant media were aspirated and replaced with 500 µL of IFA Method Inoculation Medium. Next, the tubes were centrifuged at 14,000 rpm for two minutes, 530 µL of the supernatant were aspirated, and 380 µL of IFA Inoculation Maintenance Medium were added. At the end of this processing, the total volume in the tube was 400 µL.

APPENDIX B

MEASUREMENT OF HYDROXYL RADICAL PRODUCTION (as detailed by Keenan, 2008)

For determining the concentration of hydroxyl radicals within the proposed system of this study, the use of a scavenger is required. The source water for hydroxyl measurements was pure Milli-Q 18.2 MΩ·cm at 25ºC. The pure water was selected, as opposed to other natural water sources (i.e. lake, river, groundwater), to minimize the influence of hydroxyl scavengers present in natural water.

The goal of these experiments was to use methanol to quantify the production of hydroxyl radicals in the system, thus minimization of known competing scavengers is needed to effectively accomplish the most accurate quantification of hydroxyl radical production. In the case of this study, the scavenger was methanol. The reaction between hydroxyl radicals and methanol occurs at a reaction rate constant of 10^{10} $M^{-1}s^{-1}$ (Buxton, 1988). This high reactivity of $^{\bullet}OH$ with methanol proves difficult when attempting to measure the concentration of hydroxyl radical with a measurement device. With a very high reaction rate, using a scavenger provides an opportunity to measure the best approximate production rate and/or concentration of hydroxyl radicals in a given system. The scavenger is essentially reacting with the OH radicals before it has the opportunity to react with any other ion (Mehrvar, 2001). Bicarbonate and carbonate may be oxidized during the photocatalytic oxidation process. Because the hydroxyl radical concentration depends on the solutes in the source water, inorganic compounds may affect the efficient use of hydroxyl radicals for water and wastewater treatment. This is due to the inorganic compounds having a scavenging effect on the hydroxyl radicals.

The reaction between methanol (CH_3OH) and hydroxyl radicals produces a carbon centered radical (Equation B1-B3), which proceeds through several sequential reactions to produce formaldehyde (CH_2O).

$$^{\bullet}OH + CH_3OH \longrightarrow {}^{\bullet}CH_2OH + H_2O \qquad \text{Equation 1}$$

$$^{\bullet}CH_2OH + H_2O \longrightarrow {}^{\bullet}CH_2OH + O_2 \longrightarrow {}^{\bullet}O_2CH_2OH \qquad \text{Equation 2}$$

$$^{\bullet}O_2CH_2OH \longrightarrow CH_2O + HO_2^{\bullet}$$ Equation 3

Formaldehyde can then react with 2,4 dinitrophenylhydrazine (DNPH) to produce hydrazone (Equation B3). It is the hydrazone concentration that can be measured using an HPLC. The concentration of hydrazone correlates to the concentration of formaldehyde. The final concentration of the formaldehyde will directly correlate to the quantity of hydroxyl radicals produced by the system, depending on rate constants and activation energies (Buxton, 1988).

When the known concentration of formaldehyde is provided by the HPLC, a series of equations are calculated to determine the production rate and concentration of hydroxyl radicals within a system (Equations B4-B10). The change in formaldehyde concentration over a period of time, $d[CH_2O]/dt$, is equated to the product of the reaction rate of hydroxyl radicals with methanol, k_{MEOH}, hydroxyl radical concentration, [˙OH], and methanol concentration, [MeOH].

$$\frac{d[CH_2O]}{dt} = +k_{MeOH}[^{\bullet}OH][MeOH]$$ Equation B4

The change in hydroxyl radicals over a period of time is determined by the differences between the production rate of hydroxyl radicals R_{OH}, the product of reaction rate of methanol and hydroxyl radicals, $k_{MEOH,}$ with the concentration of hydroxyl radical and methanol, and the product of the reaction rate with other species, k_{OS}, with the concentrations of hydroxyl radicals and their respective species [OS] (Equation B5). The product of the reaction rate with other species with the concentrations of hydroxyl radicals and their respective species is defined as the sum of the product of the reaction rate of bicarbonate with the hydroxyl radicals and the concentrations of hydroxyl radicals and bicarbonate concentration, with the product of the reaction rate of carbonate with the hydroxyl radicals and the concentrations of hydroxyl radicals and carbonate concentration (Equation B6). Hydroxyl radical concentration can then be determined as the quotient of the production rate of hydroxyl radicals and the product of the reaction rate of hydroxyl radicals with the concentration of methanol in the system (Equation B7). Because the source water used for the hydroxyl radical analysis is performed in Milli-Q water, the other species component is negligible than the methanol components for these series

of experiments (Equation B9). The hydroxyl radical is then determined to be the quotient of the production rate of hydroxyl radicals with the product of the rate constant between hydroxyl radicals and methanol with the concentration of methanol within a system (Equation B10).

$$\frac{d[^{\bullet}OH]}{dt} = R_{OH} - k_{MeOH}[^{\bullet}OH][MeOH] - k_{OS}[^{\bullet}OH][OS]$$

Equation B5

$$k_{OS}[^{\bullet}OH][OS] = k_{HCO_3}[^{\bullet}OH][HCO_3^-] + k_{CO_3}[^{\bullet}OH][CO_3^{2-}]$$

*DOM is not included in this equation, due to the non-presence in Milli-Q water.

Equation B6

$$[^{\bullet}OH] = \frac{R_{OH}}{k_{MeOH}[MeOH] + k_{OS}[OS]}$$

Equation B7

$$\frac{d[CH_2O]}{dt} = +k_{MeOH}[^{\bullet}OH][MeOH] = +k_{MeOH}\frac{R_{OH}}{k_{MeOH}[MeOH] + k_{OS}[OS]}[MeOH]$$

Equation B8

$$k_{OS}[OS] << k_{MeOH}[MeOH]$$

Equation B9

$$[^{\bullet}OH] = \frac{R_{OH}}{k_{MeOH}[MeOH]} = \frac{Ms^{-1}}{M^{-1}s^{-1}M} \longrightarrow \frac{k_{OBS}}{k_{MeOH}^{\bullet OH}} = \frac{s^{-1}}{M^{-1}s^{-1}} = M$$

Equation B10

B.1. REFERENCES

Berney, M., F. Hammes, F. Bosshard, H.-U. Weilenmann, and T. Egli (2007), Assessment and interpretation of bacterial viability by using the LIVE/DEAD BacLight kit in combination with flow cytometry, Applied and Environmental Microbiology, 73(10), 3283-3290.

Bukhari, Z., D. M. Holt, M. W. Ware, and F. W. Schaefer, III (2007), Blind trials evaluating in vitro infectivity of Cryptosporidium oocysts using cell culture immunofluorescence, Canadian Journal of Microbiology, 53(5), 656-663.

Buxton, G. V., C. L. Greenstock, W. P. Helman, and A. B. Ross (1988), Critical Review of rate constants for reactions of hydrated electrons, hydrogen atoms, and hydroxyl radicals in aqueous solution, Journal of Physical and Chemical Reference Data, 17(2), 513-886.

Campbell, A. T., L. J. Robertson, and H. V. Smith (1992), Viability of *Cryptosporidium parvum* oocysts correlation of invitro excystation with inclusion or exclusion of fluuorogenic vital dyes, Applied and Environmental Microbiology, 58(11), 3488-3493.

Cozon, G., D. Cannella, F. Biron, M. A. Piens, M. Jeannin, and J. P. Revillard (1992), *Cryptosporidium parvum* sporozoite staining by propidium iodide, International Journal for Parasitology, 22(3), 385-389.

Hammes, F., M. Berney, Y. Wang, M. Vital, O. Koester, and T. Egli (2008), Flow-cytometric total bacterial cell counts as a descriptive microbiological parameter for drinking water treatment processes, Water Research, 42(1-2), 269-277.

Hoefel, D., W. L. Grooby, P. T. Monis, S. Andrews, and C. P. Saint (2003), Enumeration of water-borne bacteria using viability assays and flow cytometry: a comparison to culture-based techniques, Journal of Microbiological Methods, 55(3), 585-597.

Mehrvar, M., W. A. Anderson, and M. Moo-Young (2001), Photocatalytic degradation of aqueous organic solvents in the presence of hydroxyl radical scavengers, International Journal of Photoenergy, 3.

Ongerth, J. E., and H. H. Stibbs (1987), Identification of *Cryptosporidium* oocysts in river water, Applied and Environmental Microbiology, 53(4), 672-676.

Schets, F. M., G. B. Engels, A. During, and A. A. D. Husman (2005), Detection of infectious Cryptosporidium oocysts by cell culture immunofluorescence assay: Applicability to environmental samples, Applied and Environmental Microbiology, 71(11), 6793-6798.

Slifko, T. R., D. Freidman, J. B. Rose, and W. Jakubowski (1997), An in vitro method for detecting infectious Cryptosporidium oocysts with cell culture, Applied and Environmental Microbiology, 63(9), 3669-3675.

Stibbs, H. H., and J. E. Ongerth (1986), Immunofluorescence detection of *Cryptosporidium* oocysts in fecal smears, Journal of Clinical Microbiology, 24(4), 517-521.

Upton, S. J., M. Tilley, and D. B. Brillhart (1995), Effect of select medium supplements on in-vitro development of *Cryptosporidium parvum* in HCT-8 cells, Journal of Clinical Microbiology, 33(2), 371-375.

Vesey, G., J. S. Slade, and C. R. Fricker (1991), Taking the eye strain out of environmental *Cryptosporidium* analysis, Letters in Applied Microbiology, 13(2), 62-65.

Vesey, G., P. Hutton, A. Champion, N. Ashbolt, K. L. Williams, A. Warton, and D. Veal (1994), Application of flow cytometry methods for the routine detection of *Cryptosporidium* and Giardia in water, Cytometry, 16(1), 1-6.